EVENT-TRIGGERED ADAPTIVE CONTROL OF NETWORKED NONLINEAR SYSTEMS WITH APPLICATION TO MOBILE ROBOTS

A Thesis Submitted
in Partial Fulfilment of the Requirements
for the Degree of

DOCTOR OF PHILOSOPHY

By

SAMI AL ISSA

Department of Electronics and Electrical Engineering
Indian Institute of Technology Guwahati
Guwahati - 781 039, INDIA.

February, 2022

EVENT-TRIGGERED ADAPTIVE CONTROL OF NETWORKED NONLINEAR SYSTEMS WITH APPLICATION TO MOBILE ROBOTS

SAMI AL ISSA

भारतीय प्रौद्योगिकी संस्थान गुवाहाटी
INDIAN INSTITUTE OF TECHNOLOGY GUWAHATI
DEPARTMENT OF ELECTRONICS & ELECTRICAL ENGINEERING

CERTIFICATE

This is to certify that the thesis entitled "**Event-triggered Adaptive Control of Networked Nonlinear Systems with Application to Mobile Robots**", submitted by **SAMI AL ISSA** (176102006), a research scholar in the *Department of Electronics and Electrical Engineering, Indian Institute of Technology Guwahati*, for the award of the degree of **Doctor of Philosophy**, is a record of an original research work carried out by him under my supervision and guidance. The thesis has fulfilled all requirements as per the regulations of the Institute and in my opinion has reached the standard needed for submission. The results embodied in this thesis have not been submitted to any other University or Institute for the award of any degree or diploma.

Dated: **02.02.2022**
Guwahati, Assam, India.

Dr. Indrani Kar
Associate Professor
Dept. of Electronics and Electrical Engg.
Indian Institute of Technology Guwahati
Guwahati - 781039, India.

This thesis is dedicated to my parents,
my brothers & sisters
and my wife

For their endless love, support and encouragement

Acknowledgement

First and foremost, I would like to express my sincere gratitude and thanks to the almighty God who is most merciful for keeping me in good health and blessing me with knowledge. Peace and blessing of Allah be upon His Prophet (SAW).

I would like to express my deep and sincere thanks to my supervisor, Dr. Indrani Kar for rendering her technical guidance, enthusiastic encouragement & helpful discussion throughout the course for this work. Without her proper guidance it would be much difficult to complete my research work and thesis on time. I would particularly like to thank for all help in patiently and carefully correcting all my manuscripts. I am also very thankful to my doctoral committee members Prof. Chitralekha Mahanta, Dr. Hanumant S. Shekhawat and Prof. Shivashankar B. Nair for sparing their precious time to evaluate the progress of my work. Their suggestions have been valuable. I would also like to thank other faculty members of EEE department for their kind help during my academic work.

I am also sincerely grateful to Dr. Yazan Aslan, my local supervisor at Damascus University, Syria, for helping me out on a number of problems related to my study in India. I would also like to express my sincere thanks & gratefulness to Ministry of Higher Education and Scientific Research, Damascus University, Syria for supporting and giving me such an opportunity to pursue my higher studies in India with scholarship.

Thanks go out to all my friends at Control and Instrumentation Laboratory. They have always been around to provide useful suggestions, companionship and created a peaceful research environment. My friends at IITG made my life joyful and were constant source of encouragement. My work in this remote place definitely would not be possible without their love and care that helped me to enjoy my new life in IITG campus. I thank all my fellow research students for their cooperation. During these years at IITG, I have had several friends who have helped me in several ways. I would like to say a big thank you to all of them for their friendship and support.

My deepest gratitude goes to my parents, brothers and sisters for their unconditional support and patience. I would like to extend my wholehearted thanks to my dear wife, Baian El-Sebaay, for her endless love and encouragement.

Sami Khuder AL ISSA

Abstract

Over the past few years, networked control systems (NCSs) have been very popular in terms of research as well as industrial applications. Such systems enjoy the merits of low cost, flexibility, reliability, and ease of maintenance. However, due to the network-induced constraints, design and implementation of controller communicating with the system over a network is indeed challenging. These constraints, including but not limited to induced delays and band-limited channels, may result in data loss consequently leading to degraded system performance or even instability. In addition to network constraints, the presence of unknown parametric uncertainties poses another challenge to the problem of an effective NCS design. Therefore, this thesis is aimed at designing a suitable controller that is capable of eliminating the network effects without affecting the system performance and stability. The emphasis of the design algorithm is laid on compensating for network delays (induced in the sensor-to-controller and controller-to-actuator channels) and reducing the resource utilizations (quantified in terms of number of transmissions and control updates), while still guaranteeing the system stability with acceptable performance.

This thesis can be divided into two major parts. In the first part, an event-triggered adaptive backstepping control scheme is proposed for a class of uncertain nonlinear systems in the presence of network-induced delays. Then, in the second part, the developed control scheme is applied on a nonholonomic mobile robot and further extended to multiple mobile robots. To overcome the limitation of channel bandwidth in NCSs, an event-triggered control scheme is proposed in this work. As compared to the traditional time-triggered paradigm, the proposed scheme significantly reduces the computational and communication burden which is highly desirable for NCSs. Unlike conventional fixed and relative thresholds, an improved triggering condition is proposed, grounded on a Lyapunov analysis based threshold. The proposed triggering condition is directly obtained from the derivative of Lyapunov function by ensuring its negative semi-definiteness property. It leads to a substantially reduced number of transmissions and exhibits more efficiency in resource utilization. To deal with the network-induced delays, an auxiliary compensation system is incorporated to handle the input delay induced in the controller-

to-actuator channel. Further, a state-predictor is designed to handle the situation when both state and input delays are induced in the network channels. The convergence of the predicted states to the actual states is proved using the Lyapunov-Razumikhin theorem. Using graph theory concepts, the developed control scheme is further extended to a leader-follower network with multiple mobile robots.

In addition to simulation and comparison results, the proposed control scheme is validated experimentally on a real mobile robot (PatrolBot). Unlike other studies where only kinematic model of the robot is considered, the dynamic model of the robot is incorporated in this study which is a more practical consideration. To handle the hardware restrictions, the dynamic model is modified to admit direct velocity commands as control input which is desirable for commercial mobile robots. The obtained results guarantee faithful trajectory tracking in the presence of both state and input delays with a substantial saving of channel bandwidth and computational resources. These results also substantiate the suitability of the theoretical propositions for practical network-based applications.

Keywords: *Adaptive control, Backstepping, Event-triggered, Mobile robots, Networked control systems, PatrolBot, State predictor, Uncertainties, Time-delays.*

Contents

List of Figures

List of Tables

List of Acronyms

C/A	Controller-to-actuator channel
ET	Event-triggered
ETAC	Event-triggered adaptive control
ETSMC	Event-triggered sliding mode control
ISE	Integral of square error
ISS	Input-to-state stable
MIMO	Multiple-input Multiple-output
NCS	Networked control system
PID	Proportional integral derivative
S/C	Sensor-to-controller channel
SISO	Single-input single-output
SMC	Sliding model control
TT	Time-triggered
ZOH	Zero-order-hold

List of Symbols

$\forall$	For all
inf	Infimum
$\in$	Belong to
$\mathbb{R}$	The space of real numbers
$\mathbb{R}^n$	The space of real valued vectors of dimension n
$\mathbb{R}^{n\times m}$	The space of real valued $n \times m$ matrices
$\lvert \cdot \rvert$	Absolute value of a scalar argument
$\lVert \cdot \rVert$	Euclidian norm for vectors and spectral norm for matrices
$(\cdot)^T$	Transpose of the argument (vector or matrix)
$\max(\cdot)$	The maximum of the arguments
$\min(\cdot)$	The minimum of the arguments
$\dot{y},\ \ddot{y}$	First and second derivative of y with respect to time
$y^{(i)}$	i^{th} derivative of y with respect to time
$\lambda_{min}(\cdot)$	Minimum eigenvalue of the argument
I_n	Identity matrix of dimension n
$\Gamma,\ \Gamma_1,\ \Gamma_2$	Positive definite diagonal matrices
u	Control input
u^{ET}	Event-triggered control input
$\tau_r,\ \tau_l$	The torques on the right and left motors
$V,\ V_1, \ldots, V_n$	Lyapunov function
x	System state
x^{ET}	The event-triggered system state
$y,\ q$	System output
$y_d,\ q_d$	Desired output
τ_{ca}	Induced delay in the controller-to-actuator channel
τ_{sc}	Induced delays in the sensor-to-controller channel

List of Publications

Book Chapter

1. **S. Al Issa** and I. Kar, "Adaptive Backstepping Control of Multiple Mobile Robots under Limited Communication; An Event-triggered Approach," in *Communication and Control for Robotic Systems*, Springer, pp. 107-122. Springer, Singapore, 2021. [Presented in *International Symposium on Control, Communication and Embedded System for Robotics, India, 2020.*]

Refereed Journals

From thesis:

1. **S. Al Issa**, A. Chakravarty, and I. Kar, "Improved event-triggered adaptive control of non-linear uncertain networked systems," in *IET Control Theory & Applications*, vol. 13, no. 13, pp. 2146–2152, 2019.
2. **S. Al Issa** and I. Kar, "Design and implementation of event-triggered adaptive controller for commercial mobile robots subject to input delays and limited communications", in *Control Engineering Practice*, 114, 2021: 104865.
3. **S. Al Issa** and I. Kar, "Adaptive control of uncertain non-linear systems over a network under input delay and limited resources," in *International Journal of Dynamics and Control*, pp. 1–8, 2021.
4. **S. Al Issa** and I. Kar, "Design and implementation of predictor-based Event-triggered Tracking Control of Nonholonomic Mobile Robot under Networked Time-delays and Limited Resources". [*To be submitted*].

Others:

5. M. Abbas, **S. Al Issa** and S.K. Dwivedy, "Event-Triggered Adaptive Hybrid Position-Force Control for Robot-Assisted Ultrasonic Examination System", in *Journal of Intelligent & Robotic Systems*, 102, 4, 2021: 1-19.

Conference Proceedings

1. **S. Al Issa**, M. Sharma, and I. Kar, "Event-triggered backstepping control scheme for networked mobile robots," in *Proceedings of the Advances in Robotics (AIR-2019)*, Chennai, India, 2019.

2. **S. Al Issa**, A. Chakravarty, and I. Kar, "Adaptive control of a networked mobile robot subject to parameter uncertainties and limited communications," in *2019 Indian Control Conference (ICC)*, Hyderabad, India, 2019.

3. **S. Al Issa** and I. Kar, "Predictor-based Event-triggered Control of Nonlinear Systems with State and Input Delays," in 7^{th} *International Conference on Advances in Control and Optimization of Dynamical Systems (IFAC-ACODS), 2022.*

4. **S. Al Issa** and I. Kar, "Event-triggered Adaptive Backstepping Control of Nonlinear Uncertain Systems with Input Delay," in 7^{th} *International Conference on Advances in Control and Optimization of Dynamical Systems (IFAC-ACODS), 2022.*

1

Introduction

Contents

1.1 Background

With the ever-increasing demand and requirements of growing industrial applications, traditional point-to-point based control becomes incompetent in meeting their desired ambitious objectives. In view of the same, recent years have witnessed a paradigm shift in the ways feedback controllers interact with the system dynamics [5]. Essentially, controlling systems using feedback with network in the loop emerges to be a competitive and viable alternative rendering the desired control objectives while satisfying practical and operational constraints in real-time applications. Such systems, popularly known as networked control systems (NCSs), enjoy the merits of low cost, flexibility, reliability, and ease of maintenance. These merits open the area for many applications, such as remote-controlled robotics, unmanned aerial vehicles, environment monitoring, and industrial automation [6]. Albeit all the prolific features of NCSs, ascribed to network uncertainties; design, analysis, and stability of controller communicating with the system over a wireless channel is indeed challenging [7, 8]. These network uncertainties, apparently encountered in the form of limits on channel bandwidth, packet loss and disorder due to congestion and time delay in transmitting information, may result in data loss consequently leading to degraded system performance or even instability [9].

The topology of a basic networked control system is illustrated in Fig. 1.1, in which a shared communication channel is employed for data exchange among the components of the systems. These components (sensors, actuators, and the controller) are located in different locations and connected via a network channel. The data transmission may be affected by network-induced delays in the sensor-to-controller and controller-to-actuator channels (represented by τ_1 and τ_2, respectively). Moreover, the transmission instants in traditional NCSs are continuously generated based on a time-triggered paradigm (represented by timers in Fig. 1.1). In such paradigm, the system states and control commands are transmitted periodically over the network. These information are continuously transmitted/updated every fixed amount of time (dt) is elapsed, without checking whether such updates are really required or not. Due to transmitting unnecessary/redundant information over the network, the time-triggered mechanism may result in inefficient utilization of the network resources, viz. channel-bandwidth, energy, and computational efforts. Instead of a time-triggered mechanism, an alternative and viable competitive strategy, called an event-triggered mechanism, is proposed recently to reduce excess waste of resources which is highly desirable for network-based applications.

In general, the research on NCSs can be classified into two main research fields, viz. *control of network* and *control over network*. In the field of *control of network*, the studies are mainly focused on network protocols, routing strategies, congestion avoidance, etc.

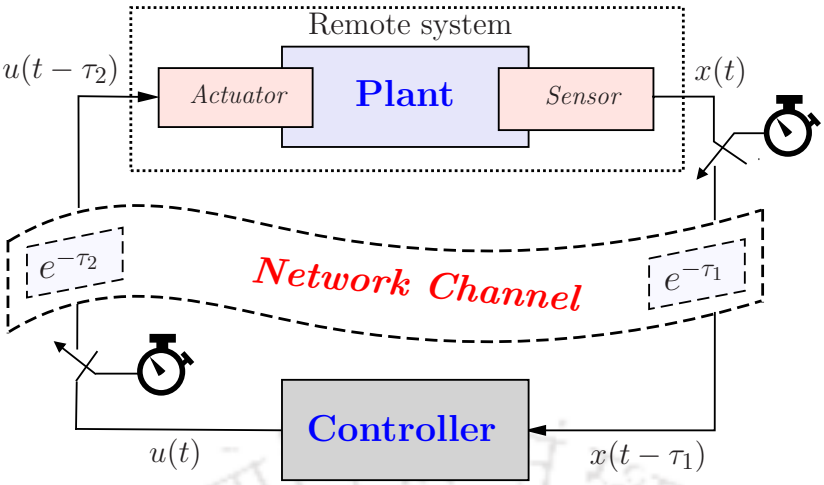

Figure 1.1: The topology of traditional time-triggered NCS.

On the other hand, the studies in the field of *control over network* are mainly involved in minimizing the effect of network uncertainties on NCSs performance and stability by exploring different control approaches and techniques. This thesis is aimed at controlling of systems *over* a network i.e. designing a suitable controller capable of eliminating the network effects without affecting the system performance and stability.

1.1.1 Event-triggered Control

Let us consider a system to be controlled over a network. The transmission/update of the system states or control inputs is called an *event*. Let $k = 1, 2, 3, \ldots, 13$ be time instants separated by a fixed time interval (dt). Fig. 1.2 presents an illustrative example for implementing the time-triggered and event-triggered strategies on a transmitted signal which may represent the system state or control input.

In time-triggered control (shown in Fig.1.2a), the system states are periodically measured and transmitted every dt. The control law is then computed based on the received states and updated over the network to actuate the plant. These transmissions are occurred at all instances ($k = 1, 2, 3, \ldots, 13$) and are continuously repeated every dt regardless of the system need. It is to be noted that this time interval (dt) is defined *a priori* based on the worst scenario such that the system stability is always ensured in all situations. This will undoubtedly result in inefficient utilization of system resources and, therefore, it is not suitable for NCSs where the network resources are generally limited.

An alternative control strategy, called event-triggered (ET) mechanism, proved to be more efficient in terms of resource utilization [10–12] and therefore it has received considerable attention in recent years (See [13–15] for linear systems and [2, 16–19] for

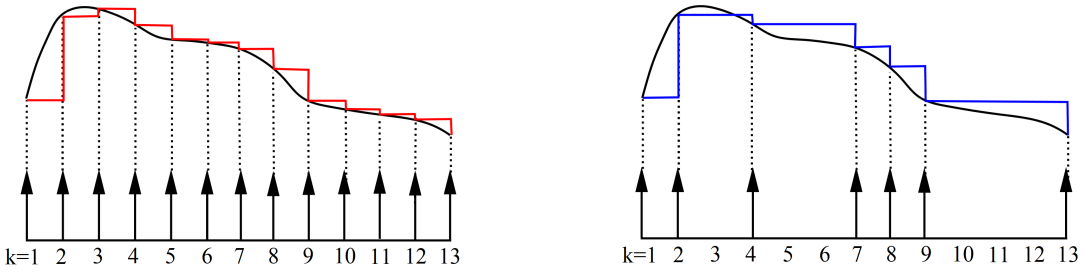

(a) Time-triggered control **(b)** Event-triggered control

Figure 1.2: An illustrative example for time-triggered and event-triggered strategies.

nonlinear systems). In event-triggered control approaches, the system state and control input are updated/transmitted over the network only when a designed *triggering condition* gets violated. Meanwhile, old/last-transmitted data are held constant till the next triggering event. In Fig. 1.2b, $k = 1, 2, 4, 7, 8, 9, 13$ represent the time instants when the triggering condition gets violated and, therefore, only at these seven instants the system states and control input are updated. As compared to periodic time-triggered control, event-triggered strategy leads to more efficient utilization of network resources since the number of updates/transmissions is significantly reduced [2, 20, 21]. Consequently, the consumed energy and packet losses will also be decreased as a result of this substantial reduction of transmitted packets over the channel. However, designing a *triggering condition* that effectively determines the triggering instants in a way that always ensures the system stability in tandem with a satisfactory performance is of great importance and indeed challenging.

Another challenge while designing an event-triggered control scheme is the exclusion of Zeno behavior i.e. the triggering mechanism shall not generate an infinite number of events within a finite time. Thus, the inter-event time between two consecutive triggering instants should always be lower bounded for the practical feasibility of the event-triggered control scheme.

1.1.2 Types of Triggering Condition

Let $s(t)$ be a signal transmitted over a network in an event-triggered fashion. This signal may represent the system state or the control input. Due to the event-triggered implementation, there will be a *measurement error* between the actual signal $s(t)$ and the received signal $s^{ET}(t)$ which is defined as $e^{ET}(t) := s(t) - s^{ET}(t)$. Based on this measurement error, several triggering conditions have been developed in the literature depending on different thresholds.

- **Fixed threshold** [22]. The triggering instants, in the triggering conditions that are based on fixed thresholds, are determined based on a predefined constant as follows.

$$\begin{aligned} t_1 &= 0, \\ t_{k+1} &= \inf\{t > t_k \mid \quad |e^{ET}(t)| \geq \varrho_1\}, \end{aligned} \tag{1.1}$$

where $\varrho_1 > 0$ is a positive constant. The measurement error in this case is always bounded by a predefined number. Although such type of triggering conditions is simple in design and implementation, it may fail to achieve the desired objectives in terms of resource utilization and system performance. In view of the same, time-varying thresholds is more desirable for network-based applications where performance is a crucial design attribute.

- **Relative threshold** [16,23,24]. The triggering instants here are determined based on the magnitude of the transmitted signal as follows.

$$\begin{aligned} t_1 &= 0, \\ t_{k+1} &= \inf\{t > t_k \mid \quad |e^{ET}(t)| \geq \sigma|s^{ET}(t)| + \varrho_2\}, \end{aligned} \tag{1.2}$$

where $0 < \sigma < 1$ and $\varrho_2 > 0$ are positive constants. The threshold is varying according to the magnitude of $s^{ET}(t)$. As compared to fixed threshold, the relative one is more flexible and it is expected to achieve better performance. However, such thresholds may fail in case of excessively large transmitted signals. In such cases, sudden jump may occur and results in degradation of the system performance.

- **Switching threshold** [2]. This triggering strategy is proposed by Xing *et al.* [2]. They suggested combining the benefits of fixed and relative thresholds. The triggering instants are now determined based on a switching threshold as follows.

$$\begin{aligned} t_1 &= 0, \\ t_{k+1} &= \begin{cases} \inf\{t > t_k \mid \quad |e^{ET}(t)| \geq \varrho_1\} & \text{if } |s^{ET}(t)| \geq \Omega \\ \inf\{t > t_k \mid \quad |e^{ET}| \geq \sigma|s^{ET}(t)| + \varrho_2\} & \text{if } |s^{ET}(t)| < \Omega \end{cases} \end{aligned} \tag{1.3}$$

where Ω is a user-defined parameter. Other parameters (σ, ϱ_1 and ϱ_2) are defined earlier. The advantages of fixed and relative thresholds are combined in this switching mechanism. It is known that a fixed threshold does not depend on the magnitude of the transmitted signal $s^{ET}(t)$ and, therefore, it will be used to avoid the sudden jump in case of excessively large signals. Based on Ω, the triggering strategy will be switched between the fixed and relative thresholds.

- **Lyapunov-based threshold**. Rather than the traditional triggering conditions based on fixed and relative thresholds, the triggering condition can be directly derived from the derivative of Lyapunov function. The threshold here is obtained based on the negative definiteness property of the derivative of Lyapunov function such that the overall system stability is always maintained under event-triggered implementation. The triggering instants are determined as follows.

$$\begin{aligned} t_1 &= 0, \\ t_{k+1} &= \inf\{t > t_k \mid \quad \dot{V} \geq 0\}, \end{aligned} \tag{1.4}$$

where $\dot{V}$ is the time derivative of Lyapunov function. This implies that as long as $\dot{V}$ is negative definite, there is no need to update/transmit a new signal over the network. The last-transmitted signal is basically held. However, this signal should be updated in case of $\dot{V} \geq 0$ in order to maintain the stability and performance of the system. It is worth mentioning that all triggering conditions proposed in this thesis are based on a Lyapunov-based threshold.

1.1.3 Configurations of Event-triggered Mechanism

According to the design requirements of a specific network-based application, the triggering mechanism might be placed either in the controller-to-actuator channel or in the sensor-to-controller channel. These two configurations are illustrated in Fig. 1.3 and discussed below.

- **Controller-to-actuator channel.** In this configuration, the event-triggered (ET) condition is evaluated at the controller-side. As shown in Fig. 1.3a, the plant is now actuated by the event-triggered control signal $u^{ET}(t)$ rather than the actual control input $u(t)$. Between two triggering instants, the last-transmitted signal is held constant at the plant-side using zero-order-holder (ZOH). The *measurement error* is defined between the actual and last-transmitted control signals as $e^{ET}(t) := u(t) - u^{ET}(t)$. A similar event-triggered configuration is reported in [2, 4, 24, 25]. This configuration is simple in design, analysis, and implementation as the measurement error appears in the control input only. Therefore, it can be directly incorporated with any traditional control approaches in a straightforward manner. In addition, there is no need for smart sensors or extra computational unit at the sensor-side in this configuration. However, as the actual control law is always required to calculate the measurement error and check the triggering condition, the computational efforts cannot be alleviated in such cases. Moreover, the system states are assumed to be always available on the controller side. In view of these considerations, it seems

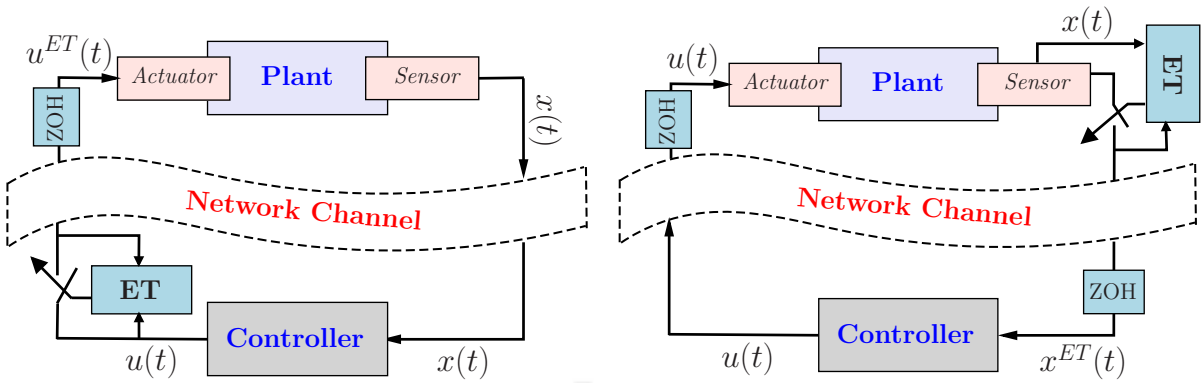

(a) Controller-to-actuator channel **(b)** Sensor-to-controller channel

Figure 1.3: Configurations of event-triggered (ET) mechanism.

that this configuration is suitable only for specific applications. Some of them are mentioned, for example, remote control of a mobile robot [4], attitude tracking of spacecraft, [24,26] and vehicle active suspension systems [27]).

- **Sensor-to-controller channel.** In this configuration, the triggering condition is evaluated at the sensor-side. The *measurement error* is defined between the actual and last-transmitted system states as $e^{ET}(t) := x(t) - x^{ET}(t)$. In such configuration, the system states are transmitted over the network only when the designed triggering condition gets violated, and the control law is then updated according to the new received states. Therefore, the computational efforts can also be decreased in this configuration since the control law is not always required to be computed and transmitted over the network. As a result, the control signal will also be event-triggered. As shown in Fig. 1.3b, the controller will be designed based on the event-triggered signal $x^{ET}(t)$ rather than the actual system states $x(t)$. Therefore, incorporating such triggering scheme with traditional control approaches is not a straightforward as the measurement errors will appear at each state, and the available controller is to be redesigned based on the event-triggered states. In addition, this configuration requires smart sensors with computational abilities or extra computation unit on the sensor-side in order to evaluate the triggering condition. A similar event-triggered configuration is reported in [19,28,29].

1.2 Literature Review

With the integration of event-triggered strategy with different control approaches, various improved control schemes have been presented in the literature. Such developed

control schemes are capable of achieving the desired performance with a significant reduction in resource utilization, and therefore, they are suitable for implementation in network-based applications where the resources are generally limited. In [30] and [31], control of continuous-time switched systems under state-based relative triggering condition is investigated. The control scheme presented in [30] considers both state-based and observer-based control. Different to the relative triggering threshold employed in [30,31], a Lyapunov-based triggering condition is proposed in [32] and [33] in order to guarantee the system stability with further reductions in the network usage. The derivative of Lyapunov function is directly employed as a threshold to formulate the triggering condition. However, these aforementioned studies consider linear systems without modeling uncertainty and external disturbances. In view of the same, various robust and adaptive control approaches have been addressed with an integrated event-triggered mechanism to achieve the desired performance in presence of system uncertainties and disturbances in nonlinear systems (for example, [2,16,34,35] for adaptive backstepping, [1,20,36–38] for sliding model control, [39] for H_∞, [17] for neural networks and [18] for fuzzy control). A passivity-based robust event-triggered controller is designed in [40] which is applicable to linear and nonlinear systems with external disturbance. In [14], Tripathy *et al.* adopted an event-triggered based robust control approach for discrete-time systems affected by mismatched uncertainties. Yet, the bounds on the uncertainties, in robust control, have to be exactly known a priori. Further, a global robust SMC is developed for linear time-invariant systems in [36] and for Lipschitz nonlinear systems in [1] to render system invariance towards matched modelling uncertainties. In [37], a practical second order SMC has also been proposed considering matched uncertainties. However, SMC strategies are generally unable to guarantee robust performance in presence of unmatched uncertainties. Moreover, the bounds of the disturbance in SMC should also be known and if unforeseen disturbances are encountered, sliding mode control may not be able to ensure stability or tracking. Besides, SMC results in, even if we use event-triggered, more frequent updates of the control and smaller inter-event time which consequently leads to more transmission energy and bandwidth requirements. In these cases, adaptive control is considered as a powerful approach used in controller design for systems affected by unknown parametric uncertainty and external perturbations. Moreover, it does not require a priori information about the bounds on these uncertainties [41].

In the context of adaptive control synthesis for systems affected by both modeling and network uncertainties, e.g., loss of information due to bandwidth constraints; very few results have been reported lately. Xing *et al.* proposed an event-triggered adaptive control scheme for uncertain nonlinear systems [2,25]. In [2], a novel triggering strategy based on switched threshold is proposed which combines both preselected fixed and rel-

ative thresholds. An improved Lyapunov-based triggering threshold is developed in [34], in which adaptive controller was designed based on backstepping approach for a class of uncertain nonlinear systems. The improved threshold is directly obtained from the derivative of Lyapunov function and it achieves a better results in terms of resource utilization as compared to [2]. Further, an event-triggered control adaptive output feedback control scheme has been investigated in [16] for a class of non-linear systems subject to actuator failures. It is worth mentioning that all the triggering mechanisms developed in these studies were placed in the *controller-to-actuator* channel and no restrictions were considered in the *sensor-to-controller* channel. Moreover, continuous information of system states were required at each time instance to evaluate the triggering condition. Hence, the computational efforts cannot be alleviated. This limitation makes these frameworks inappropriate for remote applications in which the sensors and controllers are located in two different locations. In [17–19], a triggering mechanism is developed in the sensor-to-controller channel for a class of strict-feedback non-linear SISO systems. The nonlinearities in [17, 18] were approximated using fuzzy/neural networks. This approximation leads to estimation errors that affect the convergence of the system. Moreover, the proposed scheme in [19] does not take care of system uncertainties which is not a practical consideration. In addition, all aforementioned studies assume ideal communications and do not consider any induced delays in the channels.

Delays are inevitable in any physical transmission. In NCSs, the network-induced delays may deteriorate the system performance or even result in instability of the overall closed-loop system [42]. To mitigate the impact of induced delays in NCSs, a great and significant effort has been devoted to design and analyze different control approaches and compensation strategies [43–49]. Padé approximation has been largely utilized in literature to handle the effects of induced delays. In [48, 49], an adaptive backstepping controller is designed for non-linear systems in strict-feedback form subject to input delay by using of Padé approximation. In [43], P3-DX mobile robot is remotely controlled via a wireless communication channel subject to constant time delays. These delays are handled using Padé approximation method which is largely utilized in the literature. Nevertheless, as this method is based on an approximation of time-delays, it could not handle large induced delays. In [44, 49], a novel compensation system based on integral of the input signal is developed to deal with large delays. With the incorporation of the compensating variable in the delayed system, the overall system is turned into undelayed one. Thereafter, the controller can be designed for the undelayed system using traditional control approaches. The design and analysis of the aforementioned compensating strategies seem to be straightforward and can be directly incorporated with traditional control approaches. However, such strategies are able to handle input delays only and

do not deal with state delays. In [46, 47], predictor-based controllers are designed to deal with both state and input delays for different network-based practical applications (inverted pendulum in [46] and quadrotor in [47]). The system stability is analyzed using Lyapunov–Razumikhin method in these studies. However, they are carried out under traditional time-triggered paradigm and they assume continuous control updates and signal transmissions over the network which is not practically suitable for NCSs under limited channel-bandwidth and computational resources. To analyze the stability of time-delays systems, Lyapunov-Krasovski and Lyapunov-Razumikhin can be employed which are common approaches largely utilized in literature [45]. It is worth mentioning that due to differentiating of functionals in Lyapunov-Krasovski method, the stability analysis might be complicated and, therefore, Lyapunov–Razumikhin might be an alternative simple approach while dealing with functions rather than functionals [50].

Controlling of mobile robots under network circumstances has attracted considerable attention and has been widely investigated in recent years [4, 43, 51–55]. In view of their mobility and loading capability, mobile robots have been extensively used in several applications such as automated transportation [56], autonomous wheelchairs [57], maintenance [58], surveillance systems [59] and so on. However, it has been observed that the majority of these studies are based on time-triggered framework [60–65], and very few works have been addressed in event-triggered framework [51, 66–68]. Moreover, in the context of remote control of mobile robots, the unified problem of performance improvement in presence of uncertainties and communication channel constraints (induced delays and bandwidth restrictions) between the remote controller and the system, has rarely been attempted so far. In [4, 51], an event-triggered strategy is employed to eliminate the unnecessary calls and reduce the total number of required transmissions. The proposed tracking control schemes are validated experimentally on real mobile robots (Khepera-III in [51] and Pioneer P3-DX in [52]). In these studies, the triggering mechanism was placed in the *controller-to-robot* channel and continuous transmissions were assumed in the *sensor-to-controller* channel. On similar lines, a holonomic omnidirectional robot is studied in [66]. A self-triggered controller in the sensor-to-robot channel is proposed in [68] and the results are then extended to the formation control of multiple mobile robots in [53]. An event-triggered based model predictive controller for trajectory tracking of nonholonomic mobile robot subject to external disturbances is presented in [67]. However, the mathematical models of the robot presented in [4, 51, 67, 68] consider the kinematic model only which does not capture the dynamic characteristics of the robot. Chwa [69] considers both kinematic and dynamic models of the mobile robot and proposes a tracking controller using feedback linearization. Nevertheless, a certain robot with known model parameters is considered in the study without considering the

existence of a communication channel and its underlying issues. The design is indeed theoretical considering ideal operating conditions and hence the applicability of their control algorithm for the robot may not be appreciable under practical scenarios.

From the perspective of experimental validation of the aforementioned control schemes on real mobile robots, it has been observed that the studies which consider both kinematic and dynamic models of the robot are generally restricted to simulation results. This is due to the hardware restrictions of the commercial mobile robots available in the market. Such robots have low-level velocity-based PID controllers and they are operated by direct velocity commands rather than torques or voltages of the motors. To cope with this hardware restriction, auxiliary velocity-based PD controllers are suggested and incorporated with the motors models in [70, 71]. The resultant dynamic model of the mobile robot is now actuated by linear and angular velocities. Since the parameters of internal controllers and motors models are generally not provided by manufacturers, an off-line estimation based on the least-square method is implemented in [72]. It is to be noted that the proposed control schemes in [70, 71] assume ideal communication and do not consider any restrictions on data transmissions. They are based on traditional periodic time-triggered implementation which is not preferable in networked control applications especially when channel bandwidth is limited.

In addition, recent years have witnessed compelling attention and extensive studies on multi-agent systems (See [73] for mobile robots, [74] for quad-rotors, and [75] for smart sensors networks). Consensus problem is the major topic in multi-agent systems and it is indeed challenging. This consensus can be achieved in two manners namely leader-follower and leaderless scenario. Due to its wide applications and natural physical meaning, the leader-follower scenario has been widely attempted by control theorists and practitioners (See [76–78] for linear agents and [79–81] for nonlinear agents). An adaptive fuzzy controller was designed for a class of strict-feedback nonlinear multi-agent systems in [80]. In [79], Zhao *et al.* proposed an adaptive backstepping sliding mode control scheme for multi-agent systems. The developed control scheme is applied for trajectory tracking control problem of multiple mobile robots. The graph theory is widely employed to represent the communications in the network of multiple mobile robots [82–84]. Nevertheless, the communications between these agents generally occur periodically over a shared network that has a limited bandwidth channel. As discussed earlier, these periodic transmissions undoubtedly lead to inefficient utilization of network resources [85].

1.3 Research Motivation

Controlling of uncertain systems over a communication network in the feedback loop emerges to be a fertile research problem [8]. It has provided a new research impetus to control theorists and practitioners; opening the area for many practical applications such as remote-controlled robotics, unmanned aerial vehicle, and industrial automation. At this point, it is worth mentioning that the design and stability analysis of a controller communicating with an uncertain system over a band-limited wireless channel adhering to desirable performance requirements, is indeed not straightforward [42]. Due to communication imperfections, all traditional control strategies seem to be incompetent and some modifications are needed to confront the emerging challenges such as network-induced delays, packet loss, and limited bandwidth [86]. So far, these foregoing challenges in the design of efficient and reliable NCSs, have lent enough impetuousness to solve diverse problems of networked feedback control synthesis in regards to linear dynamical systems. However, almost all dynamical systems existing in nature exhibit inherent nonlinear behavior. In addition, the presence of uncertainties in system dynamics makes the problem much more intractable. In these situations, adaptive control is one of the most rewarding control methodologies when the problem of control design for uncertain plants with completely unknown parameters is considered [41]. Moreover, different from control techniques based on optimization which only reduces the effect of uncertainties, these are online controllers which adaptively learn/estimate the unknown system parameters exactly for subsequent compensation. Hence, it is not a difficult task to infer that adaptive control is undoubtedly a potential design technique that can ensure an enhanced output performance in linear as well as nonlinear systems. However, translating adaptive control design for nonlinear systems to suit the stringent performance requirements and robustness to network uncertainties in nonlinear networked control systems is not trivial and has seldom been attempted in the open literature. The network issues further complicate the design of a stable adaptive controller for nonlinear networked control systems.

Diverting our attention to real-time implementation, applications of existing theory and methodologies of NCSs to practical robotic systems are of significant engineering importance. Controlling of mobile robots under network circumstances has been a fertile topic of great research interest in the control and robotic communities and widely studied in the last few decades [4, 51, 60–66]. In addition, recent years have witnessed compelling attention and extensive studies on multiple mobile robots. With the cooperation of these robots, many practical applications and complex control tasks would be feasible (for example, large object manipulating [87], search and rescue in large-scale areas [88], security [89] and many others). To this day, attributed to several constraints

related to communication networks in addition to highly nonlinear dynamics and nonholonomic constraints, controlling of mobile robots over a network is certainly a promising research avenue when performance is a major concern. While network constraints, manifested in the form of communication delays, information loss, etc., adversely affect system stability and convergence, unanticipated and unknown system uncertainties arising due to changes in mechanical parameters, payload variations, and disturbances due to road surface irregularities, also substantially contribute to the degradation of system performance and stability margins. In view of the same, the kinematic model based controllers are inadequate and do not provide a full description of robot characteristics. Hence, it is more practical to consider the dynamic model during controller design and analysis [62, 65, 70–72, 90–95]. However, the conventional dynamic models admit the torques of the motors as control input which is not suitable for mobile robots available in the market. Such commercial robots are operated by direct velocity commands rather than torques or voltages of the motors. Moreover, the internal parameters of the robots are not provided by manufacturers. Therefore, how to overcome these hardware restrictions is of great practical importance.

The aforementioned arguments and statements taken at face value definitely reveal that the problem of controller design for nonlinear uncertain systems under network circumstances and its applications to practical mobile robots is well motivated and the field of NCSs is promising and worth exploring.

1.4 Contributions of the Thesis

This thesis is aimed at designing an event-triggered adaptive backstepping controller for a class of nonlinear uncertain systems with application to mobile robots. In this work, the plant was controlled over a network subject to band-limited channel and induced delays. In addition, parametric uncertainties encountered in the system model are also considered, which makes the research problem indeed more challenging. Two configurations of triggering mechanism, i.e. in the controller-to-actuator channel and in the sensor-to-controller channel, are first presented in the thesis for a class of nonlinear systems. The obtained results are then validated on a real mobile robot (PatrolBot). The main contributions of the thesis can be summarized as follows.

- **Event-triggered adaptive control of a class of nonlinear uncertain SISO systems with input delay and limited communications over the controller-to-actuator channel.**

  A Lyapunov-based triggering condition is proposed, that is directly derived based on the sign of time derivative of Lyapunov function. An auxiliary compensation

system is also incorporated to handle the effects of input delay. The proposed event-triggered adaptive control scheme not only guarantees satisfactory system performance and stability but also achieves a significant improvement in channel bandwidth utilization. In addition, a comparative study with the relevant benchmark robust and adaptive control algorithms is presented which renders the proposed method with an edge over the aforementioned approaches.

- **Predictor-based event-triggered adaptive control of a class of nonlinear uncertain MIMO systems with state/input delays and limited communications over the sensor-to-controller channel.**
  A state-predictor is first designed and incorporated to handle the effects of both state and input delays. The convergence of the predicted states to the actual states is proved using the Lyapunov-Razumikhin theorem. Thereafter, an event-triggered backstepping controller is designed based on the predicted states for a class of nonlinear MIMO systems. The triggering mechanism in this configuration is placed in the sensor-to-controller channel, which results in alleviating the computational effort of the controller in addition to reducing the communication burden in both channels.

- **Event-triggered adaptive control of commercial mobile robots with limited communications and network-induced delays.**
  The developed event-triggered adaptive control schemes are implemented on a real commercial mobile robot (PatrolBot) considering the network-induced delays. Both kinematic and dynamic models of the mobile robot are presented assuming unknown system parameters. To overcome the hardware restriction of commercial mobile robots that do not accept direct torque inputs, a modified dynamic model is employed which admits direct velocity commands. The simulation and experimental results are consistent and guarantee faithful trajectory tracking with a substantial saving of channel bandwidth and computational resources.

- **Event-triggered consensus control of multiple mobile robots.**
  The obtained results are extended to multi-agent systems using graph theory. The consensus and formation control problems of a leader-followers network of multiple mobile robots under limited communication and input delay are considered. All agents are practically converged to the leader and all system signals are proved to be bounded.

1.5 Organization of the Thesis

The thesis contains seven chapters which are organized as follows.

- **Chapter 2:** This chapter investigates the event-triggered adaptive control problem of a class of nonlinear uncertain SISO systems subject to input delay and limited communication over the controller-to-actuator channel. This chapter contains two major sections. In the first section, the event-triggered adaptive controller is designed based on backstepping without consideration of input delays. An auxiliary compensation system is then introduced in the second section and the controller is modified accordingly to handle the effect of input delay. Simulation results on a single link manipulator show the effectiveness of the proposed event-triggered control scheme in terms of resource utilization.

- **Chapter 3:** This chapter investigates the event-triggered adaptive control problem of a class of nonlinear uncertain MIMO systems subject to state/input delay and limited communication over the sensor-to-controller channel. For this purpose, a state-predictor is designed here to handle the effects of both state and input delays. This chapter contains two major sections. In the first section, an event-triggered adaptive controller is designed based on backstepping without consideration for network-induced delays. A state-predictor is then incorporated in the second section to handle such delays. Thereafter, the controller is designed based on the predicted states. Simulation results on a three-link cylindrical manipulator ensure a substantial saving in computational and network resources.

- **Chapter 4:** The theoretical results obtained in Chapter 2 and Chapter 3 are then employed for the trajectory tracking control problem of a nonholonomic mobile robot in this chapter. The kinematic and dynamic models of the robot are first presented in this chapter assuming unknown system parameters. Then, two event-triggered configurations, i.e. the controller-to-robot and robot-to-controller, are employed for achieving the trajectory tracking control problem with efficient utilization of computational and channel-bandwidth resources. Simulation results show that the proposed control scheme successfully ensures faithful trajectory tracking with a substantial saving of resources as compared to traditional time-triggered control approaches.

- **Chapter 5:** Experimental validation on a real commercial mobile robot (PatrolBot) is presented in this chapter. First, a modified dynamic model is introduced to overcome the hardware restrictions of commercial mobile robots. Thereafter, the event-triggered adaptive control schemes developed in Chapter 4 are implemented

on the robot. The auxiliary compensation system and state-predictor developed in Chapter 2 and Chapter 3 are incorporated in this chapter to handle the state and input delays. Several experiments are conducted in this chapter for different values of input delays, initial conditions, and the adjustable triggering parameter, which show a faithful trajectory tracking with a significant saving in computational and communication resources in presence of state and input delays.

- **Chapter 6:** In this chapter, the obtained results are extended to multi-agent systems. The consensus tracking control problem is investigated for a leader-followers network of multi-robot systems under limited communication and induced delays. Preliminary on graph theory is first presented. Then, an event-triggered consensus controller is designed based on backstepping. Two simulation examples on consensus and formation problems of a leader-followers network show that all agents are practically converged to the leader with less number of transmissions over the network.

- **Chapter 7:** This chapter concludes the research work and outlines the scope for future research.

2

ETAC of a Class of Nonlinear Uncertain Systems over Controller-to-Actuator Channel

Contents

2.1 Introduction

Although networked control systems (NCSs) provide numerous prolific advantages over traditional point-to-point architecture, the network-induced constraints and imperfections may deteriorate the system performance and even jeopardize the stability of overall NCSs. Therefore, design and analysis of controller communicating with the system over a network is indeed challenging. In addition, the presence of uncertainties in system dynamics makes the problem much more intractable.

In this chapter[1], the network restrictions in the controller-to-actuator channel, which include the limited bandwidth and input delay, are mainly considered. In the first part of this chapter, an event-triggered adaptive controller (ETAC) is designed based on backstepping approach for a class of nonlinear uncertain networked systems without considering the input delays. Adaptive backstepping control is one of the most rewarding control methodologies when the problem of control design for uncertain nonlinear plants with completely unknown parameters is considered [41]. Moreover, event-triggered strategy is mainly employed to reduce the communication burden. Then, an auxiliary compensation system based on the integral of the input signal is introduced in the second part of the chapter to handle the input delays.

The main contributions of this chapter are summarized as follows. An improved event-triggered adaptive scheme is developed for a class of uncertain nonlinear systems with non-Lipschitz nonlinearities. Unlike existing studies based on predefined fixed [22] or relative [16, 96] thresholds, the proposed triggering mechanism is directly derived based on the negative semi-definiteness of the derivative of Lyapunov function. It guarantees system stability and Zeno exclusion with a substantially reduced number of transmissions. An auxiliary compensation system based on the integral of the input signal is also integrated with the controller design to deal with the input delays. Simulation results on a network-based manipulator illustrate the efficacy of the proposed event-triggered adaptive control scheme in terms of resource utilization. Furthermore, a comparative study with the relevant benchmark control algorithms is presented, which renders the proposed method with an edge over the aforementioned approaches.

This chapter is organized as follows. In Section 2.2, the event-triggered adaptive control scheme is presented without consideration of input delays, for which the problem is first formulated in Subsection 2.2.1. Then, the adaptive backstepping controller and event-triggered mechanism are illustrated in Subsections 2.2.2 and 2.2.3, respectively. In Section 2.3, the input delay is considered and the controller is accordingly modified

[1]This chapter is based on the article: **S. Al Issa**, A. Chakravarty, and I. Kar, "Improved event-triggered adaptive control of non-linear uncertain networked systems," in *IET Control Theory & Applications*, vol. 13, no. 13, pp. 2146–2152, 2019.

to handle the delays in the input signal. Simulation results on a single-link networked manipulator along with the comparison study are presented in Section 2.4. The chapter is summarized in Section 2.5.

2.2 ETAC of Nonlinear Uncertain Systems with Limited Resources

2.2.1 Problem formulation

Let us consider a class of nonlinear systems affine in control with unknown parameters as stated below.

$$\begin{aligned}
\dot{x}_1 &= x_2 + \Delta_1(x_1) + \varphi_1^T(x_1)\Theta^*, \\
\dot{x}_2 &= x_3 + \Delta_2(x_1, x_2) + \varphi_2^T(x_1, x_2)\Theta^*, \\
&\vdots \\
\dot{x}_i &= x_{i+1} + \Delta_i(\bar{x}_i) + \varphi_i^T(\bar{x}_i)\Theta^*, \quad 3 \leq i \leq n-1 \ , \\
\dot{x}_n &= u^{ET}(t) + \Delta_n(\bar{x}_n) + \varphi_n^T(\bar{x}_n)\Theta^* \ , \\
y &= x_1 \ ,
\end{aligned} \tag{2.1}$$

where $u^{ET} : [0, \infty) \to \mathbb{R}$ and $y \in \mathbb{R}$ denote the event-triggered control input and the system output, respectively. The i-th state vector is represented by $\bar{x}_i = [x_1, \ x_2, \ldots, \ x_i]^T \in \mathbb{R}^i, \ i = 1, \ldots, n$. The functions $\Delta_i : \mathbb{R}^i \to \mathbb{R}$ are known nonlinear functions. Further, $\varphi_i : \mathbb{R}^i \to \mathbb{R}^p$ is known function which is smooth and not necessarily Lipschitz. $\Theta^* \in \mathbb{R}^p$ is a vector of unknown parameters.

Assumption 1. *The functions Δ_i are assumed to satisfy a linear growth condition. Hence, we can write*

$$\|\Delta_i(\chi_1) - \Delta_i(\chi_2)\| \leq L_i \|\chi_1 - \chi_2\|, \quad \forall \ \chi_1, \chi_2 \in \mathbb{R}^i \tag{2.2}$$

where L_i is the Lipschitz constant, and $\|\cdot\|$ represents the Euclidean norm.

Remark 1. *The considered class of systems (2.1), described in a parametric strict feedback form, could represent a wide class of uncertain nonlinear systems. In fact, such structure is powerful enough to describe several practical engineering applications, for example, mobile robots, industrial manipulators, fan speed control system, jet engine systems, suspension systems, and many others [41]. All these practical nonlinear systems could be directly transformed to the considered structure form (2.1).*

To reduce the communication burden and circumvent the issue of channel bandwidth constraints, we resort to the use of an event-triggered controller to economically utilize

the resources to meet the desired control design objectives with respecting the restrictions of the communication channel. The event-triggered mechanism is formulated as

$$\begin{aligned} u^{ET}(t) &= u(t_k),\ \forall\ t \in [t_k, t_{k+1}) \\ t_{k+1} &= \inf\left\{\ t \mid t > t_k\ ,\quad J(e^{ET}, z_1, z_2, \ldots, z_n) > 0\right\}, \end{aligned} \tag{2.3}$$

where $e^{ET}(t) = u(t) - u^{ET}(t)$ denotes the measurement error between the actual $u(t)$ and last-transmitted $u^{ET}(t)$ control signals, $J(e^{ET}, z_1, z_2, \ldots, z_n)$ is the triggering condition to be designed later. The system configuration studied in this work is shown in Fig. 1.3a. It is considered that the control signal $u(t)$ is not directly fed to the plant. Instead, the controller communicates with the plant over a network. Hence, the plant is not actuated by the exact control input $u(t)$ calculated by the controller, as illustrated in Fig. 1.3a, owing to the presence of communication channel constraints. Rather, It is actuated by $u^{ET}(t)$ signal which is defined as $u^{ET}(t) = u(t) - e^{ET}(t)$. The control problem at this juncture is as follows. Design an event-triggered adaptive tracking control input that guarantees closed-loop signal boundedness while reducing the usage of network resources.

2.2.2 Adaptive Backstepping Control Design

The proposed control scheme utilizes an adaptive backstepping approach [41] to arrive at the final control law and is discussed in this section. Let us first define the error variables as

$$z_1 = x_1 - y_r\ , \tag{2.4}$$

$$z_i = x_i - \alpha_{i-1} - {y_r}^{(i-1)},\quad 2 \le i \le n\ , \tag{2.5}$$

where y_r represents the reference trajectory and $\alpha_1, ..., \alpha_{n-1}$ are virtual control laws to stabilize the subsystems encountered in the backstepping design procedure. The design is explained in a step-wise manner as follows.

Step 1: The derivative of the first error variable z_1 is given as

$$\begin{aligned} \dot{z}_1 &= \dot{x}_1 - \dot{y}_r \\ &= x_2 + \Delta_1 + \varphi_1^T \Theta^* - \dot{y}_r \\ &= z_2 + \alpha_1 + \Delta_1 + \varphi_1^T \Theta^*\ . \end{aligned} \tag{2.6}$$

This dynamics forms the first error subsystem to be stabilized by a suitably designed virtual control law α_1. Therefore, let us choose a Lyapunov function candidate as $V_1 = \frac{1}{2}{z_1}^2 + \frac{1}{2}\tilde{\Theta}^T \Gamma^{-1} \tilde{\Theta}$. Differentiating V_1 with respect time along the trajectories of the system

(2.1) is

$$\dot{V}_1 = z_1\dot{z}_1 - \tilde{\Theta}^T\Gamma^{-1}\dot{\hat{\Theta}} \ . \tag{2.7}$$

where $\tilde{\Theta} = \Theta^* - \hat{\Theta}$ in which $\hat{\Theta}$ is the estimate of the unknown parameter vector Θ and $\Gamma \in \mathbb{R}^{p\times p}$ is a tuning matrix associated with the adaptation law to be chosen by the designer. By substituting (2.6) into (2.7), one gets

$$\dot{V}_1 = z_1 z_2 + z_1\alpha_1 + z_1\Delta_1 + z_1\varphi_1^T\Theta^* - \tilde{\Theta}^T\Gamma^{-1}\dot{\hat{\Theta}} \ . \tag{2.8}$$

In order to make $\dot{V}_1$ equal to $-c_1{z_1}^2 + z_1z_2$, where c_1 is a positive constant, the virtual control law should be defined as

$$\alpha_1 = -c_1z_1 - \varphi_1^T\hat{\Theta} - \Delta_1 \ , \tag{2.9}$$

By substituting the virtual control law (2.9) into (2.8), it becomes

$$\dot{V}_1 = -c_1{z_1}^2 + z_1z_2 + \tilde{\Theta}^T\left(\varphi_1 z_1 - \Gamma^{-1}\dot{\hat{\Theta}}\right) \ . \tag{2.10}$$

By choosing $\dot{\hat{\Theta}} = \Gamma\varphi_1 z_1$, we have

$$\dot{V}_1 = -c_1{z_1}^2 + z_1z_2 \ . \tag{2.11}$$

Herein if $z_2 = 0$, the $\dot{V}_1$ is negative definite and the stability of z_1 is ensured.

Step 2: To stabilize the second error variable z_2 derived from (2.4), let us choose the Lyapunov function candidate as $V_2 = V_1 + \frac{1}{2}{z_2}^2 = \frac{1}{2}{z_1}^2 + \frac{1}{2}{z_2}^2 + \frac{1}{2}\tilde{\Theta}^T\Gamma^{-1}\tilde{\Theta}$. Differentiating V_2 with respect time along the trajectories of the system (2.1) is

$$\dot{V}_2 = -c_1{z_1}^2 + z_1z_2 + z_2\dot{z}_2 - \tilde{\Theta}^T\Gamma^{-1}\dot{\hat{\Theta}} \ , \tag{2.12}$$

where $\dot{z}_2$ is now expressed as

$$\begin{aligned}
\dot{z}_2 &= \dot{x}_2 - \dot{\alpha}_1 - \ddot{y}_r \\
&= x_3 + \Delta_2 + \varphi_2^T\Theta^* - \dot{\alpha}_1 - \ddot{y}_r \\
&= z_3 + \alpha_2 + \Delta_2 + \varphi_2^T\Theta^* - \dot{\alpha}_1 \\
&= z_3 + \alpha_2 + \Delta_2 + \varphi_2^T\Theta^* - \frac{\partial\alpha_1}{\partial x_1}\dot{x}_1 - \frac{\partial\alpha_1}{\partial y_r}\dot{y}_r - \frac{\partial\alpha_1}{\partial\hat{\Theta}}\dot{\hat{\Theta}} \ .
\end{aligned}$$

By substituting $\dot{x}_1$ from (2.1) and combining Θ^* terms, one gets

$$\dot{z}_2 = z_3 + \alpha_2 + \Delta_2 + \psi_2^T\Theta^* - \frac{\partial\alpha_1}{\partial x_1}(x_2 + \Delta_1) - \frac{\partial\alpha_1}{\partial y_r}\dot{y}_r - \frac{\partial\alpha_1}{\partial\hat{\Theta}}\dot{\hat{\Theta}} \ , \tag{2.13}$$

where $\psi_2^T = \left(\varphi_2^T - \frac{\partial \alpha_1}{\partial x_1}\varphi_1^T\right)$. In order to render $\dot{V}_2$ negative, the virtual control law should be defined as

$$\alpha_2 = -c_2 z_2 - z_1 - \psi_2^T \hat{\Theta} + \frac{\partial \alpha_1}{\partial x_1}(x_2 + \Delta_1) + \frac{\partial \alpha_1}{\partial y_r}\dot{y}_r + \frac{\partial \alpha_1}{\partial \hat{\Theta}}\dot{\hat{\Theta}} - \Delta_2 \ . \tag{2.14}$$

Accordingly, we have

$$\dot{V}_2 = -c_1 {z_1}^2 - c_2 {z_2}^2 + z_2 z_3 + \tilde{\Theta}^T\left(\varphi_1 z_1 + \psi_2 z_2 - \Gamma^{-1}\dot{\hat{\Theta}}\right) \ . \tag{2.15}$$

By choosing $\dot{\hat{\Theta}} = \Gamma(\varphi_1 z_1 + \psi_2 z_2)$, one gets

$$\dot{V}_2 = -c_1 {z_1}^2 - c_2 {z_2}^2 + z_2 z_3 \ . \tag{2.16}$$

Herein if $z_3 = 0$, the $\dot{V}_2$ is negative definite and the stability of z_1 and z_2 is ensured.

Step i, $(i = 3, \ldots, n-1)$: Using the same procedure as explained in the preceding steps, the virtual control law is given as follows.

$$\alpha_i = -c_i z_i - z_{i-1} - \psi_i^T \hat{\Theta} + \sum_{k=1}^{i-1} \frac{\partial \alpha_{i-1}}{\partial x_k}(x_{k+1} + \Delta_k) + \sum_{k=1}^{i-1} \frac{\partial \alpha_{i-1}}{\partial {y_r}^{k-1}} {y_r}^k + \frac{\partial \alpha_{i-1}}{\partial \hat{\Theta}}\dot{\hat{\Theta}} - \Delta_i \tag{2.17}$$

The parameter update law is also obtained as

$$\dot{\hat{\Theta}} = \Gamma\left(\varphi_1 z_1 + \sum_{k=2}^{i-1} \psi_k z_k\right), \tag{2.18}$$

where ${\psi_k}^T = \left(\varphi_k^T - \sum_{j=1}^{k-1} \frac{\partial \alpha_{k-1}}{\partial x_j}\varphi_j^T\right)$. Accordingly, one gets

$$\dot{V}_i = -\sum_{j=1}^{i} c_j {z_j}^2 + z_i z_{i+1} \ . \tag{2.19}$$

Herein if $z_n = 0$, the $\dot{V}_{n-1}$ is negative definite and the stability of $z_i, i = 1, \ldots, n-1$ is ensured. However, at the last step of backstepping procedure, the measurement error will appear in the control signal due to the event-triggered implementation. This will be handled by deriving a suitable triggering condition as follows.

2.2.3 Event-triggered Condition

It has been mentioned, in Section 2.2.1, that the controller communicates with the plant through a channel under limited communications, for which the plant is now actuated by $u^{ET}(t)$ rather than the actual control signal $u(t)$ where $u^{ET}(t) = u(t) - e^{ET}(t)$.

In this section, which represents the last step of backstepping design, the event-triggered condition is derived based on $e^{ET}(t)$ while ensuring the stability of the overall control system. Let us define the total Lyapunov function candidate as $V_n = V_{n-1} + \frac{1}{2}{z_n}^2$, whose time derivative along the system trajectories (2.1) is given as

$$\dot{V}_n = -\sum_{j=1}^{n-1} c_j {z_j}^2 + z_n z_{n+1} + z_n \left(u - e^{ET} + \varphi_n^T \Theta^* + \Delta_n - \dot{\alpha}_{n-1} - {y_r}^{(n)}\right) . \tag{2.20}$$

We have $\dot{\alpha}_{n-1}$ given as

$$\begin{aligned}\dot{\alpha}_{n-1} &= \sum_{k=1}^{n-1} \frac{\partial \alpha_{n-1}}{\partial x_k} \dot{x}_k + \sum_{k=1}^{n-1} \frac{\partial \alpha_{n-1}}{\partial {y_r}^{(k)}} {y_r}^{(k+1)} + \frac{\partial \alpha_{n-1}}{\partial \hat{\Theta}} \dot{\hat{\Theta}} \\ &= \sum_{k=1}^{n-1} \frac{\partial \alpha_{n-1}}{\partial x_k} (x_{k+1} + \Delta_k) + \sum_{k=1}^{n-1} \frac{\partial \alpha_{n-1}}{\partial x_k} \varphi_k^T \Theta^* + \sum_{k=1}^{n-1} \frac{\partial \alpha_{n-1}}{\partial {y_r}^{(k)}} {y_r}^{(k+1)} + \frac{\partial \alpha_{n-1}}{\partial \hat{\Theta}} \dot{\hat{\Theta}} .\end{aligned} \tag{2.21}$$

Then by employing $\psi_n^T = \varphi_n^T - \sum_{k=1}^{n-1} \frac{\partial \alpha_{n-1}}{\partial x_k} \varphi_k^T$ and choosing u as

$$\begin{aligned}u = &-c_n z_n - z_{n-1} - \psi_n^T \hat{\Theta} + \sum_{k=1}^{n-1} \frac{\partial \alpha_{n-1}}{\partial x_k} (x_{k+1} + \Delta_k) + \sum_{k=1}^{n-1} \frac{\partial \alpha_{n-1}}{\partial {y_r}^{(k)}} {y_r}^{(k+1)} \\ &+ \frac{\partial \alpha_{n-1}}{\partial \hat{\Theta}} \dot{\hat{\Theta}} + {y_r}^{(n)} - \Delta_n ,\end{aligned} \tag{2.22}$$

the time derivative of the Lyapunov function becomes

$$\dot{V}_n = -\sum_{j=1}^{n} c_j {z_j}^2 + \tilde{\Theta}^T \left(\sum_{j=1}^{n} \left(\varphi_n - \frac{\partial \alpha_{j-1}}{\partial x_{j-1}} \varphi_{j-1} \right) z_j - \Gamma^{-1} \dot{\hat{\Theta}} \right) - z_n e^{ET} . \tag{2.23}$$

Now, let us design the adaptation law as

$$\dot{\hat{\Theta}} = \Gamma \left(\sum_{j=1}^{n} (\varphi_n - \frac{\partial \alpha_{j-1}}{\partial x_{j-1}} \psi_{j-1}) z_j \right) . \tag{2.24}$$

Then, by substituting (2.24) in (2.23) and applying Young inequality yields

$$\begin{aligned}\dot{V}_n &\leq -\sum_{j=1}^{n} c_j z_j^2 + \|z_n\| \|e^{ET}\| \\ &\leq -\sum_{j=1}^{n} c_j z_j^2 + \frac{\|z_n\|^2}{2} + \frac{\|e^{ET}\|^2}{2}\end{aligned} \tag{2.25}$$

Adding and subtracting the term $\zeta \sum_{j=1}^{n} c_j z_j^2$, one gets

$$\dot{V}_n \leq -(1-\zeta)\sum_{j=1}^{n} c_j z_j^2 - \zeta \sum_{j=1}^{n} c_j z_j^2 + \frac{\|z_n\|^2}{2} + \frac{\|e^{ET}\|^2}{2} \tag{2.26}$$

where $\zeta > 0$ is an adjustable parameter. Now, if the triggering condition is derived by ensuring that

$$\frac{\|z_n\|^2}{2} + \frac{\|e^{ET}\|^2}{2} \leq \zeta \sum_{j=1}^{n} c_j z_j^2, \tag{2.27}$$

the derivative of Lyapunov function becomes

$$\dot{V}_n \leq -(1-\zeta)\sum_{j=1}^{n} c_j z_j^2 \tag{2.28}$$

By choosing $0 < \zeta < 1$, the negative semi-definiteness of derivative of Lyapunov function can be ensured. From (2.27), the triggering function defined in (2.3) can be written as

$$J(e^{ET}, z_1, z_2, \ldots, z_n) = \|e^{ET}\|^2 - 2\zeta \sum_{j=1}^{n} c_j {z_j}^2 + \|z_n\|^2, \tag{2.29}$$

Proposition 1. *The system dynamics (2.1) under the action of the adaptive controller (2.22) with the event-triggered scheme (2.3) is stable in the sense of Lyapunov and all states of closed-loop system are bounded. Furthermore, the error variables converge to the origin as $t \to \infty$. Moreover, the exclusion of Zeno behavior, i.e., generating infinite triggering events within a finite time, is also proved under the proposed event-triggered scheme.*

Proof. As shown in Subsection 2.2.3, the triggering condition (2.29) is derived in a way that renders the time derivative of the Lyapunov function $V = \frac{1}{2}\sum_{i=1}^{n} z_i^2 + \frac{1}{2}\tilde{\Theta}^T\Gamma^{-1}\tilde{\Theta}$ along the trajectories of system (2.1) negative semi-definite, thus the stability under this event-triggered scheme is formally guaranteed and all closed-loop signals are bounded.

Using Barbalat lemma [97], the convergence of error variables to the origin can be proved. From (2.28), we have $\ddot{V}_n = -2(1-\zeta)\sum_{j=1}^{n} c_j z_j \dot{z}_j$. Since $\dot{V}_n$ is negative semi-definite, all the closed-loop trajectories are bounded. Hence, $z_1, \ldots, z_n, \dot{z}_1, \ldots, \dot{z}_n$ are bounded for all time. Then, we can easily conclude that $\ddot{V}_n$ is also bounded. Thus, $\dot{V}_n$ is uniformly continuous. Now, we can conclude using Barbalat lemma that $\dot{V}_n \to 0$ as $t \to \infty$ which implies the convergence of state variables to the origin as $t \to \infty$.

To complete the proof, a lower bound of inter-event time should be ensured which implies the exclusion of Zeno behavior. From the definition of u (2.22), we can conclude that $\dot{u}$ is continuous and bounded as u is a function of all bounded signals. Thus, we can

write $|\dot{u}| \leq \epsilon_1$ where ϵ_1 is a positive constant. Meanwhile,

$$|u(t_{k+1}) - u(t_k)| = \left| \int_{t_k}^{t_{k+1}} \dot{u}(\lambda) d\lambda \right| \leq \int_{t_k}^{t_{k+1}} |\dot{u}(\lambda)| \, d\lambda \leq \int_{t_k}^{t_{k+1}} \epsilon_1 d\lambda = \epsilon_1 (t_{k+1} - t_k) \quad (2.30)$$

Let $e^{ET}(t_k) = 0$ and $\lim_{t \to t_{k+1}^-} e^{ET}(t) = \epsilon_2$ where ϵ_2 is a positive constant that depends on k, then we can write

$$\epsilon_2 \leq |u(t_{k+1} - u(t_k))| \quad (2.31)$$

From (2.30) and (2.31), we get

$$\epsilon_2 \leq |u(t_{k+1}) - u(t_k)| \leq \epsilon_1 (t_{k+1} - t_k) \quad (2.32)$$

Accordingly,

$$(t_{k+1} - t_k) \geq \epsilon_2 / \epsilon_1, \quad (2.33)$$

which implies that a lower bound of inter-event time can always be ensured and obtained as ϵ_2/ϵ_1 [2]. □

2.3 ETAC of Nonlinear Uncertain Systems with Input Delay

In the previous section, the event-triggered adaptive controller was designed assuming ideal communication without delay. However, the network-induced delay is practically inevitable, and it significantly affects the system's performance and stability. In this section, the input delay is considered while designing the event-triggered controller. An auxiliary compensation system is incorporated within the error variables to handle such delays, as will be explained in the sequel.

2.3.1 Problem formulation

Let us consider a class of nonlinear systems affine in control subject to input delay and unknown parameters. These systems can be described in a parametric strict feedback form as stated below.

$$\begin{aligned}
\dot{x}_1 &= x_2 + \Delta_1(x_1) + \varphi_1^T(x_1)\Theta^*, \\
\dot{x}_2 &= x_3 + \Delta_2(x_1, x_2) + \varphi_2^T(x_1, x_2)\Theta^*, \\
&\vdots \\
\dot{x}_i &= x_{i+1} + \Delta_i(\bar{x}_i) + \varphi_i^T(\bar{x}_i)\Theta^*, \quad 3 \leq i \leq n-1 \ , \\
\dot{x}_n &= u^{ET}(t-\tau) + \Delta_n(\bar{x}_n) + \varphi_n^T(\bar{x}_n)\Theta^* \ , \\
y &= x_1 \ ,
\end{aligned} \quad (2.34)$$

where $u^{ET}(t-\tau)$ denote the delayed control input, in which τ represents a constant time delay. Other variables are defined similar to the problem formulation in Subsection 2.2.1.

An event-triggered mechanism is also employed here in this section to reduce the communication burden. The triggering mechanism is similarly defined as (2.3). Relative to Section 2.2, an auxiliary compensation system is introduced in this section to handle the input delay [49], and it is defined as

$$\dot{\eta}_i = \eta_{i+1} - \kappa_i \eta_i, \quad 1 \leq i \leq n-1 \tag{2.35}$$

$$\eta_n = \int_{t-\tau}^{t} u^{ET}(\lambda) d\lambda \tag{2.36}$$

where $\kappa_i > 0$ for $i = 1, \ldots, n-1$ are positive constants. The new error variables are accordingly defined as

$$z_1 = x_1 + \eta_1 \ , \tag{2.37}$$

$$z_i = x_i - \alpha_{i-1} + \eta_i, \quad 2 \leq i \leq n \ , \tag{2.38}$$

where η_i, $i = 1, \ldots, n$ are the compensating variables and $\alpha_1, ..., \alpha_{n-1}$ are the virtual control laws to stabilize the subsystems encountered in the backstepping design procedure. For simplicity, the error variables in this section are defined for a stabilization problem.

Remark 2. *In fact, the input delay is eventually handled by the compensating variable η_n in the last step of the design procedure. This variable separates the delay out from the input signal. The control law is then designed for an un-delayed system. The other auxiliary variables η_i for $i = 1, \ldots, n-1$ are introduced to recursively handle the effects of the compensating variable η_n in the preceding steps of the backstepping design procedure.*

The system configuration studied in this section is similar to the one presented in Fig. 1.3a. However, it is considered here that the control signal $u(t)$ not only experiences loss of unnecessary information due to event-triggered implementation, but also it suffers from input-delays in the controller-to-plant channel. Hence, the plant is not actuated by the exact control input $u(t)$ calculated by the controller. Rather, It is actuated by $u^{ET}(t-\tau)$ signal. The control problem at this juncture is as follows. Design an event-triggered adaptive stabilization controller which guarantees closed-loop signal boundedness under input delays while reducing the usage of network resources.

2.3.2 Adaptive Backstepping Compensated Control Design

In this section, the control design is explained in a step-wise manner as follows.

Step 1: The derivative of the first error variable z_1 is given as

$$\begin{aligned}\dot{z}_1 &= \dot{x}_1 + \dot{\eta}_1 \\ &= x_2 + \Delta_1 + \varphi_1^T \Theta^* + \eta_2 - \kappa_1 \eta_1 \\ &= z_2 + \alpha_1 + \Delta_1 + \varphi_1^T \Theta^* - \kappa_1 \eta_1 \ . \end{aligned} \tag{2.39}$$

This dynamics forms the first error subsystem to be stabilized by virtual control law α_1. Therefore, let us choose a Lyapunov function candidate as $V_1 = \frac{1}{2}{z_1}^2 + \frac{1}{2}\tilde{\Theta}^T \Gamma^{-1} \tilde{\Theta}$. Differentiating V_1 with respect time along the trajectories of the system (2.34) is

$$\dot{V}_1 = z_1 \dot{z}_1 - \tilde{\Theta}^T \Gamma^{-1} \dot{\hat{\Theta}} \ . \tag{2.40}$$

By substituting (2.39) into (2.40), the time derivative of Lyapunov function becomes

$$\dot{V}_1 = z_1 z_2 + z_1 \alpha_1 + z_1 \Delta_1 + z_1 \varphi_1^T \Theta^* - z_1 \kappa_1 \eta_1 - \tilde{\Theta}^T \Gamma^{-1} \dot{\hat{\Theta}} \ . \tag{2.41}$$

In order to make $\dot{V}_1$ equal to $-c_1 {z_1}^2 + z_1 z_2$, where c_1 is a positive constant, the virtual control law should be defined as

$$\alpha_1 = -c_1 z_1 - \varphi_1^T \hat{\Theta} - \Delta_1 + \kappa_1 \eta_1 \ , \tag{2.42}$$

where $\hat{\Theta}$ is the estimation of the unknown parameter vector Θ and $\tilde{\Theta} = \Theta^* - \hat{\Theta}$.
By substituting the virtual control law (2.42) into the time derivative of Lyapunov function (2.41), it becomes

$$\dot{V}_1 = -c_1 {z_1}^2 + z_1 z_2 + \tilde{\Theta}^T \left(\varphi_1 z_1 - \Gamma^{-1} \dot{\hat{\Theta}} \right) \ . \tag{2.43}$$

By choosing $\dot{\hat{\Theta}} = \Gamma \varphi_1 z_1$, we have

$$\dot{V}_1 = -c_1 {z_1}^2 + z_1 z_2 \ . \tag{2.44}$$

Herein if $z_2 = 0$, the $\dot{V}_1$ is negative semidefinite and stability of z_1 is ensured.

Step 2: To stabilize the second error variable z_2 derived from (2.38), let us choose the Lyapunov function candidate as $V_2 = V_1 + \frac{1}{2}{z_2}^2 = \frac{1}{2}{z_1}^2 + \frac{1}{2}{z_2}^2 + \frac{1}{2}\tilde{\Theta}^T \Gamma^{-1} \tilde{\Theta}$. Differentiating V_2 with respect time along the trajectories of the system (2.34) is

$$\dot{V}_2 = -c_1 {z_1}^2 + z_1 z_2 + z_2 \dot{z}_2 - \tilde{\Theta}^T \Gamma^{-1} \dot{\hat{\Theta}} \ , \tag{2.45}$$

where $\dot{z}_2$ is now expressed as

$$\begin{aligned}\dot{z}_2 &= \dot{x}_2 - \dot{\alpha}_1 + \dot{\eta}_2 \\ &= z_3 + \alpha_2 + \Delta_2 + \varphi_2^T\Theta^* - \dot{\alpha}_1 - \kappa_2\eta_2 \\ &= z_3 + \alpha_2 + \Delta_2 + \varphi_2^T\Theta^* - \frac{\partial\alpha_1}{\partial x_1}\dot{x}_1 - \frac{\partial\alpha_1}{\partial\hat{\Theta}}\dot{\hat{\Theta}} - \frac{\partial\alpha_1}{\partial\eta_1}\dot{\eta}_1 - \kappa_2\eta_2 \ . \end{aligned} \tag{2.46}$$

By substituting $\dot{x}_1$ from (2.34) and combining Θ^* terms, one gets

$$\dot{z}_2 = z_3 + \alpha_2 + \Delta_2 + \psi_2^T\Theta^* - \frac{\partial\alpha_1}{\partial x_1}(x_2 + \Delta_1) - \frac{\partial\alpha_1}{\partial\hat{\Theta}}\dot{\hat{\Theta}} - \frac{\partial\alpha_1}{\partial\eta_1}\dot{\eta}_1 - \kappa_2\eta_2 \ , \tag{2.47}$$

where $\psi_2^T = \left(\varphi_2^T - \frac{\partial\alpha_1}{\partial x_1}\varphi_1^T\right)$. In order to render $\dot{V}_2$ negative, the virtual control law should be defined as

$$\alpha_2 = -c_2z_2 - z_1 - \psi_2^T\hat{\Theta} + \frac{\partial\alpha_1}{\partial x_1}(x_2 + \Delta_1) + \frac{\partial\alpha_1}{\partial\hat{\Theta}}\dot{\hat{\Theta}} + \frac{\partial\alpha_1}{\partial\eta_1}\dot{\eta}_1 + \kappa_2\eta_2 - \Delta_2 \ . \tag{2.48}$$

The time derivative of Lyapunov function V_2 becomes

$$\dot{V}_2 = -c_1{z_1}^2 - c_2{z_2}^2 + z_2z_3 + \tilde{\Theta}^T\left(\varphi_1z_1 + \psi_2z_2 - \Gamma^{-1}\dot{\hat{\Theta}}\right) \ . \tag{2.49}$$

By choosing $\dot{\hat{\Theta}} = \Gamma(\varphi_1z_1 + \psi_2z_2)$, we get

$$\dot{V}_2 = -c_1{z_1}^2 + -c_2{z_2}^2 + z_2z_3 \ . \tag{2.50}$$

Step i, $(i = 3, \ldots, n-1)$: Using the same procedure as explained in the preceding steps, the virtual control law is given as follows.

$$\alpha_i = -c_iz_i - z_{i-1} - \psi_i^T\hat{\Theta} + \sum_{k=1}^{i-1}\frac{\partial\alpha_{i-1}}{\partial x_k}(x_{k+1} + \Delta_k) + \frac{\partial\alpha_{i-1}}{\partial\hat{\Theta}}\dot{\hat{\Theta}} + \sum_{k=1}^{i-1}\frac{\partial\alpha_{i-1}}{\partial\eta_k}\eta_k + \kappa_i\eta_i - \Delta_i \tag{2.51}$$

The parameter update law is also obtained as

$$\dot{\hat{\Theta}} = \Gamma\left(\varphi_1z_1 + \sum_{k=2}^{i-1}\psi_kz_k\right) \ , \tag{2.52}$$

where $\psi_k^T = \left(\varphi_k^T - \sum_{j=1}^{k-1}\frac{\partial\alpha_{k-1}}{\partial x_j}\varphi_j^T\right)$. Accordingly, the time derivative of Lyapunov function along with system trajectories (2.34) becomes

$$\dot{V}_i = -\sum_{j=1}^{i}c_j{z_j}^2 + z_iz_{i+1} \ . \tag{2.53}$$

2.3.3 Event-triggered Condition

In this section, which represents the last step of backstepping design, the event-triggered condition is derived based on measurement error $e^{ET}(t)$ between the actual and actuated control signals while ensuring the stability of the overall control system.

The dynamics of the last error subsystem is given as follows.

$$\begin{aligned}\dot{z}_n &= \dot{x}_n - \dot{\alpha}_{n-1} + \dot{\eta}_n \\ &= u^{ET}(t-\tau) + \varphi_n^T\Theta^* + \Delta_n - \dot{\alpha}_{n-1} + \dot{\eta}_n \end{aligned} \tag{2.54}$$

From (2.36), we have $\dot{\eta}_n = u^{ET}(t) - u^{ET}(t-\tau)$. Then,

$$\dot{z}_n = u^{ET}(t) + \varphi_n^T\Theta^* + \Delta_n - \dot{\alpha}_{n-1}\ . \tag{2.55}$$

The total Lyapunov function candidate at the last step is then chosen to be $V_n = V_{n-1} + \frac{1}{2}{z_n}^2$ whose time derivative along with the trajectories of system (2.34) is given as

$$\dot{V}_n = -\sum_{j=1}^{n-1} c_j {z_j}^2 + z_n z_{n+1} + z_n\left(u(t) - e^{ET} + \varphi_n^T\Theta^* + \Delta_n - \dot{\alpha}_{n-1}\right)\ . \tag{2.56}$$

As the input delays are already handled, the control and adaptation laws can now be designed similar to previous section as

$$\begin{aligned} u &= -c_n z_n - z_{n-1} - \psi_n^T\hat{\Theta} + \sum_{k=1}^{n-1}\frac{\partial\alpha_{n-1}}{\partial x_k}\left(x_{k+1} + \Delta_k\right) + \frac{\partial\alpha_{n-1}}{\partial\hat{\Theta}}\dot{\hat{\Theta}} + \sum_{k=1}^{n-1}\frac{\partial\alpha_{n-1}}{\partial\eta_k}\eta_k - \Delta_n, \\ \dot{\hat{\Theta}} &= \Gamma\left(\sum_{j=1}^{n}(\varphi_n - \frac{\partial\alpha_{j-1}}{\partial x_{j-1}}\psi_{j-1})z_j\right) \end{aligned} \tag{2.57}$$

where $\psi_n^T = \varphi_n^T - \sum_{k=1}^{n-1}\frac{\partial\alpha_{n-1}}{\partial x_k}\varphi_k^T$. With (2.57), the derivative of the Lyapunov function becomes

$$\begin{aligned}\dot{V}_n &= -\sum_{j=1}^{n} c_j z_j^2 - z_n e^{ET} \\ &\leq -\sum_{j=1}^{n} c_j z_j^2 + \frac{\|z_n\|^2}{2} + \frac{\|e^{ET}\|^2}{2}\ . \end{aligned} \tag{2.58}$$

Similar to the analysis presented in Subsection 2.2.3, the triggering condition can be defined as

$$J(e^{ET}, z_1, z_2, \ldots, z_n) = \|e^{ET}\|^2 - 2\zeta\sum_{j=1}^{n} c_j {z_j}^2 + \|z_n\|^2, \tag{2.59}$$

which yields the derivative of Lyapunov function with respect time along the system

trajectories(2.34) as

$$\dot{V}_n \leq -(1-\zeta)\sum_{j=1}^{n} c_j z_j^2 \tag{2.60}$$

Proposition 2. *The system dynamics (2.34) under the action of the adaptive controller (2.57) with the triggering condition (2.59) is stable and the boundedness of all closed-loop signals is ensured. Furthermore, the error variables converge to the origin as $t \to \infty$. Moreover, the Zeno behavior is excluded under the event-triggered scheme.*

Proof. The triggering condition (2.59) is derived in a way that renders the time derivative of the Lyapunov function along with the trajectories of system (2.34) negative semi-definite; thus the stability in the sense of Lyapunov is ensured under the event-triggered scheme, and all signals are therefore bounded. The convergence of the error variables can be directly proved similar to the analysis in Proposition 1 by invoking Barbalat lemma [97]. Moreover, the proof of Zeno exclusion presented in Proposition 1 is also still valid and can be directly applied in case of input delays. □

2.4 Simulation and Comparative Studies

In this section, a single-link manipulator controlled over a communication network is considered. In order to illustrate the effectiveness of the proposed event-triggered control scheme, the obtained results are compared with the existing event-triggered sliding model control scheme (ETSMC) [1] and event-triggered adaptive control scheme (ETAC) [2]. In [2], fixed, relative and switching triggering conditions are presented. The details of the ETSMC scheme and selected controller parameters are provided in the Appendix A.1 for ease of reference.

The dynamics of the manipulator can be modeled as follows [2].

$$J\ddot{q}(t) + B\dot{q}(t) + Mg_aL\sin\left(q(t)\right) = u(t-\tau)\ , \tag{2.61}$$

where q and $\dot{q}$ represent the angle and angular velocity of the rigid link, respectively. J stands for the total rotation inertia of the motor and B is the overall damping coefficient that represents the unmatched uncertain term. M is the mass of the link, L is the distance from the axis of joint to the center of mass, and g_a is the gravitational acceleration. In order to transform the system into the parametric strict feedback form, let $x_1 = q, x_2 = \dot{q}$. Thus,

$$\begin{aligned} \dot{x_1} &= x_2\ , \\ \dot{x_2} &= -\frac{Mg_aL}{J}\sin(x_1) - \frac{B}{J}x_2 + u(t-\tau)\ . \end{aligned} \tag{2.62}$$

The problem is to stabilize the system (2.62) and make the angle position move back to zero ($y_r = 0$) with a reduced number of transmissions over the network. Then, the

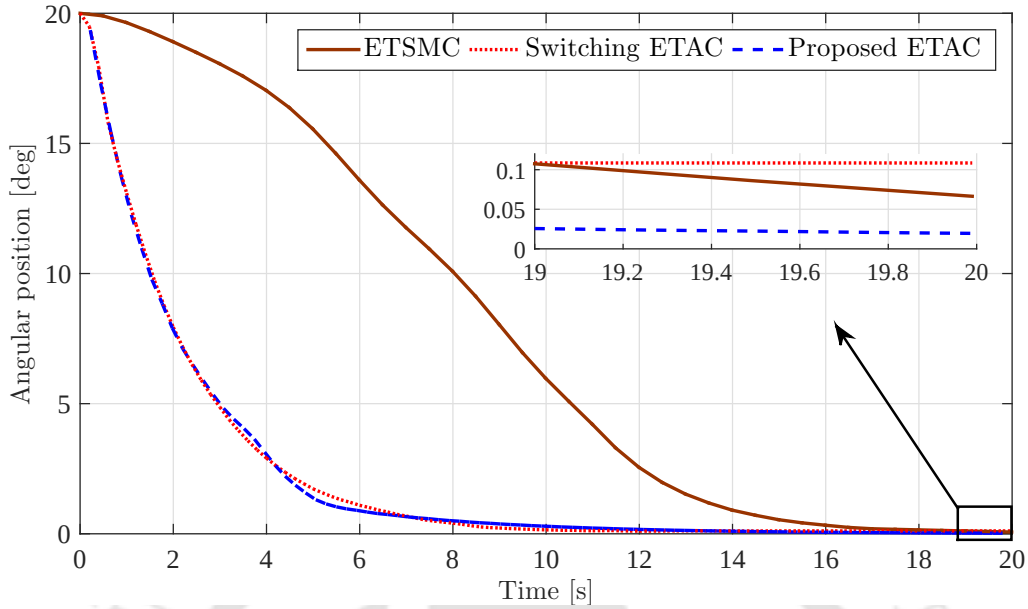

Figure 2.1: The joint angle position of the manipulator under ETSMC [1], Switching ETAC [2] and the proposed ETAC.

control law can be found using equations (2.42) and (2.48) as

$$\alpha_1 = -c_1 z_1 + \kappa_1 \eta_1 = -c_1 x_1 + \kappa_1 \eta_1, \tag{2.63}$$

$$u = \alpha_2 = -c_2 z_2 - z_1 + \frac{M g_a L}{J} \sin(x_1) + x_2 \hat{B} - c_1 x_2 + \kappa_1 \eta_2 - \kappa_1^2 \eta_1, \tag{2.64}$$

$$\dot{\hat{B}} = -\Gamma \frac{z_2 x_2}{J}. \tag{2.65}$$

The simulations are conducted using MATLAB for a total time of $20s$ with a sampling interval $T = 0.001s$. Similar to [2] and for the purpose of fair comparison, the physical parameters are given as $Mg_aL = 10, J = 1$. The other relevant parameters are chosen as $c_1 = 0.5$, $c_2 = 1$, $\Gamma = 1$, $q(0) = 20$, $\dot{q}(0) = 0$, $B = 2$, $\hat{B}(0) = 1.5$ and $\zeta = 0.5$. The input delay is chosen as $\tau = 0.1$ [s]. The parameters of the switching triggering threshold (1.3) presented in [2] are similarly selected as $\varrho_1 = 8$, $\varrho_2 = 1$, $\sigma = 0.2$, and $\omega = 30$.

The obtained results using the proposed event-triggered adaptive controller are given in Fig. 2.1–2.5. It is evident from the results that, as compared to ETSMC and ETAC, the proposed triggering rule yields better results in terms of reducing the number of required transmissions in tandem with acceptable performance. The trajectories of joint angle position under each control scheme are shown in Fig. 2.1. It is observed that the switching ETAC [2] achieves lager stabilization error as compared to the other control schemes. On the other hand, the trajectories under the proposed control scheme for different values of input delays are presented in Fig. 2.2. It is evident that the proposed control scheme is

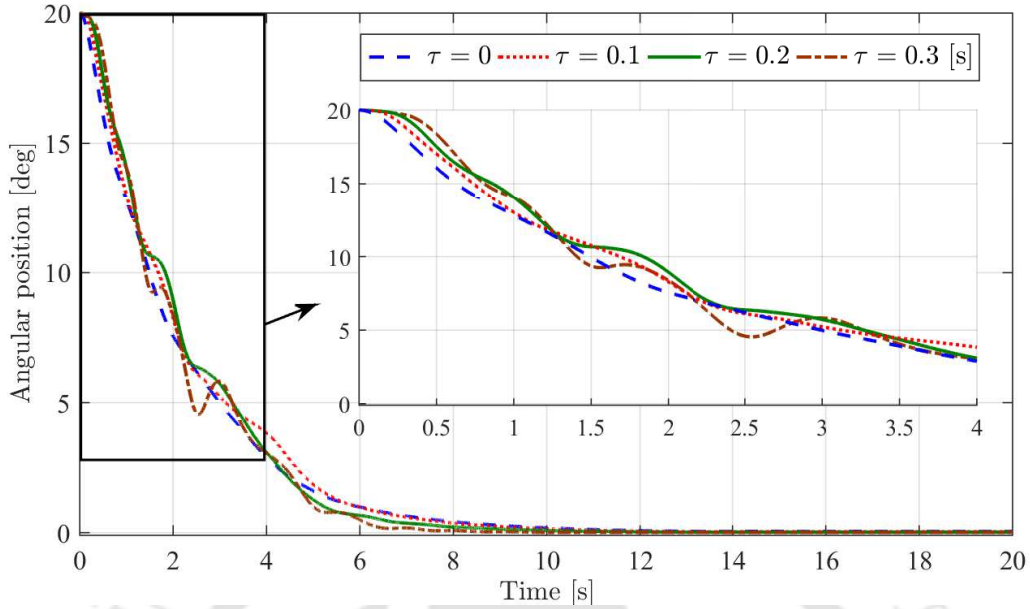

Figure 2.2: The joint angle position of the manipulator under the proposed control scheme for different values of input delays.

able to handle the input delays in tandem with an acceptable performance. The controller perform well for $\tau < 0.3$ second and a degradation is observed for values equal or greater than $\tau = 0.3$. It is worth mentioning that the scenario of input delays was not considered in [1, 2], for which the system becomes unstable even for small input delays. Therefore, it is well understood that ETAC is superior compared to ETSMC [1] and ETAC [2], and shows promise for NCS applications. The time-triggered and event-triggered control signals for each control scheme are shown in Fig. 2.3 which shows that all signals are bounded over time.

On the other hand, the inter-event times and triggering instants are depicted in Fig. 2.4 and Fig. 2.5, respectively. The required number of events, minimum and maximum values of inter-event times are shown in Table 2.1. Moreover, the average value for each scheme is calculated and found to be $0.07, 0.13$, and 0.45 for ETSMC, switching ETAC and proposed triggering scheme, respectively. It can be observed that the proposed triggering scheme has the least number of triggering events and achieves larger inter-event times as compared to other schemes, which implies the best performance in terms of limited resources utilization. It is also evident from Fig. 2.5 that the number of triggering instants in ETSMC is substantially high as compared to the ETAC schemes. This is due to the high-frequency action of SMC, for which the issue of chattering cannot be totally eliminated by using an event-triggered approach. Table 2.1 summarizes the obtained results. The results of fixed and relative thresholds presented in [2] are also

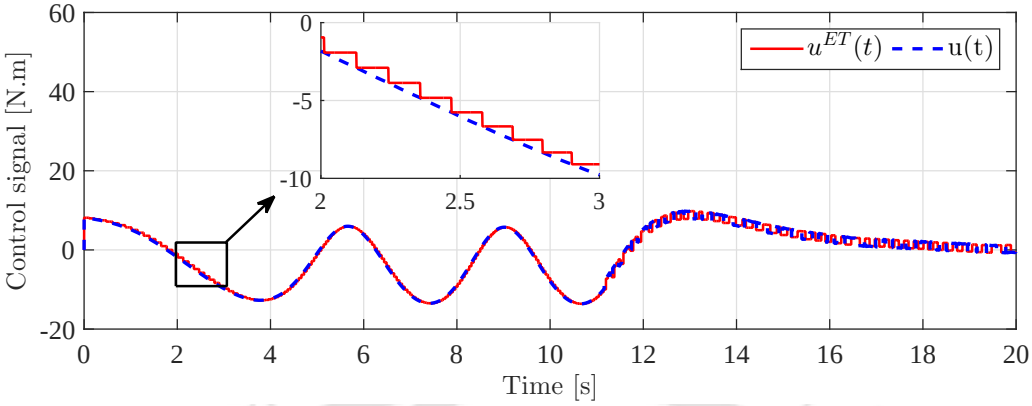

(a) ETSMC scheme [1]

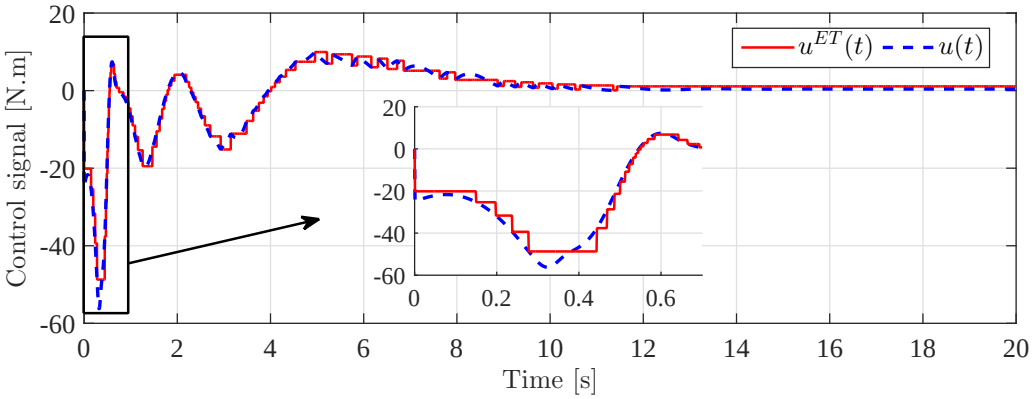

(b) Switching ETAC scheme [2]

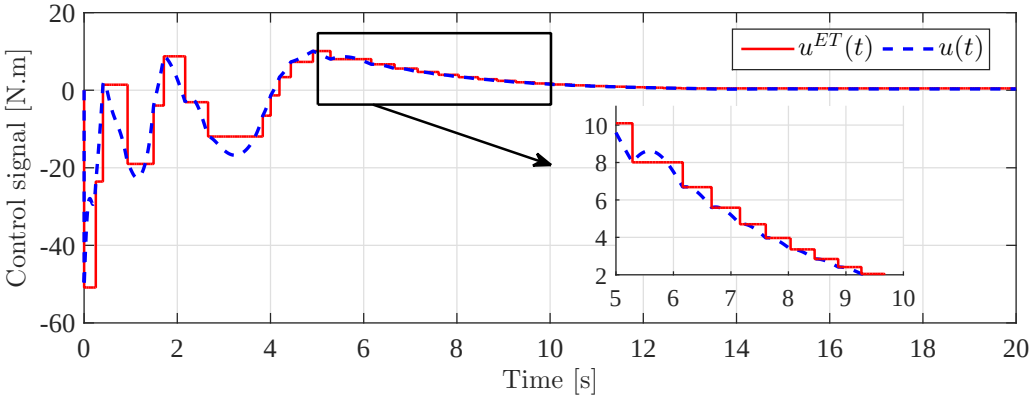

(c) The proposed ETAC scheme

Figure 2.3: Control signals for ETSMC [1], Switching ETAC [2] and the proposed ETAC.

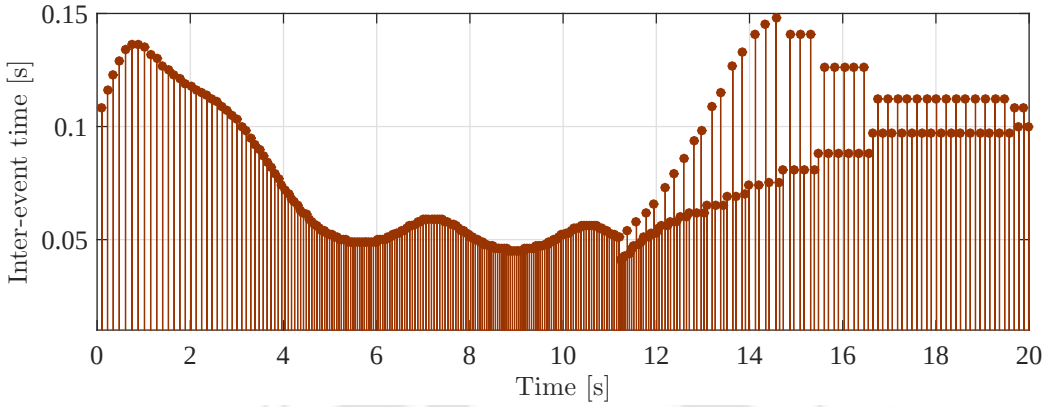

(a) ETSMC scheme [1]

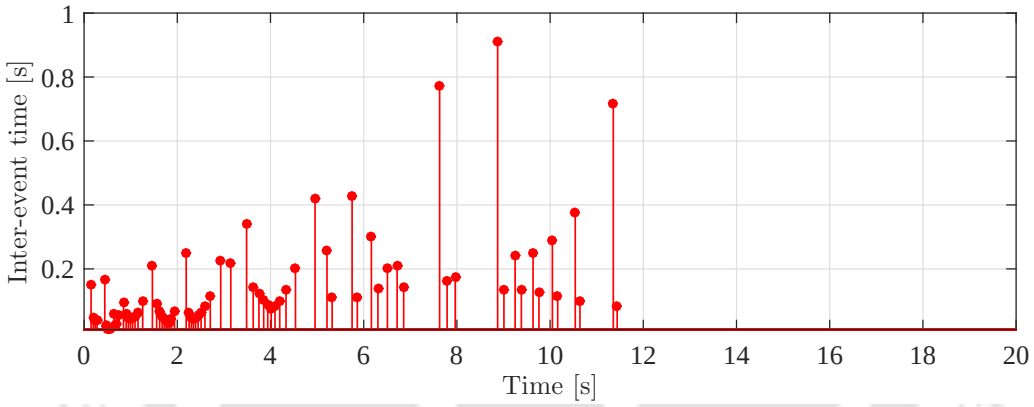

(b) Switching ETAC scheme [2]

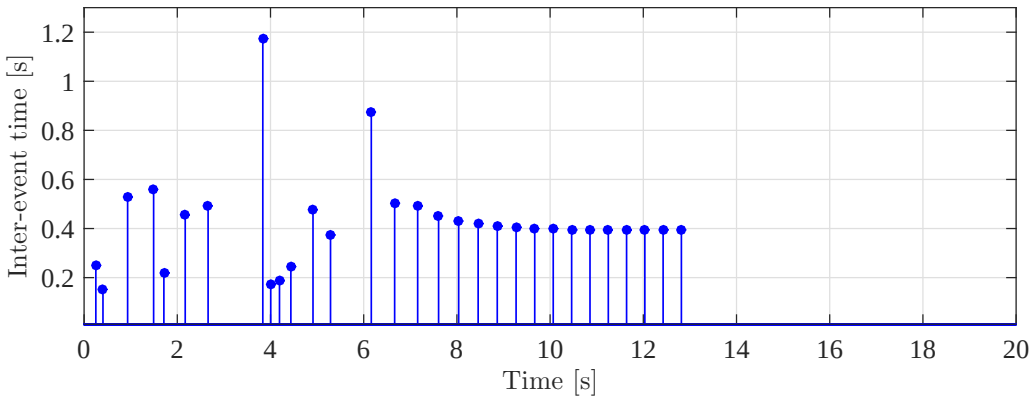

(c) The proposed ETAC scheme

Figure 2.4: Inter-event times for ETSMC [1], Switching ETAC [2] and the proposed ETAC.

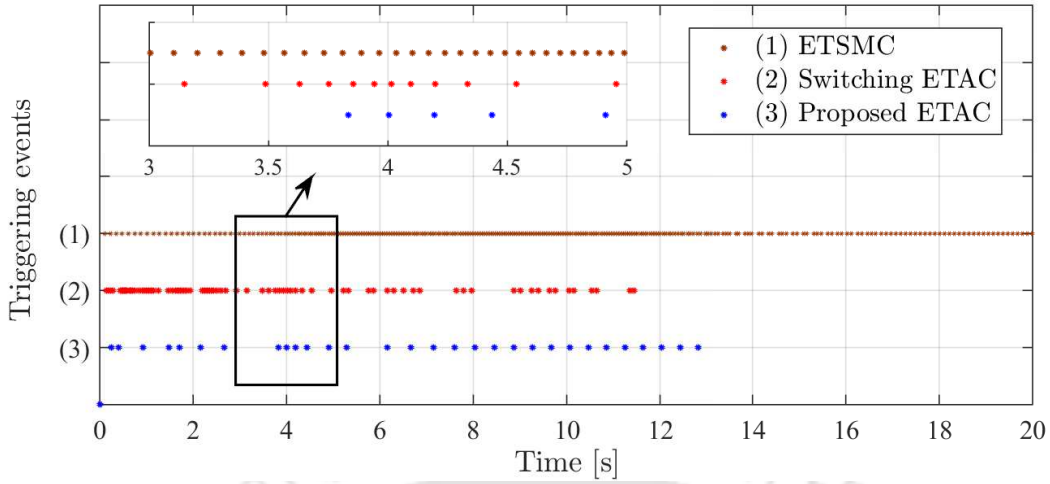

Figure 2.5: Illustration of triggering events, (1) for ETSMC scheme [1], (2) for Switching ETAC scheme [2] and (3) for the proposed ETAC scheme.

Table 2.1: Comparison of results for ETSMC [1], ETAC [2] with fixed, relative and switching thresholds, and the proposed ETAC scheme.

	ETSMC [1]	**ETAC [2]**			**Proposed Scheme**		
		Fixed	Relative	Switching	$\tau = 0$	$\tau = 0.1$	$\tau = 0.3$
#Events/transmissions	273	87	73	85	26	30	48
Stabilization error	0.034	1.190	0.032	0.110	0.035	0.047	0.011
Inter-event time (min)	0.041	0.006	0.002	0.006	0.089	0.153	0.036
Inter-event time (max)	0.148	0.362	0.922	0.910	1.641	1.174	1.154

provided in the table. It is evident that the proposed control scheme exhibits more efficiency in terms of resource utilization characterized by the number of events. It also has the ability to handle input delays.

2.5 Summary

In this chapter, an improved event-triggered adaptive control scheme has been proposed for a class of nonlinear uncertain systems subject to limited communication and input delay. Rather than simple and relative thresholds, the triggering condition has been derived on the basis of negative semi-definiteness of the derivative of Lyapunov function. Besides, an auxiliary compensation system has been introduced that effectively handled the input delays. The obtained results were compared with the existing ETSMC [2] and ETAC [1]. As compared to the ETSMC scheme, the proposed control methodology achieves invariance to matched and mismatched uncertainties not necessarily Lipschitz

without any substantial usage of control input. Based on the simulation results, the proposed triggering scheme results in significantly less number of triggering instants as compared to fixed, relative, and switching thresholds presented in [2], which is highly desirable for networked control systems. However, the event-triggered control scheme presented in this chapter was developed for single-input single-output (SISO) systems, and it considers the restrictions in the controller-to-actuator channel only. Moreover, the computational efforts could not be alleviated in this scheme as the actual control signal was always required for checking the triggering condition at each instance. In the upcoming chapter, the event-triggered mechanism will be placed on the sensor-side, for which the restrictions in the sensor-to-controller channel and computational efforts will be addressed. The results will further be extended to multiple-input multiple-output (MIMO) systems.

3

Predictor-based ETAC of a Class of Nonlinear Uncertain Systems over Sensor-to-Controller Channel

Contents

3.1 Introduction

In networked control systems (NCSs), the controller and plant are located in two different locations and communicated via network channels. Alleviating bandwidth utilization in both sensor-to-controller and controller-to-actuator channels as well as the computational effort is of great importance for network-based applications wherein the resources are generally limited. Relative to the previous chapter, the event-triggered mechanism in this chapter is placed in the sensor-to-controller channel. The previous results are also extended to a class of multi-input multi-output (MIMO) systems. On the other hand, the delays in both state and input signals are also considered in this chapter. For this purpose, a state predictor is first designed. Then, the event-triggered backstepping controller is developed based on the predicted states. It is worth mentioning that the proposed event-triggered scheme in this chapter has the ability to alleviate the computational costs in tandem with reducing the communication burden in both channels. Simulation results on a three-link cylindrical robotic arm show that the proposed control scheme successfully compensates for state and input delays and ensures a substantial saving in computational and network resources characterized by the number of required control updates and signal transmissions over the network.

The main contributions of this chapter[1] relative to existing studies are highlighted as follows. As compared to [2, 16, 34] where continuous information of system states are required from sensors to determine the control law and triggering condition, the proposed triggering scheme is placed in the sensor-to-controller channel in order to reduce the utilization of computational and channel-bandwidth resources. On the other hand, the proposed triggering condition is derived by ensuring the existence of Lyapunov function (negative definiteness of its time derivative) rather than predefined fixed or simple relative thresholds [16, 22, 96]. It also guarantees the exclusion of Zeno-behavior. Unlike [3], a predictor-based controller is designed to deal with network-induced delays, which increases the horizon of the controller.

The chapter is organized as follows. In Section 3.2, the event-triggered adaptive control scheme is presented without consideration of state and input delays, in which the problem is first formulated in Subsection 3.2.1 and then the event-triggered adaptive backstepping controller is presented in Subsection 3.2.2. In Section 3.3, the delays in both state and input signals are considered and the controller is accordingly modified to handle these delays. Simulation results on a three-link cylindrical robotic manipulator are presented in Section 3.4. The chapter is summarized in Section 3.5.

[1] This chapter is based on the article: **S. Al Issa** and I. Kar, "Adaptive control of uncertain non-linear systems over a network under input delay and limited resources," in *International Journal of Dynamics and Control*, pp. 1–8, 2021.

3.2 ETAC of Nonlinear Uncertain Systems with Limited Resources

3.2.1 Problem Formulation

In this chapter, we consider a class of multiple-input multiple-output (MIMO) nonlinear systems affected by parameter uncertainties as described below [98].

$$\begin{aligned}
\dot{x}_1 =& x_2 \\
\dot{x}_2 =& \varphi_1(x)^T\Theta + g_{11}u_1(t) + \ldots + g_{1n}u_n(t) \\
\dot{x}_3 =& x_4 \\
\dot{x}_4 =& \varphi_2(x)^T\Theta + g_{21}u_1(t) + \ldots + g_{2n}u_n(t) \\
&\vdots \\
\dot{x}_{2n-1} =& x_{2n} \\
\dot{x}_{2n} =& \varphi_n(x)^T\Theta + g_{n1}u_1(t) + \ldots + g_{nn}u_n(t)
\end{aligned} \tag{3.1}$$

where $x = [x_1,\ x_2,\ \ldots,\ x_{2n}]^T$, $u = [u_1,\ u_2,\ \ldots,\ u_n]^T$ and $y = [x_1\ x_3\ \ldots\ x_{2n-1}]$ denote the systems states, inputs and outputs, respectively. Further, $\varphi_1,\ \ldots,\ \varphi_n \in \mathbb{R}^d$ are known nonlinear functions. The vector $\Theta \in \mathbb{R}^d$ and the matrix $G = \begin{bmatrix} g_{11} & \ldots & g_{1n} \\ \vdots & & \vdots \\ g_{n1} & \ldots & g_{nn} \end{bmatrix}$ represent the unknown parameters. Let $X_1 = [x_1\ x_3 \ldots x_{2n-1}]^T \in \mathbb{R}^n$, $X_2 = [x_2\ x_4 \ldots x_{2n}]^T \in \mathbb{R}^n$, $X = [X_1\ X_2]^T$, $\Phi(X) = [\varphi_1\ \varphi_2\ \ldots\ \varphi_n] \in \mathbb{R}^{d\times n}$, then the above equations can be written as follow

$$\begin{aligned}
\dot{X}_1 &= X_2 \\
\dot{X}_2 &= \Phi(X)^T\Theta + Gu(t)
\end{aligned} \tag{3.2}$$

Assumption 2. *Each column of $\Phi(X)$ is assumed to satisfy a linear growth condition. Hence, we can write*

$$\|\Phi(U_1) - \Phi(U_2)\| \leq L\|U_1 - U_2\|, \quad \forall\ U_1, U_2 \in \mathbb{R}^{2n} \tag{3.3}$$

where L is the Lipschitz constant, and $\|\cdot\|$ represents the Euclidean norm.

Assumption 3. *The unknown parameter vector Θ and the elements of input distribution matrix G belong to known compact sets, i.e. $\exists\ \Theta^*$ and G^* such that $\|\Theta\| < \Theta^*$ and $\|G\| < G^*$.*

Remark 3. *The considered system (3.1) represents a wide class of uncertain non-linear systems. It is worth mentioning that many practical engineering applications can be*

transformed into the form (3.1). For instance, mobile robots, industrial manipulators, suspension systems, and many others [98].

To deal with the scenario of limited resources (computational and channel-bandwidth), an event-triggered (ET) mechanism is implemented in the sensor-to-controller channel as follows.

$$\begin{aligned} X^{ET}(t) &= X(t_k) \quad \forall t \in [t_k, t_{k+1}) \\ t_{k+1} &= \inf\{t |\ t > t_k, \quad J(e^{ET}, Z_1, Z_2) > 0\} \end{aligned} \tag{3.4}$$

where X and X^{ET} represent the actual and event-triggered states, respectively. $J(e^{ET}, Z_1, Z_2)$ is the triggering condition in which $e^{ET}(t) = [e_1^{ET} e_2^{ET}]^T = X(t) - X^{ET}(t)$ denotes the measurement error wherein $e_1^{ET}(t) = X_1(t) - X_1^{ET}(t)$ and $e_2^{ET}(t) = X_2(t) - X_2^{ET}(t)$. The system configuration studied in this work is similar to the one presented in Fig. 1.3b. The states of the plant will be transmitted over the network only when the designed triggering condition gets violated, and the control law is then updated according to the new received states. Thus, the channel bandwidth is efficiently utilized, and the computation burden is further reduced. It is to be noted that the controller is now designed based on the event-triggered states rather than the actual states, and it will be computed only when a new update of the states is received.

3.2.2 Event-triggered Adaptive Backstepping Control Design

In this section, the adaptive controller based on the backstepping approach [41] is designed. The event-triggered condition is derived in the last step of the design procedure by ensuring the derivative of Lyapunov function to be negative semi-definite. Let us first define the error variables as

$$\begin{aligned} Z_1 &= X_1 \\ Z_2 &= X_2 - \alpha_1 \end{aligned} \tag{3.5}$$

where α_1 is the virtual control law to be designed in the following steps. The event-triggered error variables are accordingly defined as $Z_1^{ET} = X_1^{ET}$, $Z_2^{ET} = X_2^{ET} - \alpha_1$.

Step 1: The dynamics of the first error subsystem is given as

$$\dot{Z}_1 = \dot{X}_1 = X_2 = Z_2 + \alpha_1 \tag{3.6}$$

The virtual control law α_1 is to be designed to stabilize the first subsystem (3.6). For that, a Lyapunov function candidate is chosen as $V_1 = \frac{1}{2} Z_1^T Z_1$. Differentiating V_1 with

respect time along the trajectories of the system (3.1) is

$$\dot{V}_1 = Z_1^T \dot{Z}_1 = Z_1^T (Z_2 + \alpha_1) \tag{3.7}$$

Let us choose the virtual control as

$$\alpha_1 = -C_1 Z_1^{ET} \tag{3.8}$$

where $C_1 \in \mathbb{R}^{n\times n}$ is a gain matrix with positive diagonal elements. It is to be noted that the virtual controller (3.8) is designed based on the event-triggered error variable $Z_1^{ET}(t)$ rather than actual error variable $Z_1(t)$. With (3.8), adding and subtracting $Z_1^T C_1 Z_1$ to (3.7), the time derivative of Lyapunov function (3.7) becomes

$$\dot{V}_1 = Z_1^T Z_2 - Z_1^T C_1 Z_1 + Z_1^T C_1 Z_1 - Z_1^T C_1 Z_1^{ET} \tag{3.9}$$

From (3.5) and the definition of event-triggered measurement error, we have

$$e_1^{ET}(t) = X_1(t) - X_1^{ET}(t) = Z_1(t) - Z_1^{ET}(t) \tag{3.10}$$

With (3.10), one gets

$$\begin{aligned} \dot{V}_1 &= Z_1^T Z_2 - Z_1^T C_1 Z_1 + Z_1^T C_1 e_1^{ET} \\ &\leq Z_1^T Z_2 - Z_1^T C_1 Z_1 + \|C_1\|\|Z_1\|\|e_1^{ET}\| \end{aligned} \tag{3.11}$$

It is worth mentioning that the third term which contains the measurement error will be handled in the next step while deriving the triggering condition.

Step 2: In this step, the actual control law is designed to stabilize the second error variable Z_2. Therefore, we choose a Lyapunov function candidate as

$$V_2 = V_1 + \frac{1}{2} Z_2^T Z_2 + \frac{1}{2} \tilde{\Theta}^T \Gamma_1^{-1} \tilde{\Theta} + \frac{1}{2} \text{trace}\left(\tilde{G}^T \Gamma_2^{-1} \tilde{G}\right) \tag{3.12}$$

Differentiating V_2 with respect time along the trajectories of the system (3.1) is

$$\dot{V}_2 \leq Z_1^T Z_2 - Z_1^T C_1 Z_1 + \|C_1\|\|Z_1\|\|e_1^{ET}\| + Z_2^T \dot{Z}_2 - \tilde{\Theta}^T \Gamma_1^{-1} \dot{\hat{\Theta}} - \text{trace}\left(\tilde{G}^T \Gamma_2^{-1} \dot{\hat{G}}\right) \tag{3.13}$$

where $\tilde{\Theta} = \Theta - \hat{\Theta}$ and $\tilde{G} = G - \hat{G}$ in which $\hat{\Theta}$ and $\hat{G}$ are the estimates of unknowns Θ and G, respectively. Further, $\Gamma_1 \in \mathbb{R}^{d\times d}$ and $\Gamma_2 \in \mathbb{R}^{n\times n}$ are tuning matrices associated with adaptation laws to be chosen by the designer. It is to be noted that the control signal is constant between inter-event periods and thus $\dot{\alpha}_1 = 0$. The second error dynamics $\dot{Z}_2$ is

then expressed as

$$\begin{aligned}\dot{Z}_2 = \dot{X}_2 &= \Phi^T(X)\Theta + Gu(t) \\ &= \Phi^T(X)\Theta + Gu(t) + \Phi^T(X^{ET})\Theta - \Phi^T(X^{ET})\Theta \end{aligned} \tag{3.14}$$

Now, the actual control law is chosen as

$$u = -\hat{G}^{-1}\left(C_2 Z_2^{ET} + Z_1^{ET} + \Phi^T(X^{ET})\hat{\Theta}\right), \tag{3.15}$$

where $C_2 \in \mathbb{R}^{n\times n}$ is a gain matrix with positive diagonal elements. The time derivative of Lyapunov function V_2 becomes

$$\begin{aligned}\dot{V}_2 \leq\ & Z_1^T Z_2 - Z_1^T C_1 Z_1 + \|C_1\|\|Z_1\|\|e_1^{ET}\| - Z_2^T C_2 Z_2^{ET} - Z_2^T Z_1^{ET} + Z_2^T \tilde{G} u \\ & + Z_2^T\left(\Phi^T(X) - \Phi^T(X^{ET})\right)\Theta + \tilde{\Theta}^T\left(\Phi(X^{ET})Z_2 - \Gamma_1^{-1}\dot{\hat{\Theta}}\right) - \text{trace}\left(\tilde{G}^T\Gamma_2^{-1}\dot{\hat{G}}\right)\end{aligned}$$

Adding and subtracting the term $Z_2^T C_2 Z_2 + Z_1^T Z_2$ to (3.16) and using Assumption (2), one gets

$$\begin{aligned}\dot{V}_2 \leq\ & -Z_1^T C_1 Z_1 - Z_2^T C_2 Z_2 + \|C_1\|\|Z_1\|\|e_1^{ET}\| + \|C_2\|\|Z_2\|\|e_2^{ET}\| + \|Z_2\|\|e_1^{ET}\| \\ & + L\Theta^*\|Z_2\|\|e_2^{ET}\| + \tilde{\Theta}^T\left(\Phi(X^{ET})Z_2 - \Gamma_1^{-1}\dot{\hat{\Theta}}\right) + \text{trace}\left(\tilde{G}^T(Z_2 u^T - \Gamma_2^{-1}\dot{\hat{G}})\right)\end{aligned} \tag{3.16}$$

where $e_2^{ET} = X_2 - X_2^{ET} = Z_2 - Z_2^{ET}$. As $e^{ET} = [e_1^{ET}, e_2^{ET}]^T$, then we can write $\|e_1^{ET}\| \leq \|e^{ET}\|$. Further, with the adaptation laws designed as

$$\dot{\hat{\Theta}} = \Gamma_1\Phi(X^{ET})Z_2^{ET} \quad \text{and} \quad \dot{\hat{G}} = \Gamma_2 Z_2^{ET} u^T, \tag{3.17}$$

one gets,

$$\begin{aligned}\dot{V}_2 &\leq -Z_1^T C_1 Z_1 - Z_2^T C_2 Z_2 + \|C_1\|\|Z_1\|\|e^{ET}\| + \|C_2\|\|Z_2\|\|e^{ET}\| + \|Z_2\|\|e^{ET}\| \\ &\quad + L\Theta^*\|Z_2\|\|e^{ET}\| + \tilde{\Theta}^T\Phi(X^{ET})e_2^{ET} + (e_2^{ET})^T\tilde{G}u \\ &\leq -Z_1^T C_1 Z_1 - Z_2^T C_2 Z_2 + \|C_1\|\|Z_1\|\|e^{ET}\| + \|C_2\|\|Z_2\|\|e^{ET}\| + \|Z_2\|\|e^{ET}\| \\ &\quad + L\Theta^*\|Z_2\|\|e^{ET}\| + \Theta^*\|\Phi(X^{ET})\|\|e^{ET}\| + \|\hat{\Theta}\|\|\Phi(X^{ET})\|\|e^{ET}\| \\ &\quad + G^*\|u\|\|e^{ET}\| + \|\hat{G}\|\|u\|\|e^{ET}\| \\ &\leq -Z_1^T C_1 Z_1 - Z_2^T C_2 Z_2 + \gamma\|e^{ET}\|\end{aligned} \tag{3.18}$$

where $\gamma = \|C_1\|\|Z_1\| + \|C_2\|\|Z_2\| + \|Z_2\| + L\Theta^*\|Z_2\| + G^*\|u\| + \|\hat{G}\|\|u\| + \Theta^*\|\Phi(X^{ET})\| + \|\hat{\Theta}\|\|\Phi(X^{ET})\|$ in which G^* and Θ^* are defined in Assumption (3).

Using Young inequality on the last term of (3.18), one gets

$$\dot{V}_2 \leq -Z_1^T C_1 Z_1 - Z_2^T C_2 Z_2 + \frac{\|\gamma\|^2}{2} + \frac{\|e^{ET}\|^2}{2}, \tag{3.19}$$

Adding and subtracting the term $\zeta(Z_1^T C_1 Z_1 + Z_2^T C_2 Z_2)$ from (3.19), yields

$$\dot{V}_2 \leq -(1-\zeta)(Z_1^T C_1 Z_1 + Z_2^T C_2 Z_2) - \zeta(Z_1^T C_1 Z_1 + Z_2^T C_2 Z_2) + \frac{\|\gamma\|^2}{2} + \frac{\|e^{ET}\|^2}{2}, \tag{3.20}$$

where ζ is an adjustable parameter. Now, if the triggering condition is derived by ensuring that

$$\frac{\|\gamma\|^2}{2} + \frac{\|e^{ET}\|^2}{2} \leq \zeta(Z_1^T C_1 Z_1 + Z_2^T C_2 Z_2) \tag{3.21}$$

then the derivative of Lyapunov function becomes

$$\dot{V}_2 \leq -(1-\zeta)(Z_1^T C_1 Z_1 + Z_2^T C_2 Z_2). \tag{3.22}$$

By choosing $0 < \zeta < 1$, the negative semi-definiteness of derivative of Lyapunov function can be ensured. From (3.21), the triggering function can be written as

$$J(e^{ET}, Z_1, Z_2) = \|e^{ET}\|^2 - 2\zeta\left(Z_1^T C_1 Z_1 + Z_2^T C_2 Z_2\right) + \|\gamma\|^2 \tag{3.23}$$

Remark 4. *It is worth mentioning that, in the previous analysis, the case between inter-event times $t_k < t < t_{k+1}$, $k \in \mathbb{Z}^+$ was considered. Meanwhile, for the case at event-triggering instants $t = t_k$, $k \in \mathbb{Z}^+$, the obtained results are verified as follows. It is known that the measurement error are zero at the triggering instants i.e. $e_1^{ET} = 0$ and $e_2^{ET} = 0$.*

Let us now consider the following Lyapunov function candidate:

$$V = \frac{1}{2}\left(Z_1^T Z_1 + \mathfrak{Z}_1^T \mathfrak{Z}_1\right) + \frac{1}{2}\left(Z_2^T Z_2 + \mathfrak{Z}_2^T \mathfrak{Z}_2\right) \tag{3.24}$$

where $\mathfrak{Z}_1 = Z_1^{ET}$ and $\mathfrak{Z}_2 = Z_2^{ET}$ (this notation is just utilized in this part to further simplify the expressions). The difference of V in the event-sampled instants is given as

$$\begin{aligned}\Delta V = \frac{1}{2}\big[&\left(Z_1^T(t_k)Z_1(t_k) - (Z_1^-)^T Z_1^-\right) + \left(Z_2^T(t_k)Z_2(t_k) - (Z_2^-)^T Z_2^-\right) \\ &+ \left(\mathfrak{Z}_1^T(t_k)\mathfrak{Z}_1(t_k) - (\mathfrak{Z}_1^-)^T \mathfrak{Z}_1^-\right) + \left(\mathfrak{Z}_2^T(t_k)\mathfrak{Z}_2(t_k) - (\mathfrak{Z}_2^-)^T \mathfrak{Z}_2^-\right)\big]\end{aligned} \tag{3.25}$$

We have

$$\begin{aligned}\mathfrak{Z}_1^- &= \lim_{t \to t_k^-} \mathfrak{Z}_1^-(t) = X_1(t_{k-1}) = \mathfrak{Z}_1(t_{k-1}) \\ \mathfrak{Z}_2^- &= \lim_{t \to t_k^-} \mathfrak{Z}_2^-(t) = X_2(t_{k-1}) - \alpha_1(X_1(t_{k-1})) = \mathfrak{Z}_2(t_{k-1})\end{aligned} \tag{3.26}$$

Then, we can write

$$\begin{aligned}\Delta V &= \frac{1}{2}\left[\left(Z_1^T(t_k)Z_1(t_k) - (Z_1^-)^T Z_1^-\right) + \left(Z_2^T(t_k)Z_2(t_k) - (Z_2^-)^T Z_2^-\right)\right. \\ &\left. + \left(\mathcal{Z}_1^T(t_k)\mathcal{Z}_1(t_k) - \mathcal{Z}_1^T(t_{k-1})\mathcal{Z}_1(t_{k-1})\right) + \left(\mathcal{Z}_2^T(t_k)\mathcal{Z}_2(t_k) - \mathcal{Z}_2^T(t_{k-1})\mathcal{Z}_2(t_{k-1})\right)\right] \\ &\leq -\frac{1}{2}\left((Z_1^-)^T Z_1^- + (Z_2^-)^T Z_2^-\right) + \frac{1}{2}\left[\left(\mathcal{Z}_1^T(t_k)\mathcal{Z}_1(t_k) - \mathcal{Z}_1^T(t_{k-1})\mathcal{Z}_1(t_{k-1})\right)\right. \\ &\left. + \left(\mathcal{Z}_2^T(t_k)\mathcal{Z}_2(t_k) - \mathcal{Z}_2^T(t_{k-1})\mathcal{Z}_2(t_{k-1})\right)\right] + D \end{aligned} \tag{3.27}$$

where D is the bound of $Z_1^T(t_k)Z_1(t_k) + Z_2^T(t_k)Z_2(t_k)$. As long as the following equation is established

$$\begin{aligned}&\frac{1}{2}\left((Z_1^-)^T Z_1^- + (Z_2^-)^T Z_2^-\right) + \frac{1}{2}\left[\left(\mathcal{Z}_1^T(t_k)\mathcal{Z}_1(t_k) - \mathcal{Z}_1^T(t_{k-1})\mathcal{Z}_1(t_{k-1})\right)\right. \\ &\left. + \left(\mathcal{Z}_2^T(t_k)\mathcal{Z}_2(t_k) - \mathcal{Z}_2^T(t_{k-1})\mathcal{Z}_2(t_{k-1})\right)\right] > D, \end{aligned} \tag{3.28}$$

there is $\Delta V < 0$ which confirms that Z_1, Z_2, $\mathcal{Z}_1$ and $\mathcal{Z}_2$ are bounded at the triggering instants.

Proposition 3. *Under the action of control law (3.15), adaptation laws (3.17) and the triggering condition (3.23), the system dynamics (3.1) is stable and all closed-loop signals are bounded. Furthermore, the error variables converge to the origin as $t \to \infty$. Moreover, the Zeno phenomenon is excluded in the proposed triggering scheme.*

Proof. Let us choose the Lyapunov function candidate as $V_2 = \frac{1}{2}\sum_{i=1}^{2} Z_i^T Z_i + \frac{1}{2}\tilde{\Theta}^T\Gamma_1^{-1}\tilde{\Theta} + \frac{1}{2}\text{trace}(\tilde{G}^T\Gamma_2^{-1}\tilde{G})$. Differentiating this function with respect time along the trajectories of the system (3.1) is given in (3.22). Then, if the triggering condition is designed as (3.23), the negative semi-definiteness of $\dot{V}_2$ is ensured. Hence, the overall system with the proposed triggering scheme is stable in the sense of Lyapunov and all signals are bounded.

Using Barbalat lemma [97], the convergence of the error variables can be proved. From (3.22), we have $\ddot{V}_2 = -2(1-\zeta)\left(Z_1^T C_1 \dot{Z}_1 + Z_2^T C_2 \dot{Z}_2\right)$. Since $\dot{V}_2$ is negative semi-definite, all the closed-loop trajectories are bounded. Hence, $Z_1, Z_2, \dot{Z}_1, \dot{Z}_2$ are bounded for all time. Then, we can easily conclude that $\ddot{V}_2$ is also bounded. Thus, $\dot{V}_2$ is uniformly continuous. Now, we can conclude using Barbalat lemma that $\dot{V}_2 \to 0$ as $t \to \infty$ which implies that the error variables converge to zero as $t \to \infty$.

The existence of a lower bound of inter-event time is required to complete the proof. We have

$$\begin{aligned}\dot{e}_1^{ET}(t) &= \dot{X}_1(t) - \dot{X}_1^{ET}(t) = \dot{X}_1(t) = X_2 \\ \dot{e}_2^{ET}(t) &= \dot{X}_2(t) - \dot{X}_2^{ET}(t) = \dot{X}_2(t) = \Phi^T(X)\Theta + Gu \leq \Phi_m\Theta^* + G^*\|u\| \end{aligned} \tag{3.29}$$

where Φ_m is the upper bound of Φ as it is a function of all bounded signals as already proved. Then, the overall error dynamics could be written in the form $\dot{e}^{ET} \leq A_p X + \Omega_p$ where $A_p = \begin{bmatrix} 0_{n\times n} & I_{n\times n} \\ 0_{n\times n} & 0_{n\times n} \end{bmatrix}$ and $\Omega_p = [0_{n\times 1}, \Phi_m\Theta^* + G^*\|u\|]^T$ in which $0_{n\times n} \in \mathbb{R}^{n\times n}$ and

$I_{n\times n} \in \mathbb{R}^{n\times n}$ represent the zero and identity matrices, respectively. Then, we have

$$\|\dot{e}^{ET}\| \leq \|A_p\|\|X\| + \|\Omega_p\| \tag{3.30}$$

Since $e^{ET}(t_k) = 0$ and $\frac{d}{dt}\|e^{ET}\| \leq \|\dot{e}^{ET}\|$, we get

$$\begin{aligned}\|e^{ET}\| &\leq \int_{t_k}^{t} e^{\|A_p\|(t-\tau)}\|\Omega_p\|\, d\tau \\ &= \frac{\|\Omega_p\|}{\|A_p\|}((e^{ET})^{\|A_p\|(t-\tau)} - 1), \quad \forall t \in [t_k, t_{k+1})\end{aligned} \tag{3.31}$$

Therefore,

$$t^* > \frac{1}{\|A_p\|}\ln\left(\frac{\|A_p\|}{\|\Omega_p\|}(\|e^{ET}\| + 1)\right) \geq 0 \tag{3.32}$$

Hence, the Zeno phenomenon is excluded. This completes the proof. □

3.3 Predictor-based Event-triggered Control of Nonlinear Networked Systems with State and Input Delays

In this section, the delays in both states and input signals are considered, for which a predictor-based event-triggered controller is designed based on backstepping approach [41]. First, the Lyapunov-Razumikhin theorem is introduced. Then, the stability analysis of the overall closed-loop control systems is investigated under time delays.

3.3.1 Preliminary on Lyapunov-Razumikhin Theorem

Theorem 1 (Lyapunov-Razumikhin Theorem [50]). *Let us consider the following system of the form*

$$\dot{x} = f(t, x_t), \tag{3.33}$$

where $x(t) \in \mathbb{R}^n$, $f \in \mathbb{R} \times C\big([-\varsigma, 0], \mathbb{R}^n\big)$ *and* $x_t = x(t+s)$ *for* $-\varsigma \leq s \leq 0$. *Let* W_1, W_2, $W_3 : \mathbb{R}^+ \to \mathbb{R}^+$ *be continuous functions such that* $W_1(s) > 0$, $W_2(s) > 0, W_3(s) > 0$ *for* $s > 0$ *and* $W_1(0) = W_2(0) = 0$. *Then, if there exists a continuous and differentiable function* $V : \mathbb{R} \times \mathbb{R}^{\varkappa} \to \mathbb{R}$ *such that*

- $W_1(\|x\|) \leq V(t, x) \leq W_2(\|x\|)$,
- $\dot{V}\big(t, x(t)\big) \leq -W_3(\|x\|)$,
- $V\big(t+\tau, x(t)\big) \leq pV\big(t, x(t)\big)$ *for* $\tau \in [-\varsigma, 0]$ *and* $p(s) > s$ *for* $s > 0$,

then the solution $x = 0$ *of* (3.33) *is uniformly asymptotically stable [50].*

3.3.2 Problem Formulation

Let us consider a similar class of MIMO nonlinear systems presented in Subsection 3.3.2. These systems are now considered to be controlled over communication network subject to state and input delays as

$$\begin{aligned}
\dot{x}_1^{\tau_{pc}} &= x_2^{\tau_{pc}}, \quad \dot{x}_2^{\tau_{pc}} = \varphi_1^T(X^{\tau_{pc}})\Theta + g_{11}u_1^{\tau} + \ldots + g_{1n}u_n^{\tau} \\
\dot{x}_3^{\tau_{pc}} &= x_4^{\tau_{pc}}, \quad \dot{x}_4^{\tau_{pc}} = \varphi_2^T(X^{\tau_{pc}})\Theta + g_{21}u_1^{\tau} + \ldots + g_{2n}u_n^{\tau} \\
&\vdots \\
\dot{x}_{2n-1}^{\tau_{pc}} &= x_{2n}^{\tau_{pc}}, \; \dot{x}_{2n}^{\tau_{pc}} = \varphi_n^T(X^{\tau_{pc}})\Theta + g_{n1}u_1^{\tau} + \ldots + g_{nn}u_n^{\tau}
\end{aligned} \tag{3.34}$$

where $X^{\tau_{pc}} := X(t-\tau_{pc}) = [x_1^{\tau_{pc}},\ x_2^{\tau_{pc}},\ \ldots,\ x_{2n}^{\tau_{pc}}]^T$, $u^{\tau} := u(t-\tau) = [u_1^{\tau},\ u_2^{\tau},\ \ldots,\ u_n^{\tau}]^T$ and $y = [x_1\ x_3\ \ldots\ x_{2n-1}]$ denote the delayed systems states, inputs and outputs, respectively. Here, $\tau = \tau_{pc} + \tau_{cp}$ is the round-trip time delay in which τ_{pc} and τ_{cp} are the delays in the plant-to-controller and controller-to-plant channels, respectively. Further, $\varphi_1,\ \ldots,\ \varphi_n \in \mathbb{R}^d$ are known nonlinear functions. Different from previous Section 3.2, the vector $\Theta \in \mathbb{R}^d$ and the matrix $G \in \mathbb{R}^{n\times n}$ are assumed to be known in this section to further simplify the controller and predictor design. The system equations (3.34) can be written as

$$\begin{aligned}
\dot{X}_1^{\tau_{pc}} &= X_2^{\tau_{pc}} \\
\dot{X}_2^{\tau_{pc}} &= \Phi^T(X^{\tau_{pc}})\Theta + Gu^{\tau}
\end{aligned} \tag{3.35}$$

where $X_1^{\tau_{pc}} = [x_1^{\tau_{pc}}\ x_3^{\tau_{pc}} \ldots x_{2n-1}^{\tau_{pc}}]^T \in \mathbb{R}^n$, $X_2^{\tau_{pc}} = [x_2^{\tau_{pc}}\ x_4^{\tau_{pc}} \ldots x_{2n}^{\tau_{pc}}]^T \in \mathbb{R}^n$, $\Phi(X_{pc}^{\tau}) = [\varphi_1\ \varphi_2\ \ldots\ \varphi_n] \in \mathbb{R}^{d\times n}$, and $G = \begin{bmatrix} g_{11} & \cdots & g_{1n} \\ \vdots & & \vdots \\ g_{n1} & \cdots & g_{nn} \end{bmatrix}$. Inspired by [46, 47], a state predictor is incorporated to deal with the network-induced time delays, and it designed as

$$\dot{\hat{X}}_1 = \hat{X}_2 - K_1\big(\hat{X}_1^{\tau} - X_1^{\tau_{pc}}\big) \tag{3.36}$$

$$\dot{\hat{X}}_2 = \Phi^T(\hat{X})\Theta + Gu - K_2\big(\hat{X}_2^{\tau} - X_2^{\tau_{pc}}\big) \tag{3.37}$$

where $K_1 \in \mathbb{R}^{n\times n}$ and $K_2 \in \mathbb{R}^{n\times n}$ are gain matrices with positive diagonal elements. An event-triggered scheme is also proposed here to reduce the communication and computation burden as follows

$$X_1^{ET}(t) = X_1(t_k),\ X_2^{ET}(t) = X_2(t_k), \quad | \quad \forall t \in [t_k, t_{k+1}) \tag{3.38}$$

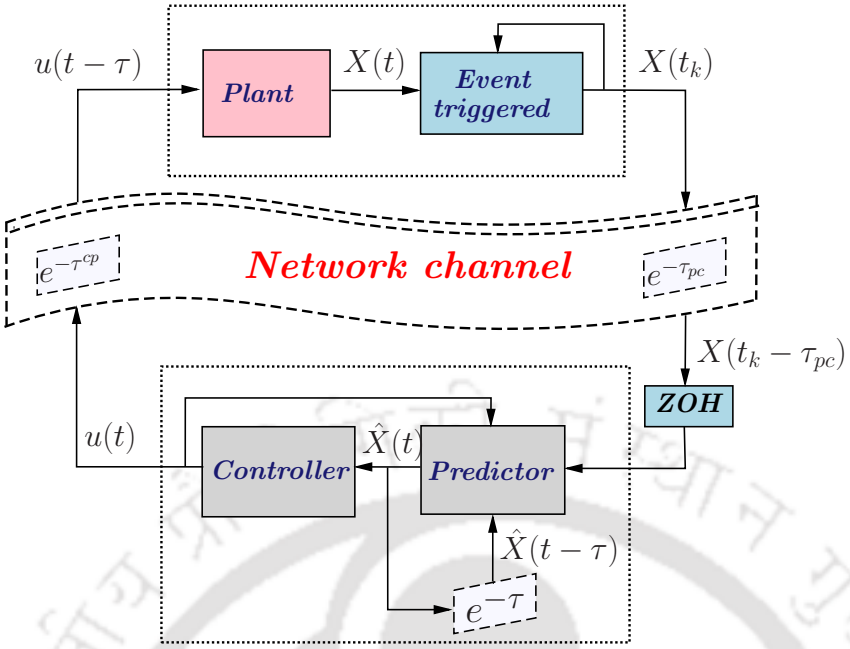

Figure 3.1: Block diagram of the system.

in which

$$t_{k+1} = \inf\{t|\ t > t_k, \quad J(e^{ET}, Z_1, Z_2) > 0\} \tag{3.39}$$

where X_1^{ET} and X_2^{ET} denote the last-received states from the plant and $J(e^{ET}, Z_1, Z_2)$ is the triggering function. Here, the measurement error is defined as $e^{ET} = [e_1^{ET} e_2^{ET}]^T$, in which $e_1^{ET}(t) = X_1(t) - X_1^{ET}(t)$ and $e_2^{ET}(t) = X_2(t) - X_2^{ET}(t)$. The block diagram of the overall system with the predictor and triggering mechanism is illustrated in Fig. 3.1.

3.3.3 State Predictor Design

In this subsection, the error dynamics of the state predictor is analyzed. The convergence of the predicted states to the actual states is also proved.
Let us define the prediction error as

$$e_{X_1} = \hat{X}_1^{\tau} - X_1^{\tau_{pc}} \tag{3.40}$$

$$e_{X_2} = \hat{X}_2^{\tau} - X_2^{\tau_{pc}} \tag{3.41}$$

Then, we have

$$\begin{aligned}\dot{e}_{X_1} &= -K_1 e_{X_1}^{\tau} + \hat{X}_2^{\tau} - X_2^{\tau_{pc}} \\ &= -K_1 e_{X_1}^{\tau} + e_{X_2} \\ &\leq -K_1 e_{X_1}^{\tau} + \|e_{X_2}\| \\ &\leq -K_1 e_{X_1}^{\tau} + \|e_X\| \end{aligned} \tag{3.42}$$

where $X = [X_1 \ X_2]^T$ and $e_X = \hat{X}^{\tau} - X^{\tau_{pc}} = [e_{X_1} \ e_{X_2}]^T$. We also have

$$\begin{aligned}\dot{e}_{X_2} &= -K_2 e_{X_2}^{\tau} + \Phi^T(\hat{X}^{\tau})\Theta + Gu^{\tau} - \Phi^T(X^{\tau_{pc}})\Theta - Gu^{\tau} \\ &= -K_2 e_{X_2}^{\tau} + (\Phi^T(\hat{X}^{\tau}) - \Phi^T(X^{\tau_{pc}}))\Theta \\ &\leq -K_2 e_{X_2}^{\tau} + \|\Phi^T(\hat{X}^{\tau}) - \Phi^T(X^{\tau_{pc}})\|\|\Theta\| \\ &\leq -K_2 e_{X_2}^{\tau} + L\|\Theta\|\|e_X\| \end{aligned} \tag{3.43}$$

The full error dynamics can be written in the following form

$$\dot{e}_X \leq -K e_X^{\tau} + \Psi \tag{3.44}$$

where

$$K = \begin{pmatrix} K_1 & 0 \\ 0 & K_2 \end{pmatrix} \quad \text{and} \quad \Psi = \begin{pmatrix} \|e_X\| \\ L\|\Theta\|\|e_X\| \end{pmatrix} \tag{3.45}$$

Proposition 4. *Let us consider the state predictor (3.36) of the system (3.34) along with the prediction error dynamics (3.44). If there exists a positive gain matrix (K) for which the following condition is satisfied*

$$\lambda_{min}(K) - \lambda_{min}(K^2)\sqrt{q}\tau - \lambda_{min}(K)\Upsilon\tau - \Upsilon > 0 \ , \tag{3.46}$$

where $\lambda_{min}(.)$ denotes the smallest eigenvalues of $(.)$ and $\Upsilon = \max\left(1, \ L\|\Theta\|\right)$ in which L is the Lipschitz constant, then the prediction error $e(t) \to 0$ as $t \to \infty$.

Proof. Let us choose the Lyapunov function candidate as $V_p = \frac{1}{2} e_X^T e_X$ whose time derivative is given as

$$\dot{V}_p = e_X^T \dot{e}_X = -e_X^T (K e_X^{\tau} - \Psi) \tag{3.47}$$

From Leibnitz's formula, we have

$$e_X^{\tau} = e_X - \int_{t-\tau}^{t} \dot{e}_X(\rho) d\rho \tag{3.48}$$

Substituting (3.48) in (3.47), one gets

$$\dot{V}_p = -e_X^T\Big(Ke_X + K^2\int_{t-\tau}^{t} e_X(\rho-\tau)d\rho + K\int_{t-\tau}^{t}\Psi(\rho)d\rho - \Psi\Big) \tag{3.49}$$

$$\leq -\lambda_{min}(K)\|e_X\|^2 - e_X^TK^2\int_{t-\tau}^{t} e_X(\rho-\tau)d\rho - e_X^TK\int_{t-\tau}^{t}\|\Psi(\rho)\|d\rho + \|e_X\|\|\Psi\| \tag{3.50}$$

The norm of the term Ψ can be written as

$$\|\Psi\| \leq \|e_X\| + L\|\Theta\|\|e_X\| \leq \Upsilon\|e_X\| \tag{3.51}$$

Using (3.51) and the relation that says $V_p\big(e_X(t+\gamma)\big) \leq qV_p\big(e_X(t)\big)$ for $-2\tau \leq \gamma \leq 0$ and $q > 1$, one gets

$$\begin{aligned}\dot{V}_p &\leq -\lambda_{min}(K)\|e_X\|^2 + \lambda_{min}(K^2)\sqrt{q}\tau\|e_X\|^2 + \lambda_{min}(K)\Upsilon\tau\|e_X\|^2 + \Upsilon\|e_X\|^2 \\ &= -\big(\lambda_{min}(K) - \lambda_{min}(K^2)\sqrt{q}\tau - \lambda_{min}(K)\Upsilon\tau - \Upsilon\big)\|e_X\|^2\end{aligned} \tag{3.52}$$

Herein, if the condition (3.46) is satisfied, $\dot{V}_p$ becomes negative definite which implies that $V_p \to 0$ as $t \to \infty$. As a result, we can conclude that the prediction error $e(t) \to 0$ as $t \to \infty$. This completes the proof. □

3.3.4 Predictor-based Event-triggered Control Design

The predictor-based event-triggered controller is now designed based on the predicted states. The event-triggered condition is consequently derived in the last step of the design procedure by ensuring the negative semi-definiteness of the derivative of Lyapunov function. Let us now redefine the error variables based on the predicted states as

$$\begin{aligned}Z_1 &= \hat{X}_1 \\ Z_2 &= \hat{X}_2 - \alpha_1\end{aligned} \tag{3.53}$$

where $\hat{X}_1$ and $\hat{X}_2$ are the predicted states, α_1 is the virtual control law to be designed in the following steps. The event-triggered error variables are accordingly defined as $Z_1^{ET} = \hat{X}_1^{ET}$, $Z_2^{ET} = \hat{X}_2^{ET} - \alpha_1$.

Step 1: The dynamics of the first error subsystem is given as

$$\dot{Z}_1 = \dot{\hat{X}}_1 = \hat{X}_2 = Z_2 + \alpha_1 \tag{3.54}$$

Similar to Section 3.2.2, the virtual control is chosen as

$$\alpha_1 = -C_1Z_1^{ET} \tag{3.55}$$

where $C_1 \in \mathbb{R}^{n\times n}$ is a gain matrix with positive diagonal elements. However, it is to be noted here that, unlike Section 3.2.2, the virtual control law (3.55) is designed based on the predicted states. Differentiating $V_1 = \frac{1}{2}Z_1^T Z_1$ with respect time along the trajectories of the system (3.34) is

$$\dot{V}_1 \leq Z_1^T Z_2 - Z_1^T C_1 Z_1 + \|C_1\|\|Z_1\|\|e_1^{ET}\| \tag{3.56}$$

Step 2: In this step, the actual control law is designed to stabilize the second error variable Z_2. The Lyapunov function candidate is therefore chosen as $V_2 = V_1 + \frac{1}{2}Z_2^T Z_2$. Differentiating V_2 with respect time is

$$\dot{V}_2 \leq Z_1^T Z_2 - Z_1^T C_1 Z_1 + \|C_1\|\|Z_1\|\|e_1^{ET}\| + Z_2^T \dot{Z}_2 \tag{3.57}$$

It is to be noted that the control signal is constant between inter-event periods. Thus $\dot{\alpha}_1 = 0$. The second error dynamics $\dot{Z}_2$ is then expressed as

$$\dot{Z}_2 = \Phi^T(\hat{X})\Theta + \Phi^T(\hat{X}^{ET})\Theta - \Phi^T(\hat{X}^{ET})\Theta + Gu \tag{3.58}$$

Now, the actual control law is chosen as

$$u = -G^{-1}(C_2 Z_2^{ET} + Z_1^{ET} + \Phi^T(\hat{X}^{ET})\Theta), \tag{3.59}$$

where $C_2 \in \mathbb{R}^{n\times n}$ is a gain matrix with positive diagonal elements. The time derivative of Lyapunov function V_2 becomes

$$\begin{aligned}\dot{V}_2 \leq\ & Z_1^T Z_2 - Z_1^T C_1 Z_1 + \|C_1\|\|Z_1\|\|e_1^{ET}\| - Z_2^T C_2 Z_2^{ET} - Z_2^T Z_1^{ET} \\ & + Z_2^T \left(\Phi^T(\hat{X}) - \Phi^T(\hat{X}^{ET})\right)\Theta\end{aligned} \tag{3.60}$$

Adding and subtracting the term $Z_2^T C_2 Z_2 + Z_1^T Z_2$ to (3.60) and using Assumption (2), one gets

$$\begin{aligned}\dot{V}_2 &\leq -Z_1^T C_1 Z_1 - Z_2^T C_2 Z_2 + \|C_1\|\|Z_1\|\|e_1^{ET}\| + \|C_2\|\|Z_2\|\|e_2^{ET}\| + \|Z_2\|\|e_1^{ET}\| + L\Theta\|Z_2\|\|e_2^{ET}\| \\ &\leq -Z_1^T C_1 Z_1 - Z_2^T C_2 Z_2 + \|C_1\|\|Z_1\|\|e^{ET}\| + \|C_2\|\|Z_2\|\|e^{ET}\| + \|Z_2\|\|e^{ET}\| + L\Theta\|Z_2\|\|e^{ET}\| \\ &\leq -Z_1^T C_1 Z_1 - Z_2^T C_2 Z_2 + \gamma\|e^{ET}\|\end{aligned} \tag{3.61}$$

where $e^{ET} = [e_1^{ET}, e_2^{ET}]^T$ and $\gamma = \|C_1\|\|Z_1\| + \|C_2\|\|Z_2\| + \|Z_2\| + L\Theta\|Z_2\|$.

Based on the results obtained in Subsection 3.2.2, the triggering condition can be directly designed as

$$J(e^{ET}, Z_1, Z_2) = \|e^{ET}\|^2 - 2\zeta\left(Z_1^T C_1 Z_1 + Z_2^T C_2 Z_2\right) + \|\gamma\|^2 \tag{3.62}$$

where ζ is an adjustable parameter. Accordingly, the derivative of Lyapunov function becomes

$$\dot{V}_2 \leq -(1-\zeta)(Z_1^T C_1 Z_1 + Z_2^T C_2 Z_2). \tag{3.63}$$

By choosing $0 < \zeta < 1$, the negative semi-definiteness of derivative of Lyapunov function can be ensured. It is worth mentioning that the triggering condition was directly obtained from the derivative of Lyapunov function. Specifically, the event is triggered only when $\dot{V}_2 \geq 0$. In this case, the states are updated over the network and the control input is consequently computed and updated based on the actual system states. In other cases, the old control input is held constant as the system stability is maintained.

3.4 Simulation Results

In this section, we consider the stabilization problem of a three-link cylindrical robotic arm controlled over a network [3]. The dynamics of this system with the state and input delays can be modeled as

$$\begin{aligned}
\dot{x}_1^{\tau_{pc}} &= x_4^{\tau_{pc}}, \\
\dot{x}_2^{\tau_{pc}} &= x_5^{\tau_{pc}}, \\
\dot{x}_3^{\tau_{pc}} &= x_6^{\tau_{pc}}, \\
\dot{x}_4^{\tau_{pc}} &= \frac{2}{J} m_2 x_3^{\tau_{pc}} x_4^{\tau_{pc}} x_6^{\tau_{pc}} + \frac{1}{J} u_1^{\tau}, \\
\dot{x}_5^{\tau_{pc}} &= g x_3^{\tau_{pc}} + \frac{1}{m_1 + m_2} u_2^{\tau}, \\
\dot{x}_6^{\tau_{pc}} &= -m_2 x_3^{\tau_{pc}} x_4^{\tau_{pc}} + \frac{1}{m_2} u_3^{\tau}.
\end{aligned} \tag{3.64}$$

The state predictor is first designed as

$$\dot{\hat{X}}_1 = \hat{X}_2 - K_1\big(\hat{X}_1^{\tau} - X_1^{\tau_{pc}}\big) \tag{3.65}$$

$$\dot{\hat{X}}_2 = \Phi^T(\hat{X})\Theta + Gu - K_2\big(\hat{X}_2^{\tau} - X_2^{\tau_{pc}}\big) \tag{3.66}$$

Accordingly, the virtual and actual control laws are designed as

$$\alpha_1 = -C_1 \hat{Z}_1 \tag{3.67}$$

$$u = -G^{-1}(C_2 \hat{Z}_2 + \hat{Z}_1 + \Phi^T(\hat{X})\Theta), \tag{3.68}$$

where $\hat{X}_1 = [\hat{x}_1, \hat{x}_2, \hat{x}_3]^T$, $\hat{X}_2 = [\hat{x}_4, \hat{x}_5, \hat{x}_6]^T$, $Z_1 = \hat{X}_1$, $Z_2 = \hat{X}_2 - \alpha_1$,
$G = diag(\frac{1}{J}, \frac{1}{m_1+m_2}, \frac{1}{m_2})$, $\Phi = diag(\hat{x}_3\hat{x}_4\hat{x}_6, \hat{x}_3, -\hat{x}_3\hat{x}_4)$ and $\Theta = [\frac{2}{J}m_2, g, m_2]^T$.

For the fair of comparison, the physical parameters and initial values are chosen sim-

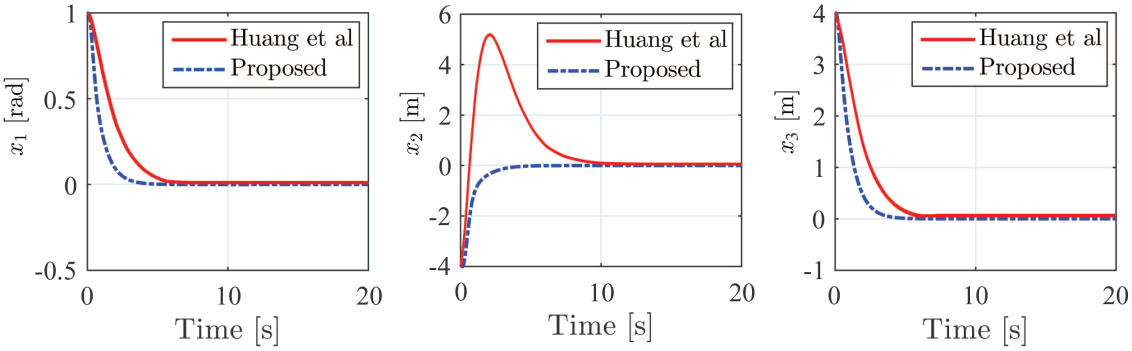

Figure 3.2: System responses under the proposed control scheme and Huang *et al.* [3]

.

ilar to Huang *et al.* [3] where $m_1 = 3$, $m_2 = 1$ and $J = 5$. The initial states are also given as $X_1 = [1, -4, 4]^T$ and $X_2 = [0, 0, 0]^T$. The control parameters are chosen as $C_1 = diag(4, 4, 4)$, $C_2 = diag(1, 1, 1)$, $K_1 = diag(2, 2, 2)$ and $K_2 = diag(2, 2, 2)$. Other parameters are given as $\zeta = 10^{-3}$ and $L = 1$.

To show the effectiveness of the proposed control scheme in handling the effects of both unknown parameters and network-induced delays, two simulations are conducted under two different scenarios in which these effects are mutually deactivated. In the first case, the scenario of unknown parameters in the system model is considered while assuming ideal communications ($\tau = 0$). The trajectories of system outputs under the proposed control scheme and the one presented by Huang *et al.* [3] are shown in Fig. 3.2. It is clear that the proposed control scheme achieves better performance in terms of transient response and convergence rate. On the other hand, the network-induced delays are considered in the second scenario assuming known parameters. The trajectories of system outputs for different values of τ is depicted in Fig. 3.3. Here, τ represents the accumulative network-induced delays in both network channels (plant-to-controller and controller-to-plant) in which $\tau = \tau_{pc} + \tau_{cp}$. It can be observed from the obtained results that the designed predictor is capable of compensating for induced delays and achieve accurate tracking. However, as the accumulative delay increases, the system performance degrades and it may become unstable for larger induced delays. It is worth mentioning that the induced delays were not considered in [3], for which the system becomes unstable even for small delays in the communication channels. The event-triggered control inputs and the triggering events are illustrated in Fig. 3.4 and Fig. 3.5, respectively. In Fig. 3.5, the time instants when the triggering rule is violated are represented by dots. At these instants, actual system states are required to be transmitted over the network, and the control inputs must be updated accordingly in order to guarantee system stability and performance. The density of triggering dots in this figure indicates how much

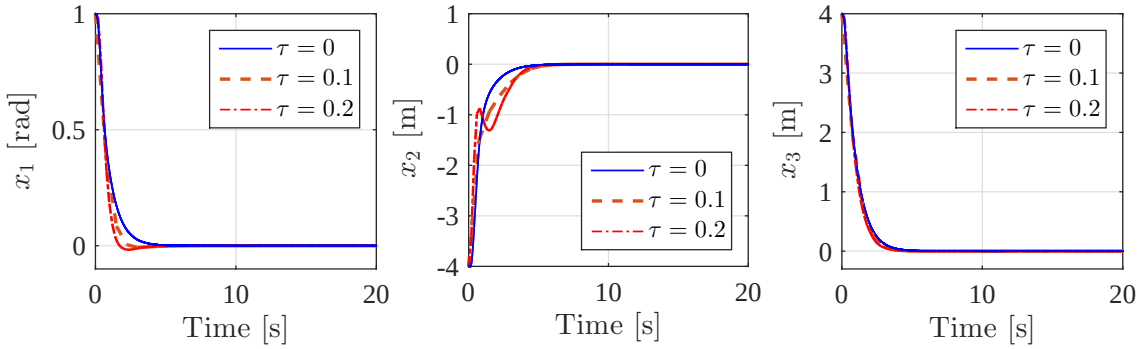

Figure 3.3: System responses under the proposed control scheme for different values of delays.

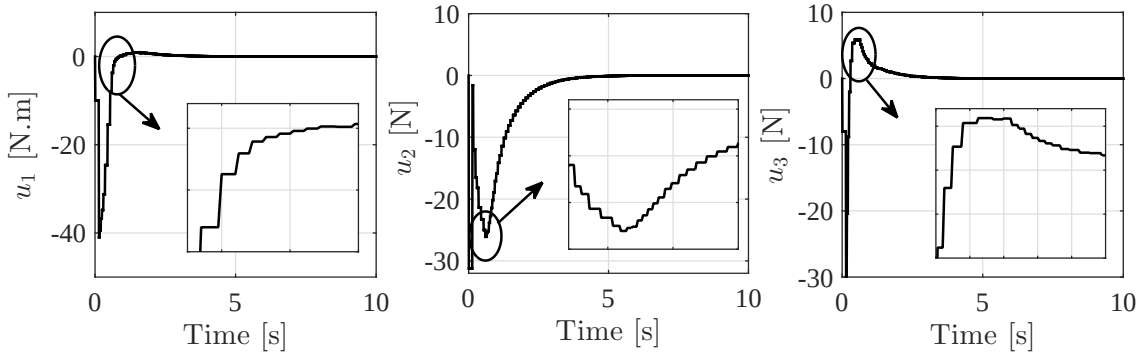

Figure 3.4: The event-triggered control signals for $\tau = 0.1$ [s].

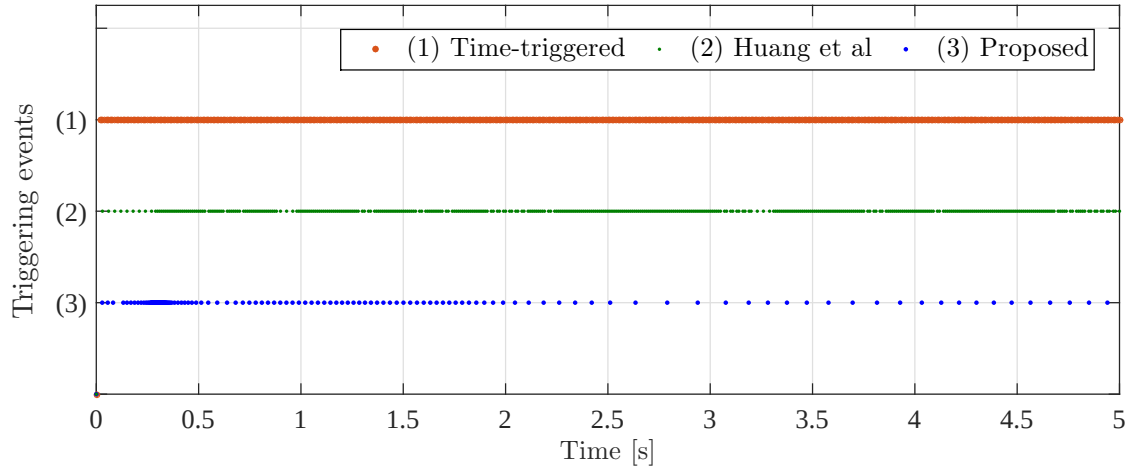

Figure 3.5: Illustration of triggering events.

the resources are used. It is evident from Fig. 3.5 that the proposed scheme leads to a significantly less number of triggering events as compared to Huang *et al.* [3]. Hence, more saving in channel bandwidth and computational resources. Precisely, 1527 control updates/transmissions over the network are observed under the event-triggered control scheme presented in [3]. However, this number is significantly reduced to 128 events under the proposed triggering condition. In comparison with traditional time-triggered implementation, 25000 event were occurred in 25 [s] of simulation run under sampling time $dt = 0.001$ [s]. This is obvious as the control signal and system states are continuously updated/transmitted over the network every dt. It is to be noted that the inter-event time in the time-triggered paradigm is fixed and equals the sampling time. This is heuristically selected based on the worst-case scenario such that the system stability and performance are always maintained. On the contrary, the sampling time in event-triggered control is not constant. Instead, it is dynamic and continuously changing according to the system's needs while maintaining the stability of the overall closed-loop system. Under the proposed control scheme, the minimum, maximum, and average inter-event time between two consecutive triggering events are calculated and found to be 0.02, 1.12, and 0.15 [s], respectively. This dynamic sampling is undoubtedly more efficient and yields superior saving in both computational and limited-bandwidth resources, which is highly desirable for network-based applications.

3.5 Summary

In this chapter, a predictor-based event-triggered adaptive control scheme has been developed for a class of nonlinear MIMO systems subject to state and input delays. The event-triggered mechanism was placed in the plant-to-controller channel and, therefore, it has the ability to alleviate the computational costs and reduce the communication burden in both channels. The triggering condition was designed by ensuring the negative semi-definiteness of the derivative of Lyapunov function. On the other hand, the delays in both states and input signals have been investigated, for which a state predictor was first designed, and the controller was then designed based on the predicted states. The convergence of the predicted states was proved using Lyapunov-Razumikhin theorem. The simulation results show that the proposed control scheme successfully compensates for state and input delays. It also leads to a significantly less number of triggering events as compared to other existing control schemes.

4

ETAC of a Mobile Robot over a Network Subject to Limited Resources

Contents

4.1 Introduction

Although inserting the network in the feedback control loop opens an arena with a multitude of applications of modern control techniques, the issue of limited bandwidth is a fundamental problem that inhibits their applicability to network-based applications. Hence, this design issue should be considered in the control design and subsequently resolved at the design phase to meet the essential requirements of such applications. In this chapter[1], a nonholonomic mobile robot controlled over a communication channel subject to limited resources is considered. The kinematic and dynamic models of the robot are first presented. Then the theoretical results obtained in Chapter 2 and Chapter 3 are applied on the overall mathematical model of the robot. Practically speaking, reducing the need for communications (decrement in the frequency of transmitting and receiving information between the remote controller and the robot) is highly desirable. Therefore, the main design concern in this work is to respect the limitation on the channel bandwidth while achieving a robust acceptable trajectory tracking by the robot. For clarity, the event-triggered control scheme is investigated in this chapter without considering the input and state delays. These network-induced delays will be considered in Chapter 5 along with the experimental validations on a real mobile robot (PatrolBot).

The main results of this chapter are divided into two parts. In the first part, the communication network is considered only in the controller-to-robot channel. The control commands are transmitted over a wireless channel with limited bandwidth. However, the robot states are assumed to be captured using a camera that is directly connected to the controller via a dedicated wired connection. A similar framework was considered in [4, 51]. On the other hand, the communication network is considered in both channels in the second part of this chapter, which is a more practical scenario. Here, the states of the robot are directly received from the robot over the wireless channel without using the vision system. Two-fold design objectives of tracking performance improvement in tandem with the minimum usage of resources are accomplished through the proposed event-triggered adaptive controller.

The contributions of this chapter are summarized as follows. The dynamic model of the robot assuming unknown system parameters is considered, for which an adaptive backstepping controller is first designed to compensate for the uncertainties in the model parameters. Then, a Lyapunov-based triggering condition is proposed and incorporated to reduce the communication burden in the controller-to-robot channel. As compared to

[1]This chapter is based on the articles: 1. **S. Al Issa**, M. Sharma, and I. Kar, "Event-triggered backstepping control scheme for networked mobile robots," in *Proceedings of the Advances in Robotics (AIR-2019)*, Chennai, India, 2019. 2. **S. Al Issa**, A. Chakravarty, and I. Kar, "Adaptive control of a networked mobile robot subject to parameter uncertainties and limited communications," in *2019 Indian Control Conference (ICC)*, Hyderabad, India, 2019.

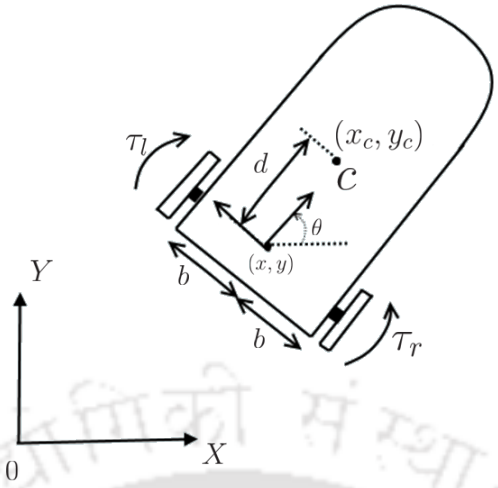

Figure 4.1: The schematic of wheeled mobile robot.

non-adaptive learning based control strategies, the trajectory tracking results obtained using the proposed control are indeed encouraging and testifies the performance improvement feature of adaptive control. Further, the mobile robot under the action of the proposed controller exhibits substantially low usage of network resources characterized by a significantly reduced number of triggering instants. To the best of our knowledge, the scenario of trajectory tracking control of mobile robots over a band-limited communication channel, under Lyapunov-based triggering framework and assuming no knowledge of dynamic model parameters, is yet to be addressed in the literature.

The remainder of this chapter is organized as follows. The mathematical model of the mobile robot is presented in Section 4.2. After that, the proposed event-triggered control scheme is discussed for the controller-to-robot and robot-to-controller channels in Section 4.3 and Section 4.4, respectively. Simulation results for tracking a circular trajectory are presented in Section 4.5. Section 4.6 gives a brief summary of the chapter.

4.2 Kinematic and Dynamic Models of Nonholonomic Mobile Robots

In this section, the mathematical model of a nonholonomic mobile robot is discussed. The motion of the robot shown in Fig. 4.1 can be described as

$$\dot{x} = v\cos\theta, \quad \dot{y} = v\sin\theta, \quad \dot{\theta} = w, \tag{4.1}$$

where x and y denote the position of the robot and θ represents its orientation. Further, v and w are linear and angular velocities of the robot, respectively. These equations can

be directly written in a matrix form as

$$\dot{q} = S(q)\nu \tag{4.2}$$

where $q = \begin{bmatrix} x & y & \theta \end{bmatrix}^T$, $\nu = \begin{bmatrix} v & w \end{bmatrix}^T$ and

$$S(q) = \begin{bmatrix} \cos\theta & 0 \\ \sin\theta & 0 \\ 0 & 1 \end{bmatrix}. \tag{4.3}$$

This represents the kinematic model of the mobile robot. On the other hand, the dynamic model can be derived based on the Euler-Lagrange method as follows.

$$\frac{d}{dt}\left(\frac{\partial L}{\partial \dot{q}}\right) - \frac{\partial L}{\partial q} = F_q, \tag{4.4}$$

where $F_q = \begin{bmatrix} F_x & F_y & \tau \end{bmatrix}^T$ denotes the generalized force/torque vector, in which

$$F_x = \frac{1}{r}\tau_r \cos\theta + \frac{1}{r}\tau_l \cos\theta + \lambda \sin\theta, \tag{4.5}$$

$$F_y = \frac{1}{r}\tau_r \sin\theta + \frac{1}{r}\tau_l \sin\theta - \lambda \cos\theta, \tag{4.6}$$

$$\tau = \frac{1}{r}\tau_r b - \frac{1}{r}\tau_l b, \tag{4.7}$$

where r and b represents the radius of wheels and distance between wheel and origin of body frame, respectively, τ_r and τ_l are the torques on right and left wheels. Further, λ denotes Lagrangian multiplier due to nonholonomic constraints. The Lagrange L can be written as

$$L = \frac{1}{2}m\left(\dot{x}_c^2 + \dot{y}_c^2\right) + \frac{1}{2}I\dot{\theta}^2, \tag{4.8}$$

where $x_c = x + d\cos\theta$ and $y_c = y + d\sin\theta$, in which d denotes the distance between center of mass and origin of body frame, m and I represent the robot mass and moment of inertia, respectively. Putting (4.5–4.8) in (4.4), a conventional dynamic model of mobile robots could be directly obtained and written as

$$M(q)\ \ddot{q} + C_c(q,\dot{q})\ \dot{q} + F_g(q) = E(q)\ u - A_k^T(q)\ \lambda\ , \tag{4.9}$$

where $M(q)$ represents the inertia matrix and $C_c(q,\dot{q})$ denotes the centripetal and Coriolis matrix. Moreover, $F_g(q)$ and $E(q)$ represent the gravitational forces and input transformation matrix, respectively. Further, $A_k(q)$ is the kinematic constraint vector. Here, the control input $u = \begin{bmatrix} \tau_r & \tau_l \end{bmatrix}^T$ is represented by the torques on the right and left wheels of

the robot. These matrices and vectors are given as

$$M := \begin{bmatrix} m & 0 & -dm\sin\theta \\ 0 & m & dm\cos\theta \\ -dm\sin\theta & dm\cos\theta & d^2m + I \end{bmatrix},$$

$$C_c := \begin{bmatrix} 0 & 0 & -dm\dot{\theta}\cos\theta \\ 0 & 0 & -dm\dot{\theta}\sin\theta \\ 0 & 0 & 0 \end{bmatrix},$$

$$E := \frac{1}{r}\begin{bmatrix} cos\theta & \cos\theta \\ sin\theta & \sin\theta \\ b & -b \end{bmatrix} \quad \text{and} \quad A_k^T := \begin{bmatrix} -\sin\theta \\ \cos\theta \\ 0 \end{bmatrix} \tag{4.10}$$

Note that $F_g(q) = 0$ for a nonholonomic planar mobile robot. From kinematic equation (4.1), we have $\ddot{q} = S\dot{\nu} + \dot{S}\nu$. Further, Equation (4.9) can be converted to unconstrained form by pre-multiplication both side with S^T, wherein $S^T A_k^T = 0$. Then, the dynamic model of the mobile robot can be directly obtained as

$$\dot{\nu} = -\bar{M}^{-1}\bar{C}\nu + \bar{M}^{-1}\bar{E}u(t)\ , \tag{4.11}$$

where $\bar{M} = S^T M S, \bar{C} = S^T(M\dot{S} + C_c S)$ and $\bar{E} = S^T E$. Substituting the expressions of $M(\cdot)$, $C_c(\cdot)$ and $E(\cdot)$ matrices, the dynamics of robot model can further be simplified and written in the following form

$$\dot{\nu} = \varphi(\nu)\Theta + Gu(t)\ , \tag{4.12}$$

where

$$\varphi(\nu) := \begin{bmatrix} w^2 & 0 \\ 0 & -vw \end{bmatrix}, \quad \Theta := \begin{bmatrix} d \\ \frac{md}{md^2+I} \end{bmatrix} \text{ and } G := \begin{bmatrix} \frac{1}{mr} & \frac{1}{mr} \\ \frac{b}{d^2m+I} & \frac{-b}{d^2m+I} \end{bmatrix} \tag{4.13}$$

This represents the dynamic model of the mobile robot, in which Θ and G denote the unknown parameters.

4.3 ETAC of a Mobile Robot over Controller-to-Robot Channel

In this section, the event-triggered mechanism is proposed in the controller-to-robot channel to reduce the communication burden, with no restrictions on the robot-to-controller channel. In such case, the actual states are assumed to be continuously available while designing the controller and triggering condition.

4.3.1 Problem Formulation

Let us consider a nonholonomic mobile robot, affected by parameter uncertainties and controlled over a communication network. From (4.2) and (4.12), the overall mathematical model of the mobile robot can be written in the following form (Refer to Section 4.2 for more details).

$$\begin{aligned} \dot{q} &= S\nu \ , \\ \dot{\nu} &= \varphi(\nu)\Theta + Gu^{ET}(t) \end{aligned} \tag{4.14}$$

To reduce the communication burden in the controller-to-robot channel, an event-triggered mechanism is introduced. Thus, the robot is now actuated by the event-triggered control signal u^{ET} rather than actual time-triggered signal u. The triggering mechanism is defined as

$$\begin{aligned} u^{ET}(t) &= u(t_k), \ \forall \ t \in [t_k, t_{k+1}) \\ t_{k+1} &= \inf \left\{ \ t \mid t > t_k \ , \quad J(e^{ET}, Z_1, Z_2) > 0 \right\} , \end{aligned} \tag{4.15}$$

where $J(e^{ET}, Z_1, Z_2)$ is the triggering condition to be designed later, in which $e^{ET} = u - u^{ET}$ denotes the measurement error.

The configuration of the event-triggered framework considered in this section is similar to Fig 1.3a. Referring to the kinematic and dynamic descriptions of the mobile robot (4.14), the control problem is stated as follows. Design an event-triggered adaptive tracking controller that guarantees boundedness of the closed-loop signals and ensures faithful reference trajectory tracking with a significant reduction in communication burden.

4.3.2 Control Design

The procedural steps of the backstepping approach that is utilized to arrive at the final control law are discussed in this section. Let us define the error variables as

$$Z_1 = q - q_r \ , \tag{4.16}$$

$$Z_2 = \nu - \alpha_1 \ , \tag{4.17}$$

where $q_r = [x_{ref} \quad y_{ref} \quad \theta_{ref}]^T$ represents the position and orientation of the reference trajectory, and α_1 is the virtual control law to stabilize the first subsystem encountered in the backstepping design procedure.

Step 1:

The derivative of the first error variable Z_1 is given as

$$\dot{Z}_1 = \dot{q} - \dot{q}_r = S\nu - \dot{q}_r = S(Z_2 + \alpha_1) - \dot{q}_r \tag{4.18}$$

The above differential equation forms the first error subsystem to be stabilized by a suitably designed virtual control α_1. Now, let us choose a Lyapunov function candidate as $V_1 = \frac{1}{2}Z_1^T Z_1$. Differentiating V_1 with respect time along the trajectories of the system (4.14) is

$$\dot{V}_1 = Z_1^T \dot{Z}_1 = Z_1^T (SZ_2 + S\alpha_1 - \dot{q}_r) \tag{4.19}$$

Let us design α_1 such that

$$S\alpha_1 = -C_1 Z_1 + \dot{q}_r \tag{4.20}$$

where $C_1 \in \mathbb{R}^{3\times 3}$ is a gain matrix with positive diagonal elements. Since $S^T S = I_2$ where $I_2 \in R^{2\times 2}$ is identity matrix, one gets

$$\alpha_1 = S^T S\alpha_1 = -S^T (C_1 Z_1 - \dot{q}_r) \ . \tag{4.21}$$

Now, the time derivative of Lyapunov function becomes

$$\dot{V}_1 = -Z_1^T C_1 Z_1 + Z_1^T S Z_2 \tag{4.22}$$

Herein if $Z_2 = 0$, $\dot{V}_1$ is negative definite and convergence of Z_1 is ensured.

Step 2:

Let us now choose Lyapunov function candidate as

$$V_2 = V_1 + \frac{1}{2}Z_2^T Z_2 + \frac{1}{2}\tilde{\Theta}^T \Gamma_1^{-1} \tilde{\Theta} + \text{trace}\left(\frac{1}{2}\tilde{G}^T \Gamma_2^{-1} \tilde{G}\right). \tag{4.23}$$

where $\tilde{\Theta} = \Theta - \hat{\Theta}$ and $\tilde{G} = G - \hat{G}$ are the estimate errors. Further, Γ_1 and Γ_2 are tuning matrices associated with adaptation laws to be chosen by designer. Differentiating V_2 with respect time along the trajectories of the system (4.14) is

$$\dot{V}_2 = \dot{V}_1 + Z_2^T \dot{Z}_2 - \tilde{\Theta}^T \Gamma_1^{-1} \dot{\hat{\Theta}} - \text{trace}\left(\tilde{G}^T \Gamma_2^{-1} \dot{\hat{G}}\right), \tag{4.24}$$

where $\dot{Z}_2$ is now expressed as

$$\begin{aligned} \dot{Z}_2 = \dot{\nu} - \dot{\alpha}_1 &= \varphi\Theta - \dot{\alpha}_1 + Gu^{ET} \\ &= \varphi\Theta - \dot{\alpha}_1 + \tilde{G}u^{ET} + \hat{G}u^{ET} = \varphi\Theta - \dot{\alpha}_1 + \tilde{G}u^{ET} + \hat{G}u - \hat{G}e^{ET} \end{aligned} \tag{4.25}$$

where $e^{ET} = u - u^{ET}$ and

$$\dot{\alpha}_1 = -\dot{S}^T(C_1 Z_1 - \dot{q}_r) - S^T(C_1 \dot{Z}_1 - \ddot{q}_r) = -\dot{S}^T(C_1 Z_1 - \dot{q}_r) - S^T\left(C_1(S\nu - \dot{q}_r) - \ddot{q}_r\right) \tag{4.26}$$

Substituting (4.22) and (4.25) in (4.24), the following equality is obtained.

$$\begin{aligned}\dot{V}_2 = &-Z_1^T C_1 Z_1 + Z_1^T S Z_2 + Z_2^T\left(\varphi\Theta - \dot{\alpha}_1 + \tilde{G}u^{ET} + \hat{G}u - \hat{G}e^{ET}\right)\\ &- \tilde{\Theta}^T\Gamma_1^{-1}\dot{\hat{\Theta}} - \text{trace}\left(\tilde{G}^T\Gamma_2^{-1}\dot{\hat{G}}\right)\end{aligned} \tag{4.27}$$

Let us design the control law as

$$u = -\hat{G}^{-1}\left(C_2 Z_2 - \dot{\alpha}_1 + S^T Z_1 + \varphi\hat{\Theta}\right) \ , \tag{4.28}$$

where $C_2 \in \mathbb{R}^{2\times 2}$ is a gain matrix with positive diagonal elements. Substituting (4.28) in (4.27), the time derivative of Lyapunov function V_2 becomes

$$\begin{aligned}\dot{V}_2 &= -Z_1^T C_1 Z_1 - Z_2^T C_2 Z_2 + Z_2^T\varphi\tilde{\Theta} - \tilde{\Theta}^T\Gamma^{-1}\dot{\hat{\Theta}} + Z_2^T\tilde{G}u^{ET} - \text{trace}\left(\tilde{G}^T\Gamma_2^{-1}\dot{\hat{G}}\right) - Z_2^T\hat{G}e^{ET}\\ &= -Z_1^T C_1 Z_1 - Z_2^T C_2 Z_2 - Z_2^T\hat{G}e^{ET} + \tilde{\Theta}^T\left(\varphi^T Z_2 - \Gamma_1^{-1}\dot{\hat{\Theta}}\right)\\ &\quad - \text{trace}\left(-\tilde{G}^T Z_2(u^{ET})^T + \tilde{G}^T\Gamma_2^{-1}\dot{\hat{G}}\right)\end{aligned} \tag{4.29}$$

Finally, by choosing the adaptive laws as

$$\dot{\hat{\Theta}} = \Gamma_1\varphi^T Z_2 \ , \quad \dot{\hat{G}} = \Gamma_2 Z_2(u^{ET})^T \tag{4.30}$$

one obtains

$$\begin{aligned}\dot{V}_2 &= -Z_1^T C_1 Z_1 - Z_2^T C_2 Z_2 - Z_2^T\hat{G}e^{ET}\\ &\leq -Z_1^T C_1 Z_1 - Z_2^T C_2 Z_2 + \frac{\left\|Z_2^T\hat{G}\right\|^2}{2} + \frac{\left\|e^{ET}\right\|^2}{2}\end{aligned} \tag{4.31}$$

Based on the results obtained in Subsection 3.2.2, the triggering condition $J(e^{ET}, Z_1, Z_2)$ defined in (4.15) can now be directly obtained as

$$J(e^{ET}, Z_1, Z_2) = \left\|e^{ET}\right\|^2 - 2\zeta\left(Z_1^T C_1 Z_1 + Z_2^T C_2 Z_2\right) + \left\|\left\|Z_2^T\hat{G}\right\|^2\right\|^2 \tag{4.32}$$

where ζ is an adjustable parameter. Accordingly, the derivative of Lyapunov function becomes

$$\dot{V}_2 \leq -(1-\zeta)(Z_1^T C_1 Z_1 + Z_2^T C_2 Z_2). \tag{4.33}$$

By choosing $0 < \zeta < 1$, the negative semi-definiteness of derivative of Lyapunov function can be ensured and all closed-loop signals can be proved to be bounded. Similar to

previous chapters, by invoking Barbalat Lemma [97], the convergence of the tracking errors to the origin could also be directly proved.

4.4 ETAC of a Mobile Robot over Robot-to-Controller Channel

In this section, the assumption of continuous availability of the robot's states is relaxed. The communication restriction will be considered in both channels. In view of the same, both the states and control signals are event-triggered, and therefore the controller will not be designed based on the actual states. Instead, it will be designed based on the event-triggered (last-received) states. The control law will be computed just at the triggering instants. This will undoubtedly lead to a significant saving in both computational efforts and channel bandwidth.

4.4.1 Problem Formulation

Unlike Section 4.3 where the event-triggered mechanism was placed in the controller-to-robot channel, the devised triggering scheme in this section is placed in the robot-to-controller channel. In such case, the triggering mechanism is defined as

$$q^{ET}(t) = q(t_k), \quad \nu^{ET}(t) = \nu(t_k) \quad | \quad \forall t \in [t_k, t_{k+1}) \tag{4.34}$$

in which

$$t_{k+1} = \inf\{t|\ t > t_k, \quad J(e^{ET}, Z_1, Z_2) > 0\} \tag{4.35}$$

where $q^{ET} = [x^{ET}, y^{ET}, \theta^{ET}]^T$ and $\nu^{ET} = [v^{ET}, w^{ET}]^T$ denote the last-received states from the robot, $J(e^{ET}, Z_1, Z_2)$ is the triggering condition. Here, the measurement error is defined as $e^{ET} = [e_q^{ET}\ e_\nu^{ET}]$, in which $e_q^{ET}(t) = q(t) - q^{ET}(t)$ and $e_\nu^{ET}(t) = \nu(t) - \nu^{ET}(t)$. The triggering function is to be designed later based on the measurement error e^{ET} such that the stability of the overall closed-loop control system are ensured under the event-triggered implementation.

The configuration of the proposed event-triggered control scheme is similar Fig 1.3b. The states of the robot are transmitted over the network only when the designed triggering condition gets violated and the control law is then updated according to the new received states. Referring to kinematic and dynamic descriptions of the mobile robot (4.14), the control problem is stated as follows. Design an event-triggered adaptive tracking controller that guarantees boundedness of the closed-loop signals and ensures faithful reference trajectory tracking with a significant reduction in communication and computational burden.

4.4.2 Control Design

The error variables are first defined as

$$Z_1 = q - q_r, \quad Z_2 = \nu - \alpha_1 \tag{4.36}$$

where $q_r = [x_{ref} \quad y_{ref} \quad \theta_{ref}]^T$ represents the position and orientation of the reference trajectory, and α_1 is the virtual control law to be designed in the first step of design process. The event-triggered error variables are accordingly defined as

$$Z_1^{ET} = q^{ET} - q_r, \quad Z_2^{ET} = q^{ET} - \alpha_1 \tag{4.37}$$

where q^{ET} and q^{ET} are the last-received states at the controller-side.

Step 1

The first error dynamic subsystem is given as

$$\dot{Z}_1 = \dot{q} - \dot{q}_r = S\nu - \dot{q}_r = S\left(Z_2 + \alpha_1\right) - \dot{q}_r \tag{4.38}$$

The Lyapunov function candidate is chosen in this step as $V_1 = \frac{1}{2} Z_1^T Z_1$. Differentiating V_1 with respect time along the trajectories of the system (4.14) is

$$\dot{V}_1 = Z_1^T \dot{Z}_1 = Z_1^T \left(SZ_2 + S\alpha_1 - \dot{q}_r + S^{ET}\alpha_1 - S^{ET}\alpha_1\right) \tag{4.39}$$

where $S^{ET} = S(q^{ET})$. Let us now design the virtual controller α_1 such as

$$S^{ET}\alpha_1 = -C_1 Z_1^{ET} + \dot{q}_r \tag{4.40}$$

where $C_1 \in \mathbb{R}^{3\times 3}$ is a gain matrix with positive diagonal elements. Since $S^T S = I_2$ where $I_2 \in R^{2\times 2}$ is identity matrix, one gets

$$\alpha_1 = (S^{ET})^T S^{ET}\alpha_1 = -(S^{ET})^T (C_1 Z_1^{ET} - \dot{q}_r) \ . \tag{4.41}$$

Unlike Section 4.3.2, the virtual controller here is designed based on the event-triggered states rather than the actual states. Accordingly, the time derivative of Lyapunov function becomes

$$\begin{aligned} \dot{V}_1 &= Z_1^T \left(SZ_2 + (S(q) - S^{ET})\alpha_1 - C_1 Z_1^{ET}\right) \\ &= -Z_1^T C_1 Z_1 + Z_1^T S Z_2 + Z_1^T C_1 e_q^{ET} + Z_1^T (S - S^{ET})\alpha_1 \\ &\leq -Z_1^T C_1 Z_1 + Z_1^T S Z_2 + \|C_1\|Z_1\|\|e_q^{ET}\| + \|\alpha_1\|Z_1\|\|e_q^{ET}\| \end{aligned} \tag{4.42}$$

Let us now add and subtract the term $\zeta Z_1^T C_1 Z_1$ to (4.42), and then design the first

triggering condition as

$$\|e_q^{ET}\| \leq \frac{\|C_1\|}{\|C_1\| + \|\alpha_1\|}\zeta\|Z_1\| \tag{4.43}$$

With (4.43), the time derivative of Lyapunov function becomes

$$\dot{V}_1 \leq -(1-\zeta)Z_1^T C_1 Z_1 + Z_1^T S Z_2 \tag{4.44}$$

Step 2

Let us choose the Lyapunov function candidate in this step as

$$\dot{V}_2 = V_1 + \frac{1}{2}Z_2^T Z_2 + \frac{1}{2}\tilde{\Theta}^T\Gamma_1^{-1}\tilde{\Theta} + \text{trace}\left(\frac{1}{2}\tilde{G}^T\Gamma_2^{-1}\tilde{G}\right), \tag{4.45}$$

Differentiating V_2 with respect time along the trajectories of the system (4.14) is

$$\dot{V}_2 \leq -(1-\zeta)Z_1^T C_1 Z_1 + Z_1^T S Z_2 + Z_2^T\dot{Z}_2 - \tilde{\Theta}^T\Gamma_1^{-1}\dot{\hat{\Theta}} + \text{trace}\left(-\tilde{G}^T\Gamma_2^{-1}\dot{\hat{G}}\right) \tag{4.46}$$

The dynamics of the second error variable is given as

$$\dot{Z}_2 = \dot{\nu} - \dot{\alpha}_1 = \varphi\Theta + Gu + \varphi^{ET}\hat{\Theta} - \varphi^{ET}\hat{\Theta} \tag{4.47}$$

If the control law is designed as

$$u = -\hat{G}^{-1}(C_2 Z_2^{ET} + S^{ET}Z_1^{ET} - \varphi^{ET}\hat{\Theta}) \tag{4.48}$$

where $C_2 \in \mathbb{R}^{2\times 2}$ is a gain matrix with positive diagonal elements and $\varphi^{ET} = \varphi(\nu^{ET})$, the time derivative of Lyapunov function becomes

$$\begin{aligned}
\dot{V}_2 &\leq -(1-\zeta)Z_1^T C_1 Z_1 - Z_2^T C_2 Z_2 + Z_2^T C_2 e_\nu^{ET} + Z_1^T S Z_2 - Z_2^T (S^{ET})^T Z_1^{ET} \\
&\quad + Z_2^T\tilde{G}u + Z_2^T\left(\varphi^T - (\varphi^{ET})^T\right)\Theta + \tilde{\Theta}^T\left((\varphi^{ET})^T Z_2 - \Gamma_1^{-1}\dot{\hat{\Theta}}\right) - \text{trace}\left(\tilde{G}^T\Gamma_2^{-1}\dot{\hat{G}}\right) \\
&\leq -(1-\zeta)Z_1^T C_1 Z_1 - Z_2^T C_2 Z_2 + Z_2^T C_2 e_\nu^{ET} + Z_1^T(S - S^{ET})Z_2 - (e_q^{ET})^T(S^{ET})^T Z_2 \\
&\quad + Z_2^T(\varphi - \varphi^{ET})\Theta + \tilde{\Theta}^T\left((\varphi^{ET})^T Z_2 - \Gamma_1^{-1}\dot{\hat{\Theta}}\right) + \text{trace}\left(\tilde{G}^T(Z_2 u^T - \Gamma_2^{-1}\dot{\hat{G}})\right) \\
&\leq -(1-\zeta)Z_1^T C_1 Z_1 - Z_2^T C_2 Z_2 + \|C_2\|\|Z_2\|\|e_\nu^{ET}\| + \|Z_1\|\|Z_2\|\|e_\nu^{ET}\| + \|Z_2\|\|e_\nu^{ET}\| \\
&\quad + L\|\Theta\|\|Z_2\|\|e_\nu^{ET}\| + \tilde{\Theta}^T((\varphi^{ET})^T Z_2 - \Gamma_1^{-1}\dot{\hat{\Theta}}) + \text{trace}\left(\tilde{G}^T(Z_2 u^T - \Gamma_2^{-1}\dot{\hat{G}})\right)
\end{aligned} \tag{4.49}$$

With the adaptation laws designed as

$$\dot{\hat{\Theta}} = \Gamma_1(\varphi^{ET})^T Z_2^{ET} \quad \text{and} \quad \dot{\hat{G}} = \Gamma_2 Z_2^{ET} u^T, \tag{4.50}$$

one gets,

$$\dot{V}_2 \leq -(1-\zeta)Z_1^T C_1 Z_1 - Z_2^T C_2 Z_2 + \|C_2\|\|Z_2\|\|e_\nu^{ET}\| + \|Z_1\|\|Z_2\|\|e_\nu^{ET}\| + \|Z_2\|\|e_\nu^{ET}\| + L\|\Theta\|\|Z_2\|\|e_\nu^{ET}\| + \gamma\|e_\nu^{ET}\| \tag{4.51}$$

where $\gamma = G^*\|u\| + \|\hat{G}\|\|u\| + \Theta^*\|(\varphi^{ET})^T\| + \|\hat{\Theta}\|\|\varphi\|$ in which G^* and Θ^* were defined in Assumption (3). Let us add and subtract the term $\zeta Z_2^T C_2 Z_2$ from (4.51), and then design the second triggering condition as

$$\|e_\nu^{ET}\| \leq \frac{\|C_2\|}{(\|C_2\| + \|Z_1\| + L\|\Theta\|\|Z_2\| + 1)\|Z_2\| + \gamma}\zeta\|Z_2\|^2 \tag{4.52}$$

With (4.52), the time derivative of Lyapunov function becomes

$$\dot{V}_2 \leq -(1-\zeta)\left(Z_1^T C_1 Z_1 + Z_2^T C_2 Z_2\right) \tag{4.53}$$

By choosing $0 < \zeta < 1$, the negative semi-definiteness of the derivative of Lyapunov function can be ensured, and therefore, the overall system is stable in the sense of Lyapunov and all closed-loop signals are bounded. Similar to previous chapters, by invoking Barbalat Lemma [97], the convergence of the tracking errors to the origin could also be directly proved.

4.5 Simulation Results

To demonstrate the applicability of the proposed event-triggered adaptive control scheme, a wheeled mobile robot controller over a network channel subject to parametric uncertainties and limited communication is considered in this section. The physical parameters of the robot are given as $m = 10$ [kg], $r = 0.1$ [m] and $b = 0.5$ [m], $d = 0.5$ [m] and $I = 2.5$ [kgm^2]. The uncertainties in d and I are given as $I(t) = I + 0.5\sin(t)$ and $d(t) = d + 0.4\sin(2t)$. We have selected a circular trajectory with radius and angular speed as $r_{ref} = 1$[m] and $w_{ref} = 0.5$ [rad/s], respectively. The design parameters are chosen as $C_1 = diag(0.4, 0.4, 4), C_2 = diag(2, 2)$, $\zeta = 0.8$ and $\Gamma_1 = \Gamma_2 = diag(10, 10)$, and the initial state is chosen as $x_1(0) = (0,\ 1.1,\ 10)^T$. The simulation is conducted on MATLAB for 30 seconds under 0.02 [s] sampling interval.

The obtained results under the designed event-triggered adaptive controller on the system dynamics (4.14) are illustrated in Fig.4.2–4.6. The performance of tracking a circular trajectory in $X-Y$ plane in the presence of parametric uncertainties with/without adaptation is shown in Fig. 4.2. The effect of uncertainties on the system performance can be clearly recognized, and it can also be observed that the designed adaptive controller is able to compensate these uncertainties and achieve a faithful tracking performance.

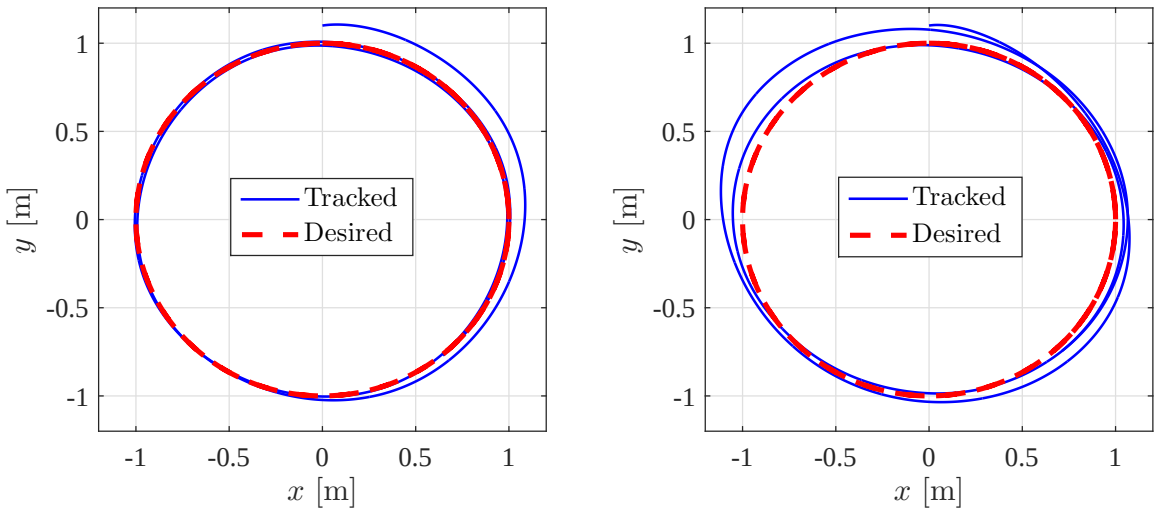

Figure 4.2: Circular trajectory tracking under the proposed control scheme in the presence of parametric uncertainties; with adaptation (left) and without adaptation (right).

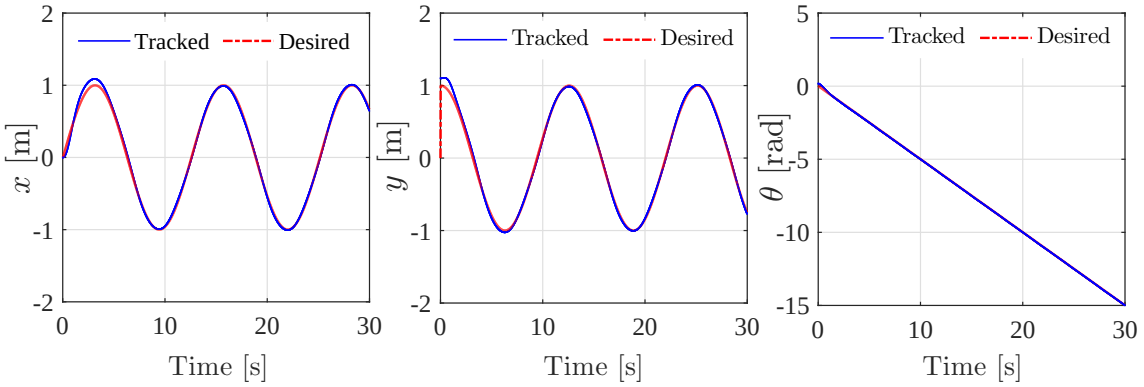

(a) Trajectories in x, y, θ directions.

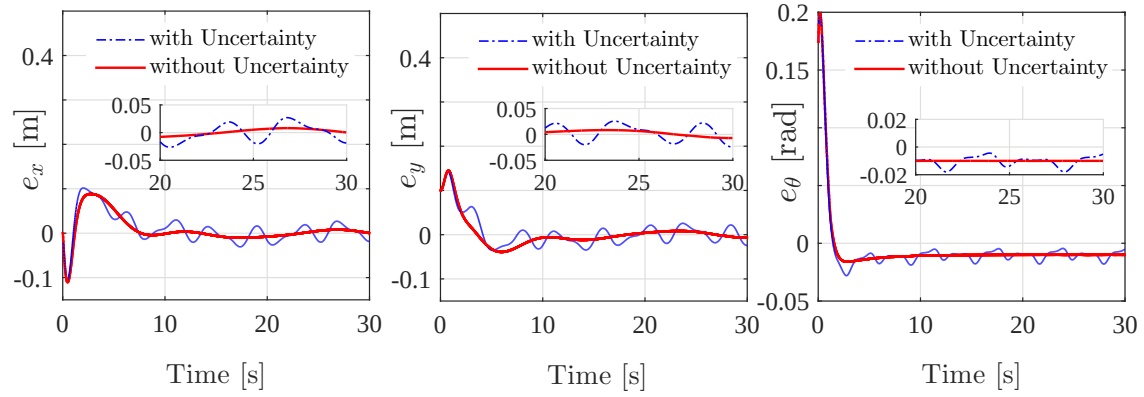

(b) Tracking errors in x, y, θ directions.

Figure 4.3: Performance of the proposed control scheme.

The trajectories in the x, y and θ directions and the tracking errors are illustrated in Fig. 4.3a and Fig. 4.3b, respectively. It is observed that the error signals converge to a small set around zero. Furthermore, the event-triggered and time-triggered control signals for right and left motors are depicted in Fig. 4.4 which are shown to be bounded over time.

With respect to resource utilization, the event-triggered control schemes presented in Section 4.3 and Section 4.4 are compared along with the traditional time-triggered control scheme. The comparison results are summarized in Table 4.1. The triggering instants for each case are illustrated in Fig. 4.5, wherein each dot in the figure represents the time instance at when the triggering condition is violated. Moreover, the inter-event times between each two executive triggering instants are also shown in Fig. 4.6. In case of time-triggered control approaches, it is well-known that the states and control updates are periodically circulated over the network, in which the inter-event time is constant and equals the sampling rate (dt). In such approaches, the number of events is always fixed and equals T/dt. Specifically, 1500 control updates and transmissions over the network channels have occurred for 30 [s] of simulation run with 0.02 sampling interval. In comparison with periodic time-triggered implementation, the proposed event-triggered schemes yield a greater saving of network resources in terms of the number of transmissions and control updates. In the following, the performance of the two triggering mechanisms presented in this chapter is discussed. In Section 4.3, the triggering mechanism was placed in the controller-to-robot channel without considering any restriction in the other channel. Although this configuration was simple in analysis and implementation, it should be noted that in such case the number of control updates could not be alleviated. Therefore, the number of control updates and transmissions over the robot-to-controller channel was 1500 similar to the time-triggered paradigm. However, the number of transmissions over the controller-to-robot channel was significantly reduced (64 and 268 triggering events in the absence and presence of the parametric uncertainties, respectively). Obviously, more transmissions are required to handle the effects of uncertainties when they are encountered in the robot model. On the other hand, the triggering mechanism presented in Section 4.4 was placed in the robot-to-controller channel, i.e. both state and control signals are now event-triggered. Therefore, the number of control updates, as well as the transmissions over robot-to-controller, are alleviated. However, it is worth mentioning that such configuration is complicated in analysis and implementation, and it does require smart sensors with computational abilities for evaluating the triggering condition. As compared to the configuration presented in 4.3, the number of transmissions over the robot-to-controller channel as well as control updates are reduced to 681 and 221 for the cases with and without uncertainties, respectively.

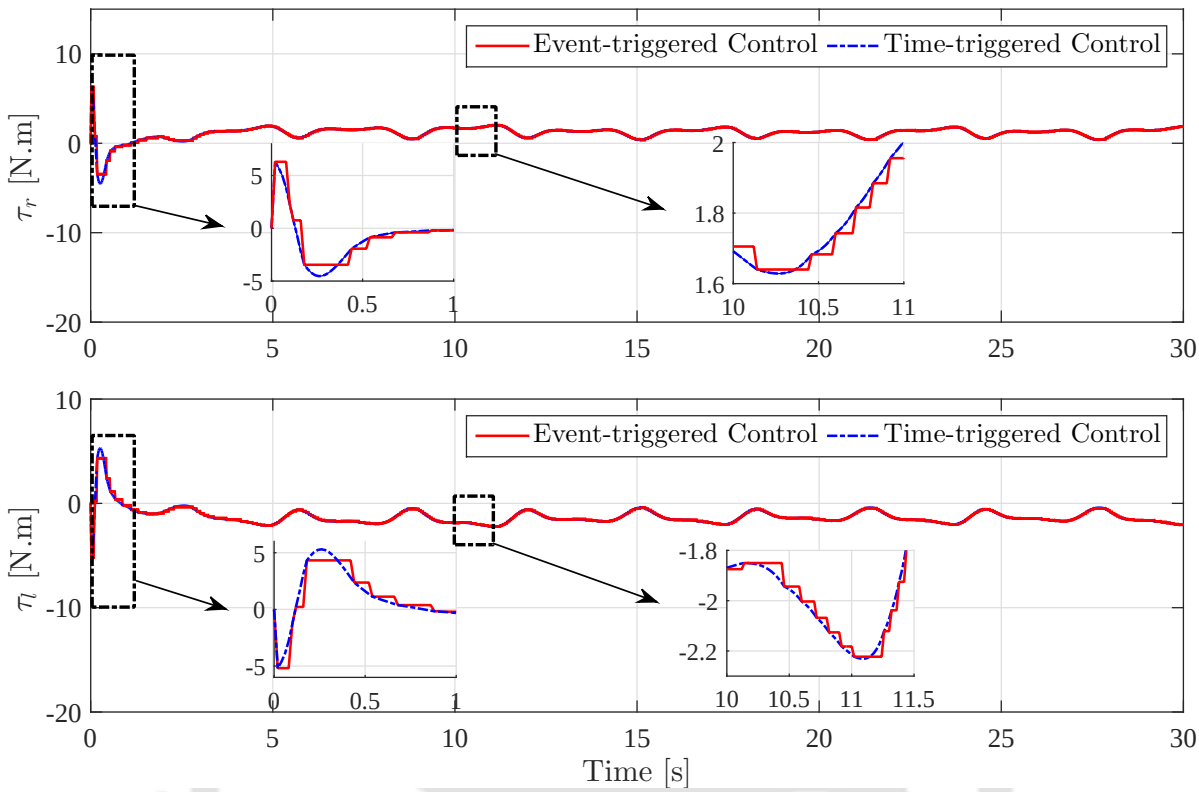

Figure 4.4: The control signal of the right and left motors

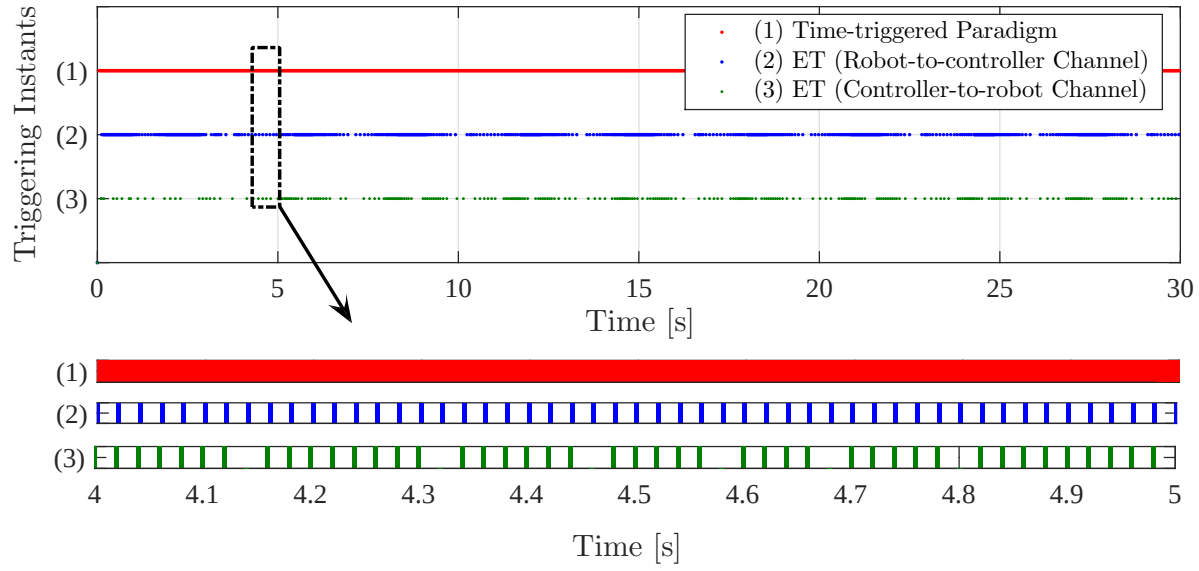

Figure 4.5: Illustration of triggering instants in the presence of parametric uncertainties.

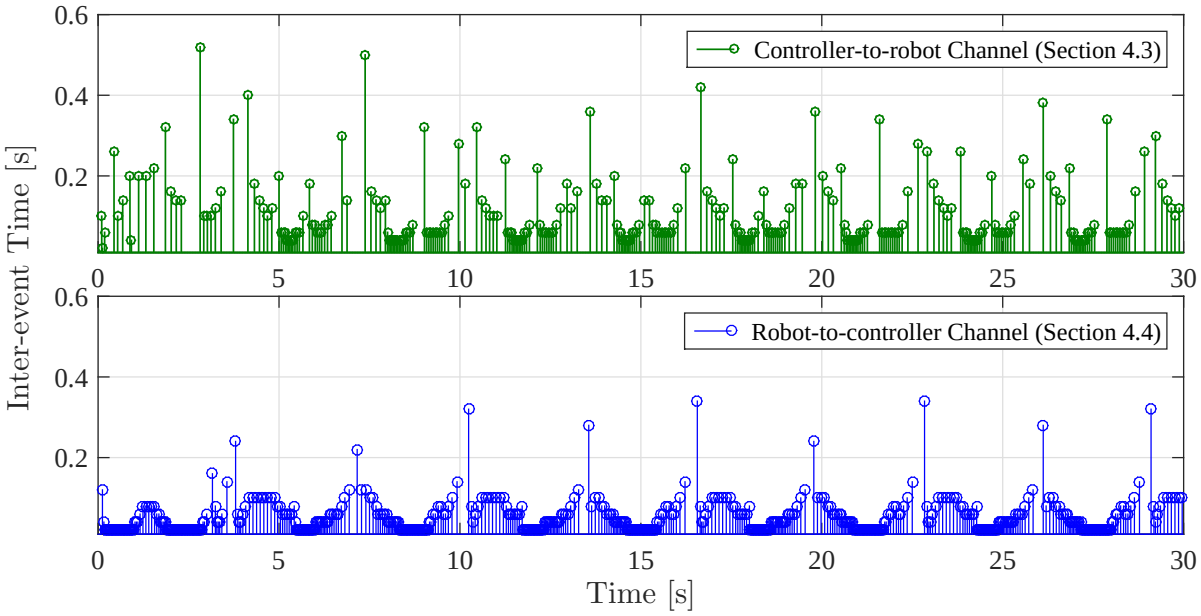

Figure 4.6: Inter-event time in the presence of parametric uncertainties.

Table 4.1: Comparison of results for time-triggered and event-triggered strategies presendted in Section 4.3 and Section 4.4.

			#Control updates	#Transmissions over Channel	
				Robot-to-controller	Controller-to-robot
Time-triggered			1500	1500	1500
Event-triggered	**Section** 4.3	without uncertainty	1500	1500	64
		with uncertainty	1500	1500	268
	Section 4.4	without uncertainty	221	221	221
		with uncertainty	681	681	681

4.6 Summary

In this chapter, the trajectory tracking control problem of a nonholonomic mobile robot subject to parametric uncertainties has been considered. The robot was controlled over a communication channel with limited resources. For this purpose, an event-triggered adaptive controller has been designed based on backstepping to achieve the control task. Moreover, two different event-triggered configurations have also been presented in the robot-to-controller and controller-to-robot channels to economically utilize the network resources. The simulation results show that the designed controller is able to compensate for the uncertainties in the robot model and ensures the desired trajectory to be tracked with satisfactory performance. As compared to the time-triggered paradigm, the proposed event-triggered scheme guarantees a significant saving in the system resources.

5

Design and Implementation of ETAC for Commercial Mobile Robots with Networked-Induced Delays

Contents

5.1 Introduction

In this chapter[1], an adaptive tracking controller is designed and implemented on a real mobile robot in an event-triggered fashion considering some practical challenges such as limited communications, network-induced delays, and hardware restrictions of commercial mobile robots. Unlike other dynamic models of mobile robots that consider torques or voltages as control inputs, a modified dynamic model that admits direct commands of desired linear and angular velocities is first presented. This is highly desirable for commercial robots available in the market. Due to the unavailability of internal parameters of the robot, an adaptive law is designed to estimate them on-line during the robot operation. The main results of this chapter are divided into two main parts. In the first part, an auxiliary compensation system is introduced along with an adjustable triggering condition to deal with the input delay and limited bandwidth restrictions. The robot states here are assumed to be captured using a camera that is directly connected to the controller via a dedicated wired connection. Therefore, the communication network is considered in the controller-to-robot channel only. However, in the second part of this chapter, the communication network is considered in both channels with state and input delays. For this purpose, a state predictor is first designed to deal with the induced delays. Thereafter, an event-triggered trajectory tracking controller is designed using backstepping approach based on the predicted states. The triggering conditions are directly derived from the derivative of Lyapunov function such that the stability of the overall control system is always guaranteed under the event-triggered implementation.

The main contributions of this chapter in comparison with existing studies are highlighted as follows. As compared to [4,43,51–53,55], both kinematic and dynamic models of mobile robot are considered in this study. Moreover, the presented dynamic model admits direct velocity commands rather than torques [62] or voltages of the motors [65]. An on-line adaptive law is also designed to estimate the unavailable model parameters. Rather than the predefined fixed [22] or relative thresholds [2,23], an adjustable triggering condition is designed by guaranteeing the existence of an appropriate Lyapunov function. It also ensures the exclusion of Zeno behavior. Unlike [4,51] where the event-triggered mechanism was placed in the controller-to-robot channel only, the devised triggering scheme in the second part of this chapter is placed in the robot-to-controller channel, which results in alleviation of computational resources and transmissions over the channel. Moreover, the designed predictor-based controller is capable to deal with both state and input delays, which increases the horizon of the controller. Finally, the proposed

[1]This chapter is based on the article: **S. Al Issa** and I. Kar, "Design and implementation of event-triggered adaptive controller for commercial mobile robots subject to input delays and limited communications", in *Control Engineering Practice*, 114, 2021: 104865.

event-triggered adaptive control schemes are experimentally validated on a commercial robot (PatrolBot). The obtained results are consistent with simulations and show an accurate tracking with a significant saving in channel bandwidth and computational resources in presence of state and input delays.

The rest of the chapter is organized as follows. A modified mathematical model for commercial mobile robots is first derived in Section 5.2. In Section 5.3, the event-triggered adaptive tracking control problem is investigated in the controller-to-robot channel with input delay. Subsection 5.3.1 formulates the problem. Thereafter, an ETAC controller is designed and the triggering rule is also derived in Subsection 5.3.2. Experimental results of the proposed control scheme on PatrolBot is provided in Subsection 5.3.3. In Section 5.4, the predictor-based event-triggered tracking control problem is investigated in the robot-to-controller with state and input delays. Subsection 5.4.1 formulates the problem. In Subsection 5.4.2, the predictor-based event-triggered controller is designed. Further, experimental results are provided in Subsection 5.4.3. The summary of the chapter is drawn in Section 5.5.

5.2 A Modified Dynamic Model for Commercial Mobile Robots

In this section, a modified dynamic model of mobile robots is presented, which admits the linear and angular velocities as control inputs rather than torques or voltages of the motors. Practically speaking, this is highly desirable for commercial mobile robots that are generally operated by direct linear and angular velocity commands. In Section 4.2 of the previous chapter, a conventional dynamic model of mobile robot was obtained based on the Euler-Lagrange method. By putting (4.5–4.8) and in (4.4), the conventional dynamic model was directly obtained as

$$M(q)\ \ddot{q} + C_c(q,\dot{q})\ \dot{q} + F_g(q) = E(q)\ u - A_k^T(q)\ \lambda\ , \tag{5.1}$$

where the parameters of the model were defined in (4.10). However, the control input $u = [\ \tau_r \quad \tau_l\ ]^T$ was represented by the torques on the right and left wheels of the robot. It is more appropriate to incorporate the actuator model and consider the motor voltage as control input as follows [92]

$$\tau_r = K_a\left(\frac{V_r - K_b w_r}{R_a}\right) \quad , \quad \tau_l = K_a\left(\frac{V_l - K_b w_l}{R_a}\right) \tag{5.2}$$

where K_a and K_b are torque constant and back EMF coefficient, respectively. R_a is the resistance and (w_r, w_l) denote the angular velocities of right and left motors. The

control signals are now represented by voltages of the motors (V_r, V_l). Nevertheless, it is worth mentioning that commercial mobile robots are operated by direct linear and angular velocity commands. They have their internal velocity-based controllers which are not accessible [72]. To cope with this restriction, we proceed further to combine two velocity-based controllers as follows

$$\frac{V_r + V_l}{2} = K_p^v (v_{in} - v) - K_d^v (\dot{v}) \tag{5.3}$$

$$\frac{V_r - V_l}{2} = K_p^w (w_{in} - w) - K_d^w (\dot{w}) \tag{5.4}$$

where

$$v = \frac{r}{2}(w_r + w_l) \quad , \quad w = \frac{r}{d}(w_r - w_l) \tag{5.5}$$

and K_p^v, K_d^v, K_p^w, K_d^w are proportional and derivative gains of PD controllers. v_{in} and w_{in} are linear and angular velocities of the robot and they represent the control inputs in the modified dynamic model. It is to be noted that PD controllers are used in (5.3) and (5.4) with neglecting $\dot{v}_{in}$ and $\dot{w}_{in}$ terms to further simplify the dynamic model.

With (5.2–5.5), a modified dynamic model of the mobile robot can be written in a matrix form as

$$M\ddot{q} + C_c\dot{q} + h = E_1 u + E_2 \nu + E_3 \dot{\nu} - A_k^T \lambda \tag{5.6}$$

where

$$M := \begin{bmatrix} m & 0 & -md\sin\theta \\ 0 & m & md\cos\theta \\ -md\sin\theta & dm\cos\theta & md^2 + I \end{bmatrix}, \quad C_c := \begin{bmatrix} \dot{m} & 0 & c_{13} \\ 0 & \dot{m} & c_{23} \\ -\dot{m}d\sin\theta & \dot{m}d\cos\theta & \dot{m}d^2 + 2md\dot{d} \end{bmatrix},$$

$$h := \begin{bmatrix} (\dot{m}\dot{d} + m\ddot{d})\cos\theta \\ (\dot{m}\dot{d} + m\ddot{d})\sin\theta \\ 0 \end{bmatrix}, \quad E_1 := \begin{bmatrix} \varsigma_1\cos\theta & 0 \\ \varsigma_1\sin\theta & 0 \\ 0 & \varsigma_2 \end{bmatrix}, \quad E_2 := \begin{bmatrix} -\varsigma_3\cos\theta & 0 \\ -\varsigma_3\sin\theta & 0 \\ 0 & -\varsigma_4 \end{bmatrix},$$

$$E_3 := \begin{bmatrix} -\varsigma_5\cos\theta & 0 \\ -\varsigma_5\sin\theta & 0 \\ 0 & -\varsigma_6 \end{bmatrix}, \text{ and } A_k^T := \begin{bmatrix} -\sin\theta & \cos\theta & 0 \end{bmatrix}$$

in which

$$\begin{aligned} c_{13} &= -md\cos\theta\dot{\theta} - (\dot{m}d + 2m\dot{d})\sin\theta, \\ c_{23} &= -md\sin\theta\dot{\theta} + (\dot{m}d + 2m\dot{d})\cos\theta, \end{aligned} \tag{5.7}$$

and

$$\varsigma_1 = \frac{2K_aK_p^v}{rR_a} \quad , \quad \varsigma_2 = \frac{2bK_aK_p^w}{rR_a}$$
$$\varsigma_3 = \frac{2K_a\left(K_p^v + K_b\right)}{rR_a} \quad , \quad \varsigma_4 = \frac{bK_a\left(2K_p^w + dK_b\right)}{rR_a}$$
$$\varsigma_5 = \frac{2K_aK_d^v}{rR_a} \quad , \quad \varsigma_6 = \frac{2bK_aK_d^w}{rR_a}.$$

In the modified dynamic model (5.6), the control input $u = [\ v_{in} \quad w_{in}\ ]^T$ is now represented by the linear and angular velocities rather than torques. To convert (5.6) to unconstrained form, we pre-multiply both side by S^T defined in (4.3) as

$$S^T\left(M\ddot{q} + C_c\dot{q}\right) + \bar{h} = \bar{E}_1 u + \bar{E}_2\nu + \bar{E}_3\dot{\nu} \tag{5.8}$$

where $\bar{h} = [\ \dot{m}\dot{d} + m\ddot{d} \quad 0\ ]^T$, $\bar{E}_1 = diag\left(\varsigma_1, \varsigma_2\right)$, $\bar{E}_2 = diag\left(-\varsigma_3, -\varsigma_4\right)$ and $\bar{E}_3 = diag\left(-\varsigma_5, -\varsigma_6\right)$. The internal parameters $(\varsigma_i,\ i = 1, \ldots, 6)$ are unknowns and they represent the internal parameters of motor models and gains of incorporated PD controllers.

From kinematic equation (4.2), we have $\ddot{q} = S\dot{\nu} + \dot{S}\nu$. Moreover, with simple rearrangements of (5.8), the dynamic model of the mobile robot could be written as

$$\bar{M}\dot{\nu} = \bar{E}_1 u + \bar{\bar{E}}\nu - \bar{h} \tag{5.9}$$

where

$$\bar{M} := S^T M S - \bar{E}_3 = \begin{bmatrix} m + \varsigma_5 & 0 \\ 0 & md^2 + I_c + \varsigma_6 \end{bmatrix},$$
$$\bar{\bar{E}} := \bar{E}_2 - S^T(M\dot{S} + C_cS) = \begin{bmatrix} \sigma_3 & mdw \\ -mdw & \sigma_4 \end{bmatrix},$$

in which,

$$\sigma_3 = -\varsigma_3 - \dot{m},$$
$$\sigma_4 = -\varsigma_4 - \dot{m}d^2 - 2md\dot{d}$$

With straightforward matrix multiplications, the dynamic model (5.9) of the mobile robot can be further simplified and finally written as

$$\dot{\nu} = \varphi(\nu)\Theta + Gu - \bar{h} \tag{5.10}$$

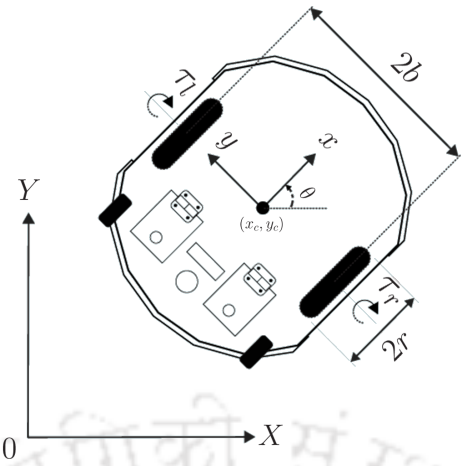

Figure 5.1: The schematic of PatrolBot wheeled mobile robot

where

$$\varphi := \begin{bmatrix} -v & w^2 & 0 & 0 \\ 0 & 0 & -vw & -w \end{bmatrix},$$
$$\Theta := \begin{bmatrix} \frac{\sigma_3}{m+\varsigma_5} & \frac{md}{m+\varsigma_5} & \frac{-md}{md^2+I_c+\varsigma_6} & \frac{\sigma_4}{md^2+I_c+\varsigma_6} \end{bmatrix}^T,$$
$$G := \bar{M}^{-1}\bar{E}_1 = \begin{bmatrix} \frac{\varsigma_1}{m+\varsigma_5} & 0 \\ 0 & \frac{\varsigma_2}{md^2+I_c+\varsigma_6} \end{bmatrix} := \begin{bmatrix} p_1 & 0 \\ 0 & p_2 \end{bmatrix}, \tag{5.11}$$
$$\bar{h} := \begin{bmatrix} m\ddot{d}+\dot{m}\dot{d} & 0 \end{bmatrix}^T := \begin{bmatrix} p_3 & 0 \end{bmatrix}^T,$$
$$u := \begin{bmatrix} v_{in} & w_{in} \end{bmatrix}^T.$$

5.3 Design and Implementation of ETAC over Controller-to-Robot Channel with Input Delay

5.3.1 Problem Formulation

Let us consider a non-holonomic wheeled mobile robot with unknown parameters and controlled via a time-delayed wireless channel under limited transmission. From (4.2) and (5.10), the kinematic and dynamic models of the robot can be written as

$$\begin{aligned} \dot{q} &= S\nu, \\ \dot{\nu} &= \varphi(\nu)\Theta + Gu^{ET}(t-\tau) - \bar{h} \end{aligned} \tag{5.12}$$

To reduce the communication burden, an event-triggered mechanism is introduced in the controller-to-robot channel. Thus, the robot is now actuated by event-triggered control signal u^{ET} rather than the actual time-triggered signal u where

$$\begin{aligned} u^{ET}(t) &= u(t_k),\ \forall\ t \in [t_k, t_{k+1}) \\ t_{k+1} &= \inf\left\{\ t \mid t > t_k\ ,\quad J(e^{ET}, Z_1, Z_2) > 0\right\}, \end{aligned} \tag{5.13}$$

where $J(e^{ET}, Z_1, Z_2)$ is the triggering function to be designed later and $e^{ET} = u - u^{ET}$ denotes the measurement error. On the other hand, an auxiliary compensation system is introduced to deal with input delay and it is defined as

$$\begin{aligned} \dot{\eta}_1 &= S\eta_2 - \kappa_1\eta_1, \\ \dot{\eta}_2 &= \hat{G}(u^{ET}(t) - u^{ET}(t-\tau)), \end{aligned} \tag{5.14}$$

where $\kappa_1 > \frac{1}{2}$ is a positive constant and $\hat{G}$ is the estimate of the unknown matrix G. The compensating variable η_2 represents the integral of input signal u^{ET} over the interval $[t-\tau,\ t]$.

The block diagram of the proposed control scheme is illustrated in Fig 5.2. In this framework, it is assumed that there are no restrictions in the robot-to-controller channel. The states of the robot are acquired using a vision system in which the camera is directly connected to the controller using a wire. Referring to the kinematic and dynamic descriptions of the mobile robot (5.12), the control problem is stated as follows. Design and implement an event-triggered adaptive tracking controller on a commercial mobile robot, that guarantees the boundedness of the closed-loop signals in the presence of input delay and ensures an accurate reference trajectory tracking with a significant reduction in communication burden.

5.3.2 Event-triggered Adaptive Control Scheme

In this section, an adaptive controller is first designed based on the backstepping method [41]. The triggering condition is then derived by guaranteeing the existence of an appropriate Lyapunov function.

5.3.2.1 Adaptive Backstepping Control Design

Let us define the error variables as

$$Z_1 = q - q_r + \eta_1\ , \tag{5.15}$$

$$Z_2 = \nu - \alpha_1 + \eta_2\ . \tag{5.16}$$

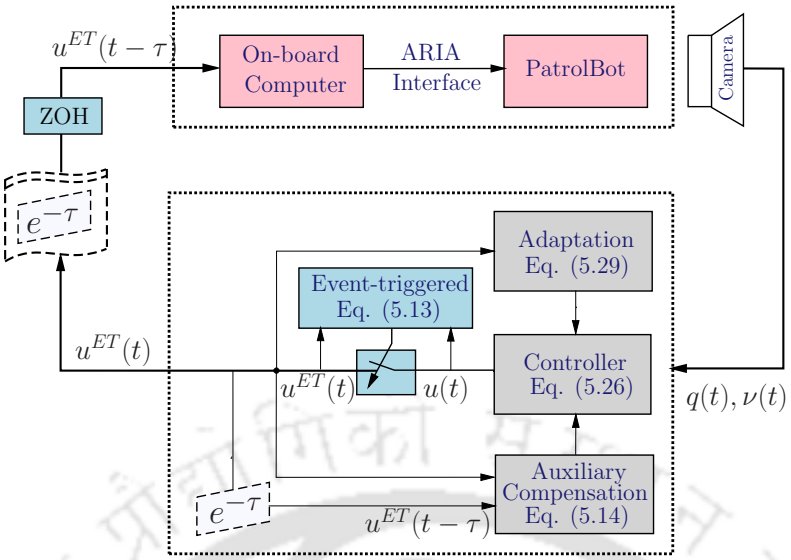

Figure 5.2: The block diagram of the proposed control scheme.

where $q_r = [x_{ref} \quad y_{ref} \quad \theta_{ref}]^T$ represents the position and orientation of the reference trajectory, and α_1 is the virtual control law to be designed in the first step of design process.

Step 1: The dynamics of the first error subsystem is given as

$$\begin{aligned} \dot{Z}_1 &= \dot{q} - \dot{q}_r + \dot{\eta}_1 \\ &= S\nu - \dot{q}_r + S\eta_2 - \kappa_1\eta_1 \\ &= SZ_2 + S\alpha_1 - \dot{q}_r - \kappa_1\eta_1 \end{aligned} \tag{5.17}$$

To stabilize the above error subsystem, a suitable virtual control α_1 is to be designed. Let us choose a Lyapunov function candidate as $V_1 = \frac{1}{2}Z_1^T Z_1$. Differentiating V_1 with respect time along the trajectories of the system (5.12) is

$$\dot{V}_1 = Z_1^T \dot{Z}_1 = Z_1^T (SZ_2 + S\alpha_1 - \dot{q}_r - \kappa_1\eta_1) \tag{5.18}$$

Let us design $S\alpha_1$ such that

$$S\alpha_1 = -C_1 Z_1 + \dot{q}_r + \kappa_1\eta_1 \tag{5.19}$$

where $C_1 \in \mathbb{R}^{3\times 3}$ is a gain matrix with positive diagonal elements. Then, one gets

$$\dot{V}_1 = -Z_1^T C_1 Z_1 + Z_1^T S Z_2 \tag{5.20}$$

It is to be noted that $S^TS = I_2$ where I_2 is identity matrix. Thus, we get from (5.19)

$$\alpha_1 = S^TS\alpha_1 = -S^T(C_1Z_1 - \dot{q}_r - \kappa_1\eta_1) \ . \tag{5.21}$$

From (5.20), $\dot{V}_1$ becomes negative definite if $Z_2 = 0$, and convergence of Z_1 is then ensured. This will be analyzed in the next step of controller design.

Step 2: Let us now choose Lyapunov function candidate as

$$V_2 = V_1 + \frac{1}{2}Z_2^TZ_2 + \frac{1}{2}\tilde{\Theta}^T\Gamma_1^{-1}\tilde{\Theta} + \frac{1}{2}\tilde{P}^T\Gamma_2^{-1}\tilde{P} \tag{5.22}$$

where $\tilde{\Theta} = \Theta - \hat{\Theta}$ and $\tilde{P} = P - \hat{P}$ in which $\hat{\Theta}$ and $\hat{P}$ are the estimates of unknown vectors Θ and P, respectively. Further, $\Gamma_1 \in \mathbb{R}^{4\times4}$ and $\Gamma_2 \in \mathbb{R}^{3\times3}$ are tuning matrices associated with adaptation laws to be chosen by the designer. Here, $P = \begin{bmatrix} p_1 & p_2 & p_3 \end{bmatrix}^T$ where p_1, p_2 and p_3 are defined in (5.11). Differentiating V_2 with respect time along the trajectories of the system (5.12) is

$$\dot{V}_2 = \dot{V}_1 + Z_2^T\dot{Z}_2 - \tilde{\Theta}^T\Gamma_1^{-1}\dot{\hat{\Theta}} - \tilde{P}^T\Gamma_2^{-1}\dot{\hat{P}} \ , \tag{5.23}$$

where the derivative of Z_2 is expressed as

$$\begin{aligned}\dot{Z}_2 = \dot{\nu} - \dot{\alpha}_1 + \dot{\eta}_2 &= \varphi\Theta - \bar{h} - \dot{\alpha}_1 + Gu^{ET}(t-\tau) + \hat{G}\big(u^{ET}(t) - u^{ET}(t-\tau)\big) \\ &= \varphi\Theta - \bar{h} - \dot{\alpha}_1 + \tilde{G}u^{ET}(t-\tau) + \hat{G}u(t) - \hat{G}e^{ET}(t),\end{aligned} \tag{5.24}$$

Substituting (5.20) and (5.24) in (5.23), the following equality is obtained.

$$\begin{aligned}\dot{V}_2 = &-Z_1^TC_1Z_1 + Z_1^TSZ_2 - \tilde{\Theta}^T\Gamma_1^{-1}\dot{\hat{\Theta}} - \tilde{P}^T\Gamma_2^{-1}\dot{\hat{P}} \\ &+ Z_2^T\left(\varphi\Theta - \hat{\bar{h}} - \tilde{\bar{h}} - \dot{\alpha}_1 + \tilde{G}u^{ET}(t-\tau) + \hat{G}u - \hat{G}e^{ET}\right)\end{aligned} \tag{5.25}$$

where $\tilde{G} = G - \hat{G}$ and $\tilde{\bar{h}} = \bar{h} - \hat{\bar{h}}$ in which $\hat{G}$ and $\hat{\bar{h}}$ represent the estimates of unknowns G and $\bar{h}$, respectively. Let us now design the control law as

$$u = -\hat{G}^{-1}\left(C_2Z_2 + \varphi\hat{\Theta} - \hat{\bar{h}} - \dot{\alpha}_1 + S^TZ_1\right) \tag{5.26}$$

where $C_2 \in \mathbb{R}^{2\times2}$ is a gain matrix with positive diagonal elements. Substituting (5.26) in (5.25), the time derivative of Lyapunov function V_2 becomes

$$\begin{aligned}\dot{V}_2 = &-Z_1^TC_1Z_1 - Z_2^TC_2Z_2 + Z_2^T\left(\tilde{G}u^{ET}(t-\tau) - \tilde{\bar{h}} - \hat{G}e^{ET}\right) \\ &+ \tilde{\Theta}^T\left(\varphi^TZ_2 - \Gamma^{-1}\dot{\hat{\Theta}}\right) - \tilde{P}^T\Gamma_2^{-1}\dot{\hat{P}}\end{aligned} \tag{5.27}$$

Let us write $Z_2 = [\ Z_{21} \quad Z_{22}\ ]^T$ and simplify the third term in (5.27). Then,

$$\dot{V}_2 = -Z_1^T C_1 Z_1 - Z_2^T C_2 Z_2 - Z_2^T \hat{G} e^{ET} + \tilde{\Theta}^T \left(\varphi^T Z_2 - \Gamma_1^{-1}\dot{\hat{\Theta}}\right) + \tilde{P}^T \left(\bar{\Psi} - \Gamma_2^{-1}\dot{\hat{P}}\right) \quad (5.28)$$

where $\bar{\Psi} = [\ Z_{21} v_{in}^{ET}(t-\tau) \quad Z_{22} w_{in}^{ET}(t-\tau) \quad -Z_{21}\ ]^T$. Now, by choosing adaptive laws as

$$\dot{\hat{\Theta}} = \Gamma_1 \varphi^T Z_2 \quad \text{and} \quad \dot{\hat{P}} = \Gamma_2 \bar{\Psi}, \quad (5.29)$$

one obtains

$$\dot{V}_2 = -Z_1^T C_1 Z_1 - Z_2^T C_2 Z_2 - Z_2^T \hat{G} e^{ET} \quad (5.30)$$

In the following subsection, the triggering rule is to be designed in such a way that guarantees the negative semi-definiteness of $\dot{V}_2$.

5.3.2.2 Proposed Event-triggered Control Scheme

According to the measurement error that is appeared in the last term of (5.30), the threshold of the triggering condition will be defined in this subsection. Using Young inequality on the last term of (5.30), one gets

$$\begin{aligned} \dot{V}_2 &\leq -Z_1^T C_1 Z_1 - Z_2^T C_2 Z_2 + \|Z_2^T \hat{G}\| \|e^{ET}\| \\ &\leq -Z_1^T C_1 Z_1 - Z_2^T C_2 Z_2 + \frac{\|Z_2^T \hat{G}\|^2}{2} + \frac{\|e^{ET}\|^2}{2}, \end{aligned} \quad (5.31)$$

Adding and subtracting the term $\zeta(Z_1^T C_1 Z_1 + Z_2^T C_2 Z_2)$ from (5.31), yields

$$\dot{V}_2 \leq -(1-\zeta)(Z_1^T C_1 Z_1 + Z_2^T C_2 Z_2) - \zeta(Z_1^T C_1 Z_1 + Z_2^T C_2 Z_2) + \frac{\|Z_2^T \hat{G}\|^2}{2} + \frac{\|e^{ET}\|^2}{2}, \quad (5.32)$$

where ζ is an adjustable parameter. Now, if the triggering condition is derived by ensuring that

$$\frac{\|Z_2^T \hat{G}\|^2}{2} + \frac{\|e^{ET}\|^2}{2} \leq \zeta(Z_1^T C_1 Z_1 + Z_2^T C_2 Z_2) \quad (5.33)$$

then the derivative of Lyapunov function becomes

$$\dot{V}_2 \leq -(1-\zeta)(Z_1^T C_1 Z_1 + Z_2^T C_2 Z_2). \quad (5.34)$$

By choosing $0 < \zeta < 1$, the negative semi-definiteness of derivative of Lyapunov function can be ensured. From (5.33), the triggering function defined in (5.13) can be written as

$$J(e^{ET}, Z_1, Z_2) = \|e^{ET}\|^2 - 2\zeta\left(Z_1^T C_1 Z_1 + Z_2^T C_2 Z_2\right) + \|Z_2^T \hat{G}\|^2 \quad (5.35)$$

Proposition 5. *Under the action of the designed controller (5.26) and adaptation law (5.29) with the event-triggered scheme (5.13), the robot dynamics (5.12) is stable in the sense of Lyapunov and all states of closed-loop system are bounded. Furthermore, the tracking errors converge to the origin as $t \to \infty$. Moreover, Zeno behavior is excluded under the proposed ET scheme.*

Proof. Based on the previous analysis, the triggering function (5.35) was finally defined in a way that guarantees the time derivative of Lyapunov function $V_2 = \frac{1}{2}\sum_{i=1}^{n} Z_i^T Z_i + \frac{1}{2}\tilde{\Theta}^T\Gamma_1^{-1}\tilde{\Theta} + \frac{1}{2}\tilde{P}^T\Gamma_2^{-1}\tilde{P}$ to be negative semi-definite. Thus, the stability in the sense of Lyapunov is ensured under proposed event-triggered scheme and all closed-loop signals are bounded. On the other hand, the boundedness of the auxiliary compensating system (5.14) is also required to complete the proof. Let us take $V_\eta = \frac{1}{2}\eta_1^T\eta_1 + \frac{1}{2}\eta_2^T\eta_2$ as Lyapunov function candidate whose derivative is given as

$$\begin{aligned}\dot{V}_\eta &= -\eta_1^T\kappa_1\eta_1 + \eta_1^T S\eta_2 + \eta_2^T\hat{G}u(t) - \eta_2^T\hat{G}u(t-\tau) \\ &\leq -\kappa_1\|\eta_1\|^2 + \|\eta_1\|\|S\|\|\eta_2\| + \|\eta_2^T\hat{G}\|\|u(t)\| + \|\eta_2^T\hat{G}\|\|u(t-\tau)\| \\ &\leq -(\kappa_1 - \frac{1}{2})\|\eta_1\|^2 + \bar{O} \end{aligned} \tag{5.36}$$

where $\bar{O} = \frac{\|u(t)\|^2}{2} + \frac{\|u(t-\tau)\|^2}{2} + \frac{\|\eta_2\|^2}{2} + \|\hat{G}\eta_2\|^2$. Since the control input (5.26) is a function of all bounded signals, the term $\bar{O}$ is bounded. Moreover, by choosing $\kappa_1 > \frac{1}{2}$, boundedness of auxiliary variables is ensured.

The convergence of the tracking errors can be directly proved similar to the analysis in Proposition 3 by invoking Barbalat lemma [97]. Furthermore, the proof of Zeno exclusion presented in Proposition 1 is still valid and can be directly applied in this scenario. □

5.3.3 Experimental Results

To validate the obtained theoretical results and demonstrate the applicability of the proposed ETAC scheme, a real-time experimental study is presented in this section for the trajectory tracking problem of mobile robot (5.12). The experiment setup that is shown in Fig. 5.3 consists of PatrolBot, on-board computer, remote-center, and camera (vision system). The PatrolBot is a programmable differential-drive mobile robot manufactured by Adept MobileRobots Inc. for research purposes. It can be programmed and controlled using ARIA (Advanced Robotics Interface for Applications). The control algorithm is implemented on a remote-center using MATLAB. The on-board computer receives the control commands through IEEE 802.11g wireless channel and actuates the motors using ARIA functions written in C++ language. The communications are based on client/server architecture. It is worth mentioning that localization (position and orientation) is acquired by the vision system. The camera is directly connected to the remote-control unit via a wired connection. Hence, no network restrictions in the robot-to-controller channel.

Figure 5.3: Experiment setup

A lemniscate path is chosen as a reference trajectory and it is defined as

$$x_{ref} = \frac{a_{ref}\sin(w_{ref}t)}{1+\sin^2(w_{ref}t)}\ ,\ y_{ref} = \frac{a_{ref}\sin(w_{ref}t)\cos(w_{ref}t)}{1+\sin^2(w_{ref}t)}, \tag{5.37}$$

where $a_{ref} = 1.2$ and $w_{ref} = 0.1$. The initial position of the robot is mainly chosen as $(0, 0, 10)$. Other parameters are chosen as $C_1 = \text{diag}(0.8,\ 0.9,\ 1.2)$, $C_2 = \text{diag}(4,\ 4)$, $\kappa_1 = 6$, $\Gamma_1 = I_4$, $\Gamma_2 = I_3$ and $\tau = 0.1$ [s]. Three different values are considered for the adjustable parameter of event-triggered condition ($\zeta = 0.4,\ 0.6$ and 0.8).

The obtained experimental results under proposed controller (5.26), adaptive law (5.29), and triggering function (5.35) on robot dynamics (5.12) are illustrated in Fig. 5.4–5.9. The tracking performance in the X-Y plane for different values of ζ is shown in Fig. 5.4. It can be observed that the designed controller is able to compensate for input delays while achieving accurate tracking. Furthermore, the proposed event-triggered and time-triggered control signals are illustrated in Fig. 5.5 and Fig. 5.6. To evaluate the tracking performance under the proposed scheme, the integral square error (ISE) and the maximum of the absolute tracking errors are provided. Moreover, the L_2 norm of the

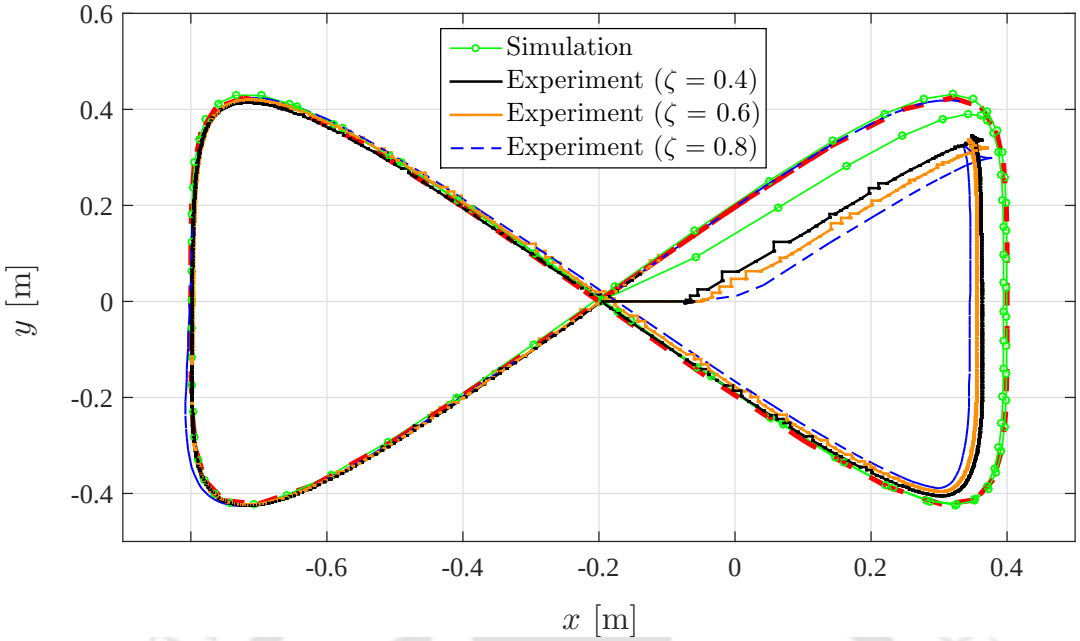

Figure 5.4: Trajectory tracking in X-Y plane for different values of ζ.

control signal is also provided for each value of ζ. The experiments are repeated 15 times (5 for each value of ζ) and the average values of the obtained results are summarized in Table 5.1.

In order to further show the effectiveness of the proposed control scheme in handling the effects of parametric uncertainties and input delays, several simulations are also conducted under different scenarios where these effects are mutually deactivated. In the first scenario, the effect of uncertainties in system parameters is evaluated assuming ideal communications ($\tau = 0$). The parametric uncertainties are defined as $\Theta(t) = \Theta(0) + \Delta\Theta$ wherein $\Delta\Theta = \frac{1}{2}\Theta(0)\sin(t)$. The system performance under this scenario using the kinematic controller and dynamic controller with/without adaptation is shown in Figs. 5.7a–5.7c. The tracking performance under different initial conditions is also shown in Fig. 5.7d and the obtained results are summarized in Table 5.2. On the other hand, the induced delay is considered in the second scenario assuming known parameters ($\Delta\Theta = 0$). The effect of input delay on system performance and stability is illustrated in Fig. 5.8, in which the trajectories in the X-Y plane with and without the incorporation of the auxiliary compensation variables are depicted in Fig. 5.8a and Fig. 5.8b, respectively. It can be observed from the obtained results that the auxiliary system is capable to compensate for input delays and achieve accurate tracking. However, as the input delay increases, the system performance degrades and it may become unstable for larger input delays. From the zoomed figure, it can also be observed that the overshoot is increasing for the case of

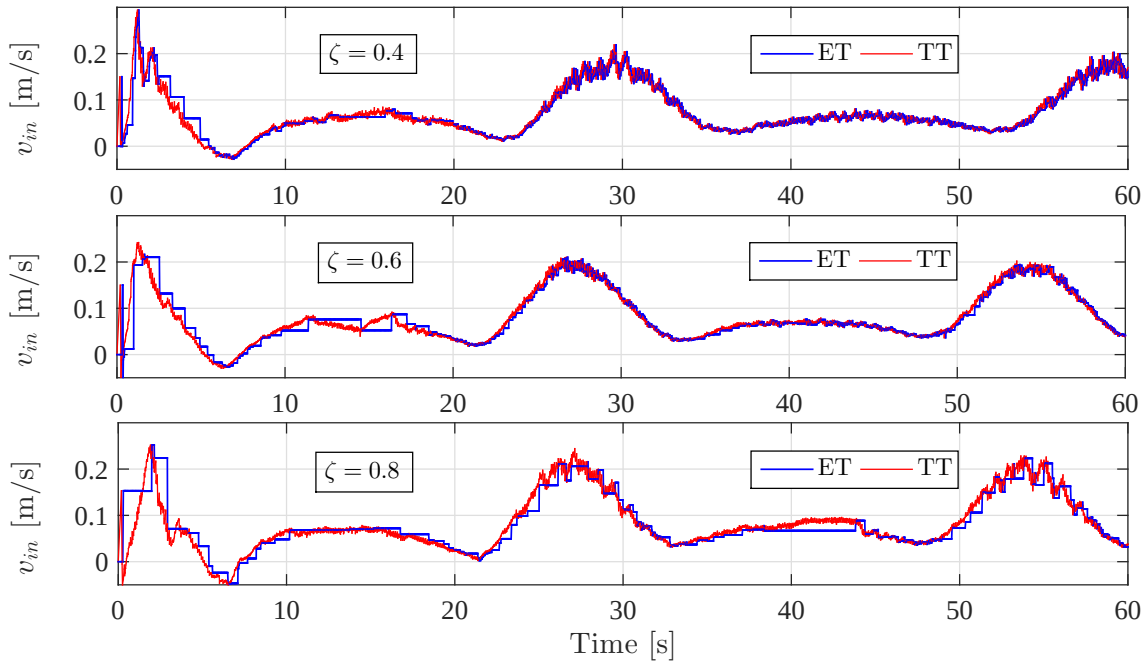

Figure 5.5: Event-triggered and time-triggered linear velocities for different values of ζ.

$\tau > 0.3$. Moreover, the performance is further degraded and a large tracking error is obtained for the case of $\tau > 1$, which is undesirable for practical applications. On the other hand, the actual trajectory converges to the desired one comparatively faster in case of $\tau < 0.3$. Besides, Fig. 5.9 depicts the triggering time instants for each value of ζ where the actual control is updated/transmitted through the network. It can be observed that, as the value of ζ increases and approaches 1, the number of triggering/transmissions decreases. Hence, the communication burden is significantly reduced. However, these savings in resources are achieved at the cost of tracking accuracy and control efforts. Yet, a trade-off between the resource utilization in tandem with an acceptable performance could be achieved by adjusting ζ. The channel usage is calculated as

$$\text{Channel Usage} = \text{Number of Updates} \times \frac{dt}{T} \times 100\ \% \tag{5.38}$$

where dt and T are sampling time and the total time of experiment run, respectively. As compared to time-triggered (TT) implementation, it is worth mentioning that 3000 control updates/transmissions are needed for 60 seconds of the experiment run under 0.02 sampling interval for the TT scenario. It can be observed that this number is further decreased under the proposed ET strategy yielding a significant saving in the usage of network resources.

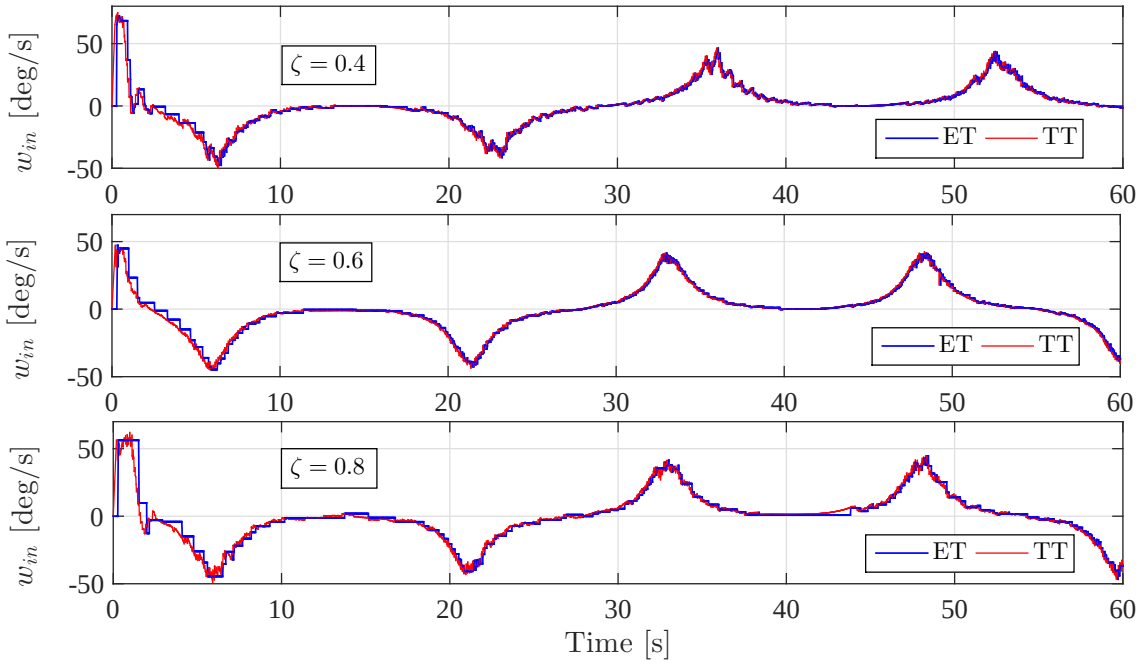

Figure 5.6: Event-triggered and time-triggered angular velocities for different values of ζ.

Table 5.1: Comparison of results for different values of the adjustable parameter ζ.

	Resource utilizations			Performance metrics			
				Tracking error			
	#Control update	%Channel usage	%Saving	ISE	Max Absolute Error [0-T/2]	Max Absolute Error [T/2-T]	L_2 norm (u)
$\zeta = 0.4$	1774	59.13	40.87	0.083	0.14	0.036	18.00
$\zeta = 0.6$	726	24.21	75.79	0.095	0.16	0.040	18.38
$\zeta = 0.8$	271	9.04	90.96	0.102	0.17	0.047	19.68

Table 5.2: Comparison of results for different initial conditions.

Initial condition	Resource utilizations			Performance metrics			
				Tracking error			
	#Control update	%Channel usage	%Saving	ISE	Max Absolute Error [0-T/2]	Max Absolute Error [T/2-T]	L_2 norm (u)
(0.1,0)	231	6.60	93.40	0.09	0.13	0.032	19.96
(-0.4,-0.1)	243	6.95	93.05	0.23	0.41	0.031	20.80
(-0.1,-0.2)	216	6.17	93.83	0.37	0.29	0.032	20.82
(-0.4,0.2)	219	6.26	93.74	0.45	0.41	0.030	20.32

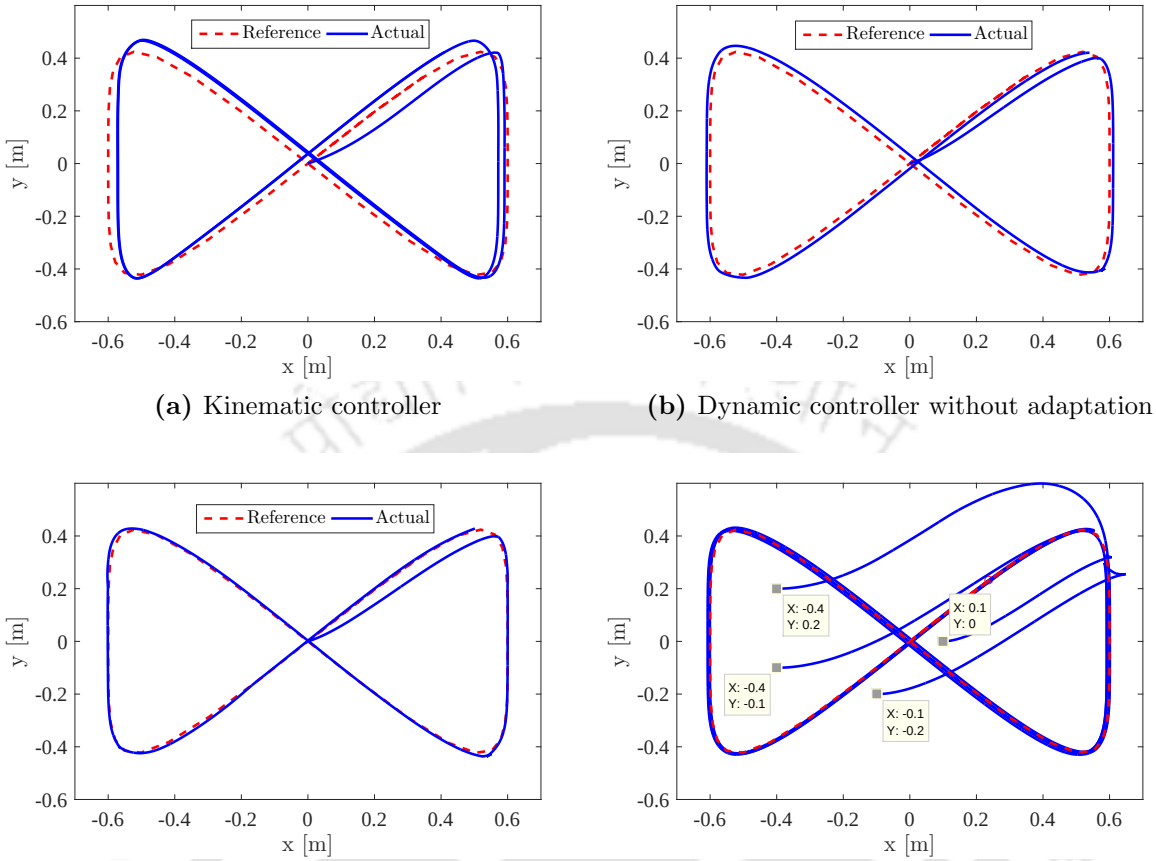

(a) Kinematic controller (b) Dynamic controller without adaptation

(c) Dynamic controller with adaptation (d) Initial condition trials

Figure 5.7: The effect of system uncertainties and different initial conditions.

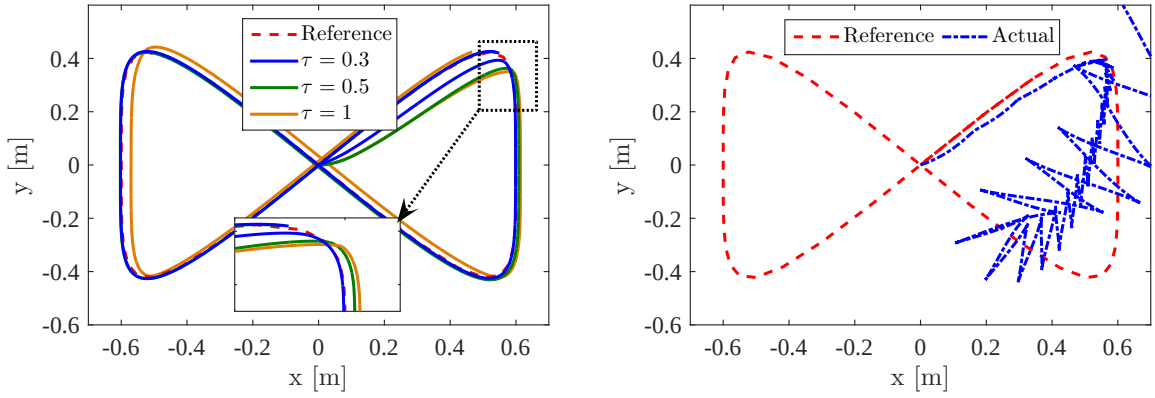

(a) With auxiliary compensation (b) Without auxiliary compensation

Figure 5.8: The effect of input delay.

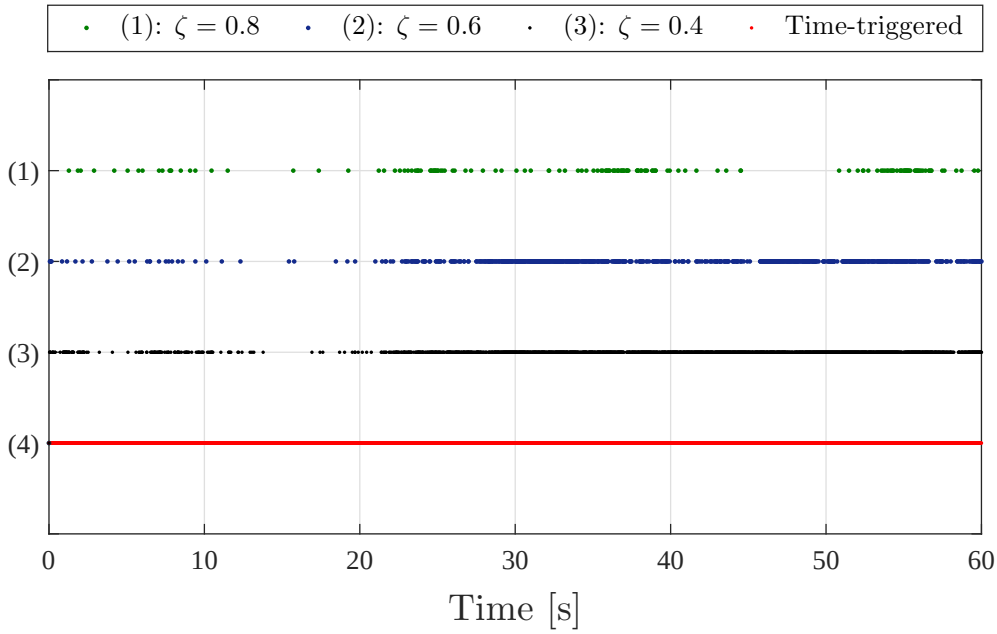

Figure 5.9: Illustration of triggering events for different values of ζ in comparison with time-triggered implementation (TT).

5.4 Design and Implementation of Predictor-based Event-triggered Controller over Robot-to-Controller Channel with State/Input Delays

5.4.1 Problem Formulation

Let us now consider a nonholonomic wheeled mobile robot controlled via a network channel under limited resources and subject to both state and input delays. The block diagram of the considered configuration is shown in Fig. 5.10. From Section 5.2, the combined kinematic and dynamic models of the mobile robot under state and input delays can be given as

$$\begin{aligned} \dot{q}_{\tau_{rc}} &= S(q_{\tau_{rc}})\nu_{\tau_{rc}}, \\ \dot{\nu}_{\tau_{rc}} &= \varphi(\nu_{\tau_{rc}})\Theta + Gu(t-\tau) \end{aligned} \tag{5.39}$$

where $q_{\tau_{rc}} := q(t-\tau_{rc}) = [x_{\tau_{rc}}\ y_{\tau_{rc}}\ \theta_{\tau_{rc}}]^T$, $\nu_{\tau_{rc}} = [v_{\tau_{rc}}\ w_{\tau_{rc}}]^T$ and $S(q_{\tau_{rc}}) = \begin{bmatrix} \cos\theta_{\tau_{rc}} & 0 \\ \sin\theta_{\tau_{rc}} & 0 \\ 0 & 1 \end{bmatrix}$

$$\varphi(\nu_{\tau_{rc}}) = \begin{bmatrix} -v_{\tau_{rc}} & w_{\tau_{rc}}^2 & 0 & 0 \\ 0 & 0 & -v_{\tau_{rc}}w_{\tau_{rc}} & -w_{\tau_{rc}} \end{bmatrix}, \text{ and } u(t-\tau) = \begin{bmatrix} v_{in}(t-\tau) & w_{in}(t-\tau) \end{bmatrix}^T \tag{5.40}$$

where $\tau = \tau_{rc} + \tau_{cr}$ is the round-trip time delay, in which τ_{rc} and τ_{cr} are the delays in the robot-to-controller and controller-to-robot channels, respectively. Let $\Theta := [\Theta_1\ \Theta_2\ \Theta_3\ \Theta_4]^T$ and $G := diag(g_1, g_2)$. Then, the overall mathematical model of the robot can be written as

$$\begin{aligned} \dot{x}_{\tau_{rc}} &= v_{\tau_{rc}}\cos\theta_{\tau_{rc}} \\ \dot{y}_{\tau_{rc}} &= v_{\tau_{rc}}\sin\theta_{\tau_{rc}} \\ \dot{\theta}_{\tau_{rc}} &= w_{\tau_{rc}} \\ \dot{v}_{\tau_{rc}} &= -\Theta_1 v_{\tau_{rc}} + \Theta_2 w_{\tau_{rc}}^2 + g_1 v_{in}(t-\tau) \\ \dot{w}_{\tau_{rc}} &= -\Theta_3 v_{\tau_{rc}} w_{\tau_{rc}} - \Theta_4 w_{\tau_{rc}} + g_2 w_{in}(t-\tau) \end{aligned} \tag{5.41}$$

Relative to Section 5.3.1 of this chapter, the internal and specification parameters of the robot represented by vector Θ and matrix G are assumed to be known in this section to further simplify the controller and predictor design. To deal with the network induced

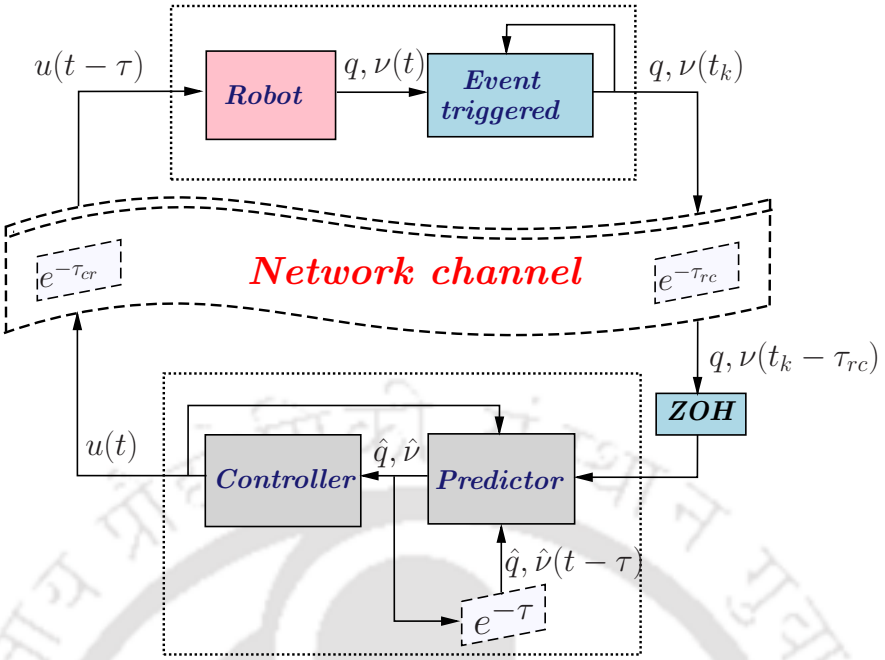

Figure 5.10: Block diagram of the system.

time delays, a state predictor is incorporated and designed as

$$\begin{aligned}
\dot{\hat{x}} &= \hat{v}\cos\hat{\theta} - k_1\big(\hat{x}(t-\tau) - x(t-\tau_{rc})\big)\\
\dot{\hat{y}} &= \hat{v}\sin\hat{\theta} - k_2\big(\hat{y}(t-\tau) - y(t-\tau_{rc})\big)\\
\dot{\hat{\theta}} &= \hat{w} - k_3\big(\hat{\theta}(t-\tau) - \theta(t-\tau_{rc})\big)\\
\dot{\hat{v}} &= -\Theta_1\hat{v} + \Theta_2\hat{w}^2 + g_1 v_{in}(t) - k_4\big(\hat{v}(t-\tau) - v(t-\tau_{rc})\big)\\
\dot{\hat{w}} &= -\Theta_3\hat{v}\hat{w} - \Theta_4\hat{w} + g_2 w_{in}(t) - k_5\big(\hat{w}(t-\tau) - w(t-\tau_{rc})\big)
\end{aligned} \tag{5.42}$$

Besides, an event-triggered scheme is proposed in the robot-to-controller channel to reduce the communication and computation burden as follows

$$q^{ET}(t) = q(t_k), \quad \nu^{ET}(t) = \nu(t_k) \quad | \quad \forall t \in [t_k, t_{k+1}) \tag{5.43}$$

in which

$$t_{k+1} = \inf\{t|\ t > t_k, \quad J(e^{ET}, Z_1, Z_2) > 0\} \tag{5.44}$$

where $q^{ET} = [x^{ET}, y^{ET}, \theta^{ET}]^T$ and $\nu^{ET} = [v^{ET}, w^{ET}]^T$ denote the last-received states from the robot. The triggering function $J(e^{ET}, Z_1, Z_2)$ is to be designed later in a way that ensures the stability of overall closed-loop control system under the event-triggered

implementation. Here, the measurement error is defined as $e^{ET} = [e_q^{ET} \; e_\nu^{ET}]$, in which $e_q^{ET}(t) = q(t) - q^{ET}(t)$ and $e_\nu^{ET}(t) = \nu(t) - \nu^{ET}(t)$.

5.4.2 Predictor-based Control Design

5.4.2.1 State Predictor

Let us define the prediction error as

$$e_x = \hat{x}(t-\tau) - x(t-\tau_{rc}) \tag{5.45}$$
$$e_y = \hat{y}(t-\tau) - y(t-\tau_{rc}) \tag{5.46}$$
$$e_\theta = \hat{\theta}(t-\tau) - \theta(t-\tau_{rc}) \tag{5.47}$$
$$e_v = \hat{v}(t-\tau) - v(t-\tau_{rc}) \tag{5.48}$$
$$e_w = \hat{w}(t-\tau) - w(t-\tau_{rc}) \tag{5.49}$$

Then, we have

$$\begin{aligned}\dot{e}_x &= -k_1 e_x(t-\tau) + \hat{v}_\tau \cos\hat{\theta}_\tau - v_{\tau_{rc}} \cos\theta_{\tau_{rc}} \\ &= -k_1 e_x(t-\tau) + e_v \cos(e_\theta + \theta_{\tau_{rc}}) + v_{\tau_{rc}} \cos(e_\theta + \theta_{\tau_{rc}}) - v_{\tau_{rc}} \cos\theta_{\tau_{rc}}\end{aligned} \tag{5.50}$$

The linearized form of (5.50) is given as

$$\dot{e}_x = -k_1 e_x(t-\tau) - v_{\tau_{rc}} \sin(\theta_{\tau_{rc}}) e_\theta + \cos\theta_{\tau_{rc}} e_v \tag{5.51}$$

Similarly, we get

$$\dot{e}_y = -k_2 e_y(t-\tau) + v_{\tau_{rc}} \cos(\theta_{\tau_{rc}}) e_\theta + \sin\theta_{\tau_{rc}} e_v \tag{5.52}$$
$$\dot{e}_\theta = -k_3 e_\theta(t-\tau) + e_w \tag{5.53}$$

We also have

$$\begin{aligned}\dot{e}_v &= -k_4 e_v(t-\tau) - \Theta_1 \hat{v}_\tau + \Theta_2 \hat{w}_\tau^2 + \Theta_1 v_{\tau_{rc}} - \Theta_2 w_{\tau_{rc}}^2 \\ &= -k_4 e_v(t-\tau) - \Theta_1 e_v + \Theta_2 (e_w + w_{\tau_{rc}})^2 - \Theta_2 w_{\tau_{rc}}^2 \\ &= -k_4 e_v(t-\tau) - \Theta_1 e_v + \Theta_2 e_w^2 + 2\Theta_2 w_{\tau_{rc}} e_w\end{aligned} \tag{5.54}$$

and

$$\begin{aligned}\dot{e}_w &= -k_5 e_w(t-\tau) - \Theta_3 \hat{v}_\tau \hat{w}_\tau - \Theta_4 \hat{w}_\tau + \Theta_3 v_{\tau_{rc}} w_{\tau_{rc}} + \Theta_4 w_{\tau_{rc}} \\ &= -k_5 e_w(t-\tau) - \Theta_3 \big(e_v e_w + w_{\tau_{rc}} e_v + v_{\tau_{rc}} e_w\big) - \Theta_4 e_w\end{aligned} \tag{5.55}$$

The linearized form of (5.54) and (5.55) are given as

$$\dot{e}_v = -k_4 e_v(t-\tau) - \Theta_1 e_v + 2\Theta_2 w_{\tau_{rc}} e_w \tag{5.56}$$

$$\dot{e}_w = -k_5 e_w(t-\tau) - \Theta_3\big(w_{\tau_{rc}} e_v + v_{\tau_{rc}} e_w\big) - \Theta_4 e_w \tag{5.57}$$

Let $e = [e_x\ e_y\ e_\theta\ e_v\ e_w]^T$. The full error dynamics can be written in the following form

$$\dot{e} = -Ke(t-\tau) + \Psi \tag{5.58}$$

where

$$K = \begin{pmatrix} k_1 & 0 & 0 & 0 & 0 \\ 0 & k_2 & 0 & 0 & 0 \\ 0 & 0 & k_3 & 0 & 0 \\ 0 & 0 & 0 & k_4 & 0 \\ 0 & 0 & 0 & 0 & k_5 \end{pmatrix} \quad \text{and} \quad \Psi = \begin{pmatrix} -v_{t_{rc}} \sin(\theta_{\tau_{rc}}) e_\theta + cos(\theta_{\tau_{rc}}) e_v \\ v_{t_{rc}} \cos(\theta_{\tau_{rc}}) e_\theta + sin(\theta_{\tau_{rc}}) e_v \\ e_w \\ -\Theta_1 e_v + 2\Theta_2 w_{\tau_{rc}} e_w \\ -\Theta_3\big(w_{\tau_{rc}} e_v + v_{\tau_{rc}} e_w\big) - \Theta_4 e_w \end{pmatrix} \tag{5.59}$$

Proposition 6. *Let us consider the state predictor (5.42) of system (5.41) along with the prediction error dynamics (5.58). If there exists a positive gain matrix (K) for which the following condition is satisfied*

$$\lambda_{min}(K) - \lambda_{min}(K^2)\sqrt{q}\tau - \lambda_{min}(K)\Upsilon\tau - \Upsilon > 0\ , \tag{5.60}$$

where $\lambda_{min}(.)$ denotes the smallest eigenvalues of $(.)$ and Υ is a positive bound to be defined later, then, the prediction error $e(t) \to 0$ as $t \to \infty$.

Proof. Let us choose the Lyapunov function candidate as $V_p = \frac{1}{2}e^T e$ whose time derivative is given as

$$\dot{V}_p = e^T \dot{e} = -e^T(Ke(t-\tau) - \Psi) \tag{5.61}$$

From Leibnitz's formula, we have

$$e(t-\tau) = e(t) - \int_{t-\tau}^{t} \dot{e}(\rho) d\rho \tag{5.62}$$

Substituting (5.62) in (5.61), one gets

$$\dot{V}_p = -e^T\Big(Ke(t) + K^2 \int_{t-\tau}^{t} e(\rho-\tau)d\rho + K\int_{t-\tau}^{t}\Psi(\rho)d\rho - \Psi\Big) \tag{5.63}$$

$$\leq -\lambda_{min}(K)\|e\|^2 - e^T K^2 \int_{t-\tau}^{t} e(\rho-\tau)d\rho - e^T K \int_{t-\tau}^{t} \|\Psi(\rho)\|d\rho + \|e\|\|\Psi\| \tag{5.64}$$

Under the assumption that the magnitude of linear and angular velocities are bounded,

the norm of the term Ψ can be written as

$$\begin{aligned}\|\Psi\| &\leq V^*|e_\theta| + |e_v| + V^*|e_\theta| + |e_v| + |e_w| + \Theta_1|e_v| + 2\Theta_2 W^*|e_w| \\ &\quad + \Theta_3 W^*|e_v| + \Theta_3 V^*|e_w| + \Theta_4|e_w| \\ &\leq \Upsilon\|e\| \end{aligned} \tag{5.65}$$

where $V^* = \max\big(|v_{\tau_{rc}}|\big)$, $W^* = \max\big(|w_{\tau_{rc}}|\big)$ and $\Upsilon = \max\big(2V^*,\ 2 + \Theta_1 + 2\Theta_2 W^*,\ 1 + 2\Theta_2 W^* + \Theta_3 V^* + \Theta_4\big)$.

Using (5.65) and the relation that says $V_p\big(e(t+\gamma)\big) \leq qV_p\big(e(t)\big)$ for $-2\tau \leq \gamma \leq 0$ and $q > 1$, one gets

$$\begin{aligned}\dot{V}_p &\leq -\lambda min(K)\|e\|^2 + \lambda_{min}(K^2)\sqrt{q}\tau\|e\|^2 + \lambda_{min}(K)\Upsilon\tau\|e\|^2 + \Upsilon\|e\|^2 \\ &= -\big(\lambda_{min}(K) - \lambda_{min}(K^2)\sqrt{q}\tau - \lambda_{min}(K)\Upsilon\tau - \Upsilon\big)\|e\|^2 \end{aligned} \tag{5.66}$$

Herein, if the condition (5.60) is satisfied, $\dot{V}_p$ becomes negative definite which implies that $V_p \to 0$ as $t \to \infty$. As a result, we can conclude that the prediction error $e(t) \to 0$ as $t \to \infty$. This completes the proof. □

5.4.2.2 Predictor-based Event-triggered Control Design

The proposed event-triggered controller is designed based on the backstepping approach that is here composed of two steps. Based on the predicted states, the virtual controller is designed in the first step. Then, the actual control law is proposed in the second step. At each step, a triggering condition is derived by maintaining the derivative of Lyapunov function to be negative semi-definite. Thus, the overall closed-loop system can be proved to be stable in the sense of Lyapunov. Let us first defined the error variables as

$$Z_1 = \hat{q} - q_r, \quad Z_2 = \hat{\nu} - \alpha_1 \tag{5.67}$$

where $\hat{q}$ and $\hat{\nu}$ are the predicted states, $q_r = [x_{ref}\ \ y_{ref}\ \ \theta_{ref}]^T$ represents the position and orientation of the reference trajectory, and α_1 is the virtual control law to be designed in the first step of design process. The event-triggered error variables are then given as

$$Z_1^{ET} = \hat{q}^{ET} - q_r, \quad Z_2^{ET} = \hat{\nu}^{ET} - \alpha_1 \tag{5.68}$$

where $\hat{q}^{ET}$ and $\hat{\nu}^{ET}$ are the event-triggered of predicted states.

Step 1: The first error dynamic subsystem is given as

$$\dot{Z}_1 = \dot{\hat{q}} - \dot{q}_r = \hat{S}\hat{\nu} - \dot{q}_r = \hat{S}\left(Z_2 + \alpha_1\right) - \dot{q}_r \tag{5.69}$$

where $\hat{S} = S(\hat{q})$. The Lyapunov function candidate is chosen in this step as $V_1 = \frac{1}{2}Z_1^T Z_1$.

Differentiating V_1 with respect time along the trajectories of the system (5.39) is

$$\dot{V}_1 = Z_1^T \dot{Z}_1 = Z_1^T \left(\hat{S} Z_2 + \hat{S}\alpha_1 - \dot{q}_r + \hat{S}^{ET}\alpha_1 - \hat{S}^{ET}\alpha_1 \right) \tag{5.70}$$

where $\hat{S}^{ET} = S(\hat{q}^{ET})$. Let us now design the virtual controller α_1 such as

$$\hat{S}^{ET}\alpha_1 = -C_1 Z_1^{ET} + \dot{q}_r \tag{5.71}$$

where $C_1 \in \mathbb{R}^{3\times 3}$ is a gain matrix with positive diagonal elements. Since $\hat{S}^T\hat{S} = I_2$ where $I_2 \in R^{2\times 2}$ is identity matrix, one gets

$$\alpha_1 = (\hat{S}^{ET})^T \hat{S}^{ET}\alpha_1 = -(\hat{S}^{ET})^T (C_1 Z_1^{ET} - \dot{q}_r) \ . \tag{5.72}$$

As compared to Subsection 5.3.2, it is to be noted that the virtual controller is designed here based on the event-triggered predicted states rather than the actual states. Substituting (5.71) in (5.70), one gets,

$$\begin{aligned} \dot{V}_1 &= Z_1^T \left(\hat{S} Z_2 + (\hat{S} - \hat{S}^{ET})\alpha_1 - C_1 Z_1^{ET} \right) \\ &= -Z_1^T C_1 Z_1 + Z_1^T \hat{S} Z_2 + Z_1^T C_1 e_q^{ET} + Z_1^T (\hat{S} - \hat{S}^{ET})\alpha_1 \\ &\leq -Z_1^T C_1 Z_1 + Z_1^T \hat{S} Z_2 + \|C_1\|Z_1\|\|e_q^{ET}\| + \|\alpha_1\|Z_1\|\|e_q^{ET}\| \end{aligned} \tag{5.73}$$

Let us now add and subtract the term $\zeta Z_1^T C_1 Z_1$ from (5.73) and then design the first triggering condition as

$$\|e_q^{ET}\| \leq \frac{\|C_1\|}{\|C_1\| + \|\alpha_1\|} \zeta \|Z_1\| \tag{5.74}$$

With (5.74), the time derivative of Lyapunov function becomes

$$\dot{V}_1 \leq -(1-\zeta) Z_1^T C_1 Z_1 + Z_1^T \hat{S} Z_2 \tag{5.75}$$

Step 2: Let us choose the Lyapunov function candidate in this step as $\dot{V}_2 = V_1 + \frac{1}{2} Z_2^T Z_2$. Differentiating V_2 with respect time along the trajectories of the system (5.39) is

$$\dot{V}_2 \leq -(1-\zeta) Z_1^T C_1 Z_1 + Z_1^T \hat{S} Z_2 + Z_2^T \dot{Z}_2 \tag{5.76}$$

The dynamics of the second error variable is given as

$$\dot{Z}_2 = \dot{\hat{\nu}} - \dot{\alpha}_1 = \hat{\varphi}\Theta + Gu \tag{5.77}$$

where $\hat{\varphi} = \varphi(\hat{\nu})$. Here $\dot{\alpha} = 0$ as the control signal is constant between inter-event periods.

If the control law is designed as

$$u = -G^{-1}(C_2 Z_2^{ET} + \hat{S}^{ET} Z_1^{ET} - \hat{\varphi}^{ET}\Theta) \tag{5.78}$$

where $C_2 \in \mathbb{R}^{2\times 2}$ is a gain matrix with positive diagonal elements and $\hat{\varphi}^{ET} = \varphi(\hat{\nu}^{ET})$. The derivative of Lyapunov function becomes

$$\begin{aligned}
\dot{V}_2 &\leq -(1-\zeta)Z_1^T C_1 Z_1 - Z_2^T C_2 Z_2 + Z_2^T C_2 e_\nu^{ET} + Z_1^T \hat{S} Z_2 \\
&\quad - Z_2^T (\hat{S}^{ET})^T Z_1^{ET} + Z_2^T (\hat{\varphi} - \hat{\varphi}^{ET})\Theta \\
&\leq -(1-\zeta)Z_1^T C_1 Z_1 - Z_2^T C_2 Z_2 + \|C_2\|\|Z_2\|\|e_\nu^{ET}\| \\
&\quad + Z_1^T (\hat{S} - \hat{S}^{ET}) Z_2 - (e_q^{ET})^T (\hat{S}^{ET})^T Z_2 + Z_2^T (\hat{\varphi} - \hat{\varphi}^{ET})\Theta \\
&\leq -(1-\zeta)Z_1^T C_1 Z_1 - Z_2^T C_2 Z_2 + \|C_2\|\|Z_2\|\|e_\nu^{ET}\| \\
&\quad + \|Z_1\|\|Z_2\|\|e_\nu^{ET}\| + \|Z_2\|\|e_\nu^{ET}\| + L\|\Theta\|\|Z_2\|\|e_\nu^{ET}\|
\end{aligned} \tag{5.79}$$

Let us now add and subtract the term $\zeta Z_2^T C_2 Z_2$ from (5.79) and then design the second triggering condition as

$$\|e_\nu^{ET}\| \leq \frac{\|C_2\|}{\|C_2\| + \|Z_1\| + L\|\Theta\|\|Z_2\| + 1}\zeta\|Z_2\| \tag{5.80}$$

With (5.80), the time derivative of Lyapunov function becomes

$$\dot{V}_2 \leq -(1-\zeta)\left(Z_1^T C_1 Z_1 + Z_2^T C_2 Z_2\right) \tag{5.81}$$

By choosing $0 < \zeta < 1$, the negative semi-definite of $\dot{V}_2$ can be ensured, and therefore, the overall system is stable in the sense of Lyapunov and all closed-loop signals are bounded.

5.4.3 Experimental Results

In this section, the trajectory tracking problem of a commercial mobile robot is presented. The obtained experimental results demonstrate the applicability of the proposed control scheme and validate the theoretical results presented in Subsection 5.4.2. The experiment setup is shown in Fig. 5.3. However, the states in this section are directly obtained and received from the robot via a wireless channel (IEEE 802.11g) i.e. the network restrictions are also imposed in the robot-to-controller channel. The on-board computer also receives the control commands through a wireless channel, and the motors are then actuated using ARIA functions. A circular reference trajectory is defined as $x_{ref} = r\sin(w_{ref}t)$ and $y_{ref} = -r\cos(w_{ref}t) + r$ where $r = 0.6$ [m] and $w_{ref} = 0.5$ [rad/s]. The initial position of the robot is chosen as $(0, 0.4)$. Other parameters are selected as $C_1 = \text{diag}(0.3, 0.3, 0.1)$, $C_2 = \text{diag}(6, 4)$, $K = \text{diag}(2, 2, 2, 2, 2)$, $\zeta = 0.6$ and

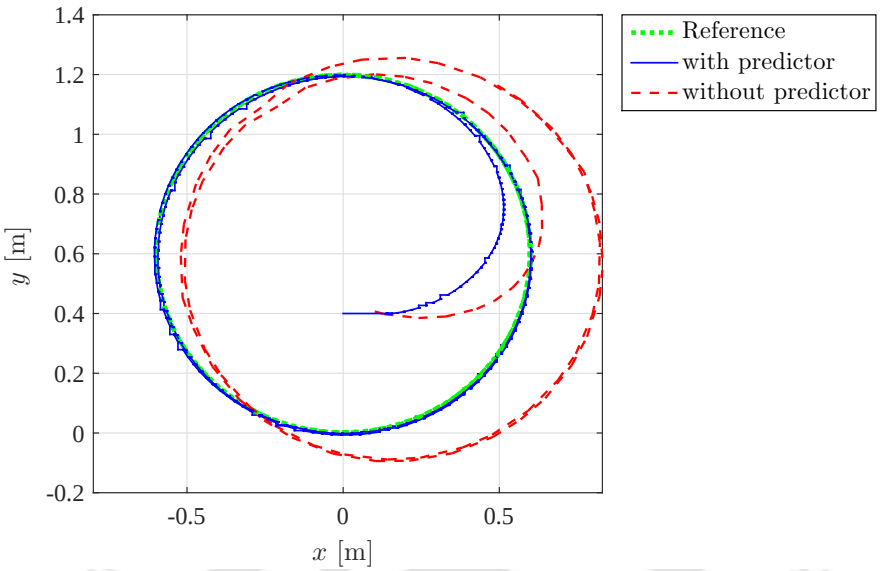

Figure 5.11: Trajectory tracking in the X-Y plane.

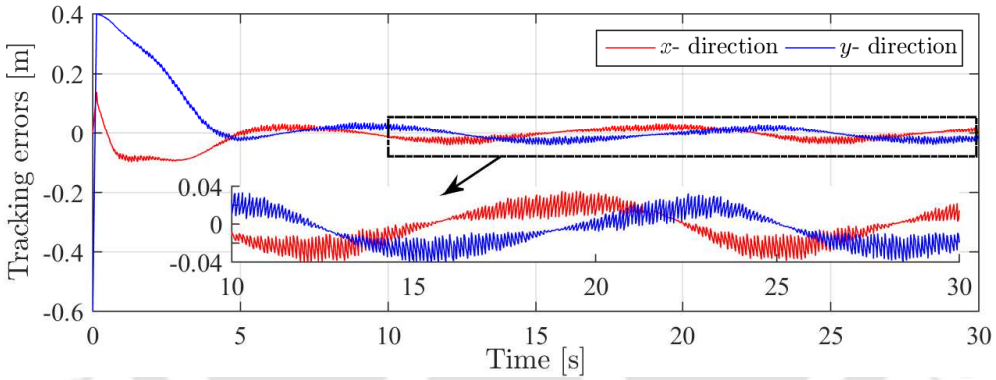

Figure 5.12: Tracking errors under the predictor-based control scheme.

$L = 1$. The delay in the robot-to-controller and controller-to-robot channels are chosen as $\tau_{rc} = \tau_{cr} = 0.1$ [s], i.e. $\tau = 0.1 + 0.1 = 0.2$ [s].

The obtained experimental results under the proposed predictor-based controller and event-triggered mechanism are illustrated in Fig. 5.11– 5.15. The performance of trajectory tracking in the X-Y plane with and without the designed state-predictor is shown in Fig. 5.11. Moreover, the tracking errors are depicted in Fig. 5.12. It can be observed that in spite of the presence of both state and input delays, the tracking errors converge to small set around zero and the designed predictor-based controller is able to achieve accurate tracking. Besides, both the time-triggered and the proposed event-triggered control signals are depicted in Fig. 5.13. It can be observed that the event-triggered control is held constant till the next triggering instant which is defined according to the designed triggering condition. This not only reduces the communication burden and

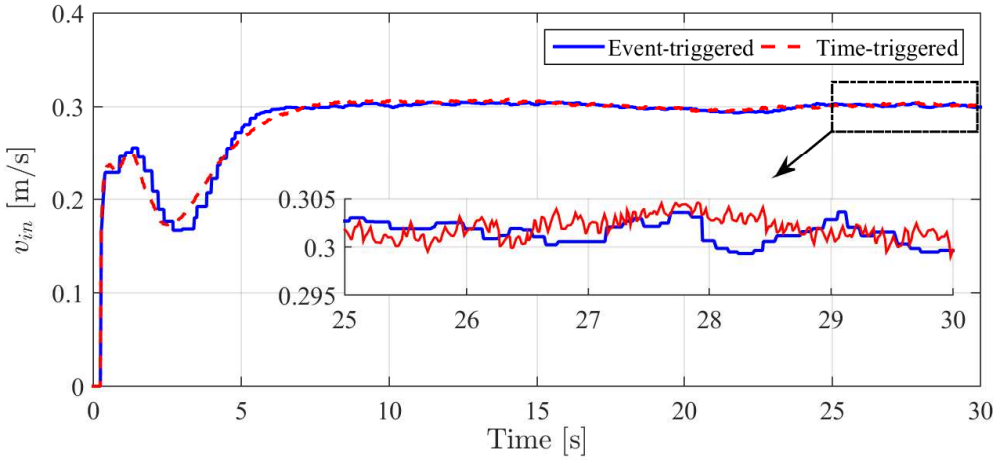

(a) Linear velocity

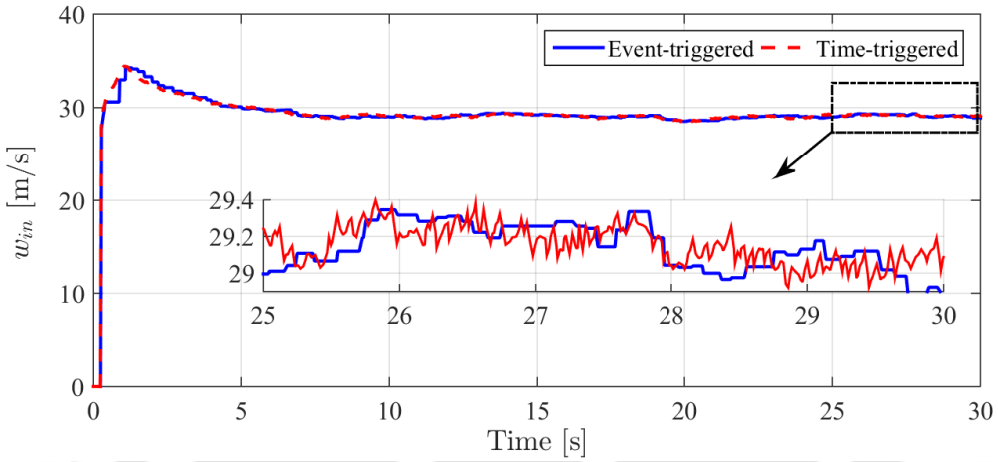

(b) Angular velocity

Figure 5.13: Comparison of event-triggered and time-triggered control signals.

computational efforts, but also helps in protecting the actuators as it eliminates the unnecessary oscillations in the control input. Furthermore, the triggering instants and inter-event times are illustrated in Fig. 5.14 and Fig. 5.15, respectively. As compared to the traditional time-triggered implementation where the data transmissions and control updates are carried out continuously every fixed sampling time is elapsed, these events have occurred just at the triggering instants with a dynamic rate in the event-triggered paradigm. It is evident that the number of triggering (control updates and transmissions) under the proposed event-triggered scheme is drastically decreased which yields a significant saving in the usage of network resources. From the perspective of resource utilization, the obtained results are compared to traditional time-triggered paradigm and event-triggered strategies [2, 4]. The comparison results are presented in Table 5.3, in which the total saving is calculated as the average of the achieved savings in the compu-

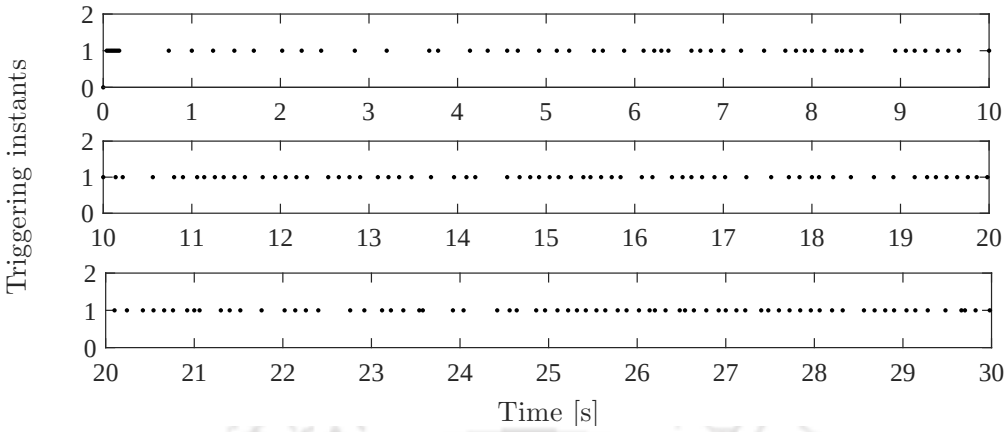

Figure 5.14: Illustration of triggering instants.

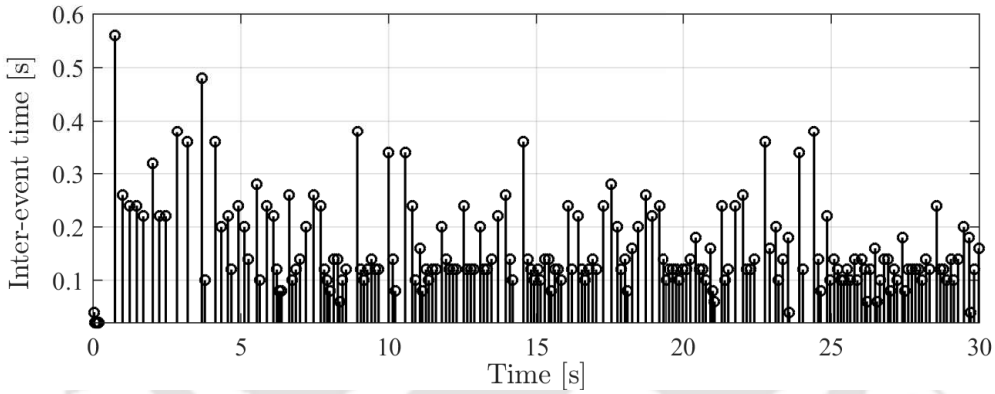

Figure 5.15: Inter-event times.

Table 5.3: Comparison of results with the time-triggered and event triggered strategies presented in [2] and [4].

		Resource utilizations			
		#Control update	Channel usage		Saving
			Robot-to-controller	Controller-to-robot	
Time-triggered		1500	100%	100%	-
Event-triggered	[2]	1500	100%	20%	about 40%
	[4]	100	100%	5-10%	about 45%
	Proposed	230	15%	15%	85%

tational effort and channel bandwidth in both channels. In the time-triggered approach, 1500 control updates/transmissions are always required for 30 seconds of simulation run subject to 0.02 sampling time. However, in the proposed triggering scheme, only 230 control updates/transmissions out of 1500 are required to achieve the control task which represents 15% of resource usage relative to time-triggered implementation. Regarding the event-triggering mechanisms presented in [2, 4], it is worth mentioning that these mechanisms are placed in the controller-to-plant channel only and continuous/periodic transmissions are assumed in the plant-to-controller channel. Therefore, the channel usage can be reduced on the controller side only. Moreover, in [2], computing of the actual control law is always required for evaluating the triggering condition and, therefore, the number of control updates cannot be reduced. Unlike these studies, the communication burden in both robot-to-controller and controller-to-robot channels can be reduced under the proposed control scheme. Furthermore, the number of control updates can also be decreased. This leads to more efficient utilization of channel bandwidth and computational resources, which is highly desirable for network-based applications.

Comparison with related works

In view of related studies in the context of trajectory tracking of mobile robots, it is observed that, due to hardware restrictions and robot operation mode, most of the studies that validate the theoretical results experimentally are mainly based on the kinematic model only [4, 43, 51–53, 55]. These works do not consider the dynamic model of the robot. In [70–72, 95], a modified velocity-based dynamic model is developed to tackle the hardware restrictions of available commercial mobile robots. However, these works are based on the traditional time-triggered paradigm and do not consider the scenario of controlling over a network or any other challenges such as limited resources or input/state delays. The above-mentioned studies are summarized and compared in Table 5.4. Relevant to these aforementioned works, the proposed control scheme deals with the scenario of controlling the mobile robot over the network and combines the challenges of input/state delays and limited resources scenario in a unified framework under event-triggered implementation.

5.5 Summary

In this chapter, an adaptive dynamic controller based on the backstepping method has been designed for the trajectory tracking problem of commercial mobile robots un-

Table 5.4: Comparison with related studies on mobile robots (K:= Kinematic, D:= Dynamic, TT:= Time-triggered, ET:= Event-triggered).

Reference	Model		Mechanism		Time delay		Network channel		Control signal	Platform
	K	D	TT	ET	Input	State	Sensor	Controller		
[4, 51]	✓	✗	–	✓	✗	✗	✗	✓	Velocity	Khepera-III
[52, 53]	✓	✗	–	✓	✓	✓	✓	✓	Velocity	Pioneer P3-DX
[54]	✓	✗	✓	✗	✗	✗	✗	✗	Velocity	QBot2
[55]	✓	✗	✓	✗	✓	✓	✓	✗	Velocity	NetCon-STM32
[62, 90, 91]	✓	✓	✓	✗	✗	✗	✗	✗	Torque	*Simulation*
[65, 92]	✓	✓	✓	✗	✗	✗	✗	✗	Voltage	*Simulation*
[93, 94]	✓	✓	–	✓	✗	✗	✗	✓	Torque	*Simulation*
[70, 72, 95]	✓	✓	✓	✗	✗	✗	✗	✗	Velocity	Pioneer P3-DX
[99]	✓	✓	–	✓	✓	✗	✗	✓	Velocity	PatrolBot
Proposed	✓	✓	–	✓	✓	✓	✓	✓	**Velocity**	**PatrolBot**

der network-induced delays, limited bandwidth, and hardware restrictions. A modified dynamic model has been first presented to overcome the hardware restrictions of commercial mobile robots. Thereafter, the event-triggered strategy has been employed to reduce the control updates and communication burden, in which an adjustable triggering condition was directly derived based on the derivative of Lyapunov function. To deal with the network-induced delays, an auxiliary compensation system has been presented to deal with input delay only. Another solution based on a state-predictor has also been developed to handle both state and input delays. It has been observed from experimental results that a significant saving in network resources is achieved under the proposed event-triggered schemes. Besides, the designed controllers cope with the input/state delays and ensure effective trajectory tracking.

6

Event-triggered Consensus Control of Multiple Mobile Robots

Contents

6.1 Introduction

Recent years have witnessed compelling attention and extensive studies on multi-agent systems. Without the cooperation of such agents, many practical applications and complex control tasks would not have been feasible. Consensus problem is a significant topic in multi-agent systems wherein the states of all agents converge to a common desired quantity. This states' agreement can be achieved in two manners, namely leader-follower and leaderless scenarios. Due to its wide applications and natural physical meaning, the leader-follower scheme has been widely attempted by control theorists and practitioners for linear [76–78, 100] and nonlinear [79–81] agents. The graph theory is widely employed to represent the communications in the network of multiple mobile robots [82–84]. Nevertheless, the communications between these agents generally occur periodically over a shared band-limited network channel. Such periodic communications result in inefficient utilization of resources, as explained in previous chapters.

In this chapter[1], the theoretical results of Chapter 4 are further extended to multi-agent systems. The consensus problem of a leader-followers network of multiple mobile robots under limited communication and input delays is attempted. Both kinematic and dynamic models are considered for mobile robot agents. To deal with limited bandwidth restrictions, an event-triggered strategy is incorporated at the controller-side resulting in reducing the communication burden. Besides, an auxiliary compensation system is also introduced to handle the input delays. Similar to previous chapters, the triggering instants are determined based on the sign of the derivative of Lyapunov function rather than employing fixed [22] or relative [96] triggering conditions. It is proved that under the proposed control scheme, all agents are practically converged to the leader and all system signals are bounded. Simulation results show the effectiveness of the proposed event-triggered scheme in terms of resource utilization as compared to traditional time-triggered control.

The work presented in this chapter represents an initial attempt toward the extension of the developed event-triggered control scheme to multi-agent systems. For simplicity, identical agents and an ideal environment with no loss of connections are assumed.

This chapter is organized as follows. A preliminary on graph theory is first introduced in Section 6.2. The problem is then formulated in Section 6.3. The consensus control design based on the backstepping approach and the event-triggering mechanism are presented in Section 6.4 and Section 6.4.1, respectively. Simulation results for two examples are shown in Section 6.5. The summary of this chapter is presented in Section 6.6.

[1]This chapter is based on the article: **S. Al Issa** and I. Kar, "Adaptive Backstepping Control of Multiple Mobile Robots under Limited Communication; An Event-triggered Approach," in *Communication and Control for Robotic Systems*, Springer, pp. 107-122. Springer, Singapore, 2021.

6.2 Preliminary on Graph Theory

In this section, some basic concepts of graph theory, which is utilized to represent the communication between the agents in the network, are briefly presented.
Let $G = \{V, E\}$ be a directed graph where V and E denote the sets of nodes and edges, respectively. The edges represent the communication between the agents (nodes). For example, an edge (i, j) in G implies that the agent j is able to receive information from agent i via direct communication. This does not imply that agent i can receive information from agent j in case of a direct graph. The set of neighbors for agent i are defined as $N_i = \{V_j |\ (V_j, V_i) \in E,\ i \neq j\}$. Let us now define the adjacency $A = [a_{i,j}] \in \mathbb{R}^{N\times N}$ and augmented $B = \text{diag}\{b_i\} \in \mathbb{R}^{N\times N}$ matrices. The adjacency matrix represent the communications of an agent with its neighbors. The element $a_{i,j}$ of the adjacency matrix are defined as follows.

$$a_{i,j} = \begin{cases} 1 & \text{if } (V_j, V_i) \in E \\ 0 & \text{Otherwise} \end{cases} \tag{6.1}$$

Let us also define the matrix $\bar{A} = \text{diag}\{\bar{a}_i\} \in \mathbb{R}^{N\times N}$ wherein its elements are defined as $\bar{a}_i = \sum_{j\in N_i} a_{i,j}$. On the other hand, the augmented matrix represents the communication of an agent with the leader. The elements b_i of this matrix are defined as follows.

$$b_i = \begin{cases} 1 & \text{if agent } i \text{ receives direct information from the leader} \\ 0 & \text{Otherwise} \end{cases} \tag{6.2}$$

Example:

Let us consider the following two directed graphs of leader-follower networks shown in Fig. 6.1. The matrices A, $\bar{A}$ and B for graph-I shown in Fig. 6.1a are given as

$$A = \begin{bmatrix} 0 & 0 & 0 & 0 \\ 1 & 0 & 0 & 0 \\ 1 & 0 & 0 & 0 \\ 0 & 0 & 1 & 0 \end{bmatrix},\ \bar{A} = \begin{bmatrix} 0 & 0 & 0 & 0 \\ 0 & 1 & 0 & 0 \\ 0 & 0 & 1 & 0 \\ 0 & 0 & 0 & 1 \end{bmatrix},\ B = \begin{bmatrix} 1 & 0 & 0 & 0 \\ 0 & 0 & 0 & 0 \\ 0 & 0 & 0 & 0 \\ 0 & 0 & 0 & 0 \end{bmatrix}$$

Similarly, these matrices can be found for graph-II shown in Fig. 6.1b as

$$A = \begin{bmatrix} 0 & 0 & 0 & 0 & 0 & 0 \\ 0 & 0 & 0 & 0 & 0 & 0 \\ 1 & 0 & 0 & 1 & 0 & 0 \\ 1 & 0 & 1 & 0 & 1 & 0 \\ 0 & 1 & 0 & 1 & 0 & 1 \\ 0 & 1 & 0 & 0 & 1 & 0 \end{bmatrix},\ \bar{A} = \begin{bmatrix} 0 & 0 & 0 & 0 & 0 & 0 \\ 0 & 0 & 0 & 0 & 0 & 0 \\ 0 & 0 & 2 & 0 & 0 & 0 \\ 0 & 0 & 0 & 3 & 0 & 0 \\ 0 & 0 & 0 & 0 & 3 & 0 \\ 0 & 0 & 0 & 0 & 0 & 2 \end{bmatrix},\ B = \begin{bmatrix} 1 & 0 & 0 & 0 & 0 & 0 \\ 0 & 1 & 0 & 0 & 0 & 0 \\ 0 & 0 & 0 & 0 & 0 & 0 \\ 0 & 0 & 0 & 0 & 0 & 0 \\ 0 & 0 & 0 & 0 & 0 & 0 \\ 0 & 0 & 0 & 0 & 0 & 0 \end{bmatrix}$$

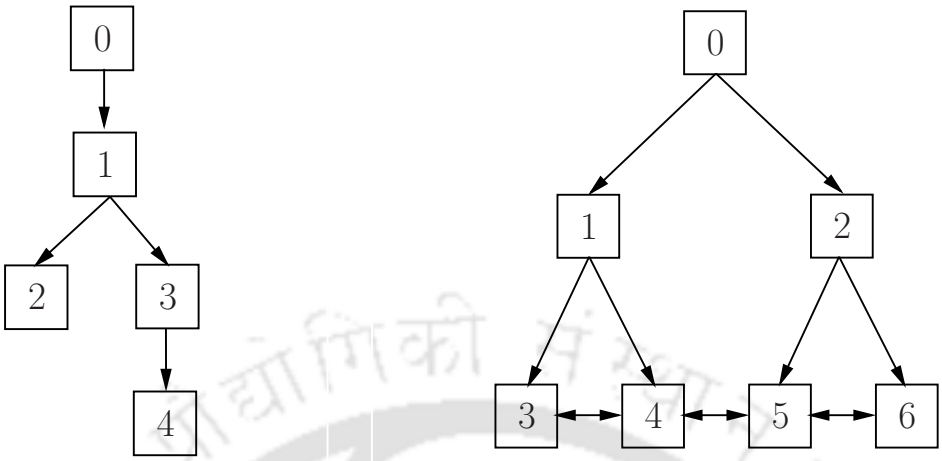

(a) Graph-I **(b)** Graph-II

Figure 6.1: Examples of two directed graph of leader-followers networks.

6.3 Problem Formulation

In this work, a multi-mobile robots system is considered which consists of one leader and N follower agents. From (4.2) and (4.12) of Chapter 4, the overall mathematical model of the i^{th} follower, shown in Fig. 4.1, can be written in the following form.

$$\begin{aligned} \dot{q}_i &= S_i(q_i)\nu_i, \\ \dot{\nu}_i &= \varphi_i(\nu_i)\theta_i + G_i u_i^{ET}(t-\tau_i) \ , \\ y_i &= q_i \ . \end{aligned} \tag{6.3}$$

where all vectors and matrices were previously defined in Section 4.2. Here, τ_i represents a constant delay in the input signal of i^{th} agent. For this, auxiliary compensation systems are introduced to deal with these input delays and are defined as follows.

$$\dot{\eta}_{i,1} = S_i\eta_{i,2} - \kappa_i\eta_{i,1}, \tag{6.4}$$

$$\dot{\eta}_{i,2} = G_i\left(u_i^{ET}(t) - u_i^{ET}(t-\tau_i)\right), \tag{6.5}$$

where $\kappa_i > \frac{1}{2}$ are positive constants. It is to be noted from (6.3) that followers are not actuated by the actual control signal u_i. Instead, they are actuated by u_i^{ET} where

$u_i^{ET} = u_i - e_i^{ET}$. This is due to the incorporation of event-triggered strategy where e_i^{ET} represents the measurement error of i^{th} agent. The triggering mechanism is defined as

$$\begin{aligned} u_i^{ET}(t) &= u_i(t_k),\ \forall\ t \in [t_k, t_{k+1}) \\ t_{k+1} &= \inf\left\{\ t \mid t > t_k\ ,\quad J_i(e_i^{ET}, Z_{i,1}, Z_{i,2}) > 0\right\}, \end{aligned} \tag{6.6}$$

where $J_i(e_i^{ET}, Z_{i,1}, Z_{i,2})$ represents the triggering condition to be designed later for i^{th} agent.

The control problem at this juncture is stated as follows. Design an event-triggered consensus control scheme for multiple mobile robots such that all agents eventually converge to the leader while ensuring that the over-usage of resources is alleviated.

Assumption 4. *It is assumed that the desired trajectory and its time-derivative are available only for the leader.*

6.4 Event-triggered Consensus Control Design

In this section, the controller is designed based on the backstepping method which is a powerful technique largely utilized in literature for stabilizing nonlinear systems [41]. Besides, the triggering condition is also derived in this section based on the negative semi-definiteness of the derivative of Lyapunov function. Let us first define the consensus error variables as

$$\begin{aligned} Z_{i,1} &= \sum_{j \in N_i} a_{ij}(q_i - q_j + \eta_{i,1}) + b_i(q_i - q_0 + \eta_{i,1}) \\ Z_{i,2} &= \nu_i + \eta_{i,2} - \alpha_{i,1}\ . \end{aligned} \tag{6.7}$$

where q_0 is the position and orientation of the leader and $\alpha_{i,1}$ for $i = 1,\ \ldots,\ N$ are the virtual controllers to be designed in the first step of the design procedure.

Remark 5. *In reality, it might be desirable to maintain a fixed distance between agents rather than converging to the exact quantity. Based on that, the consensus errors defined in (6.7) could be modified as follows.*

$$\begin{aligned} Z_{i,1} &= \sum_{j \in N_i} a_{ij}(q_i + \Delta_i - q_j - \Delta_j + \eta_{i,1}) + b_i(q_i + \Delta_i - q_0 + \eta_{i,1}) \\ Z_{i,2} &= \nu_i + \eta_{i,2} - \alpha_{i,1}\ , \end{aligned} \tag{6.8}$$

where Δ_i and Δ_j represent the displacement vectors which define the geometry of the desired formation.

Step 1: The dynamics of the first error variable can be written as

$$\dot{Z}_{i,1} = (\bar{a}_i + b_i)[S_i\nu_i + S_i\eta_{i,2} - \kappa_i\eta_{i,1}] - \sum_{j\in N_i} a_{ij}[S_j\nu_j] - b_i\dot{q}_0 \tag{6.9}$$

The Lyapunov function candidate is chosen at the first step as $V_{i,1} = \frac{1}{2}Z_{i,1}^T Z_{i,1}$. Differentiating V_1 with respect time along the trajectories of the system (6.3) is

$$\dot{V}_{i,1} = Z_1^T\dot{Z}_1 = Z_{i,1}^T\left((\bar{a}_i + b_i)[S_iZ_{i,2} + S_i\alpha_{i,1} - \kappa_i\eta_{i,1}] - \sum_{j\in N_i} a_{ij}[S_j\nu_j] - b_i\dot{q}_0\right) \tag{6.10}$$

The virtual control is now designed as

$$S_i\alpha_{i,1} = \frac{1}{\bar{a}_i + b_i}\left(-C_{i,1}Z_{i,1} + \sum_{j\in N_i} a_{ij}[S_j\nu_j] + b_i\dot{q}_0 + \kappa_i\eta_{i,1}\right) \tag{6.11}$$

which renders the time derivative of the Lyapunov function as

$$\dot{V}_{i,1} = -Z_{i,1}^T C_{i,1}Z_{i,1} + (\bar{a}_i + b_i)Z_{i,1}^T S_iZ_{i,2} \tag{6.12}$$

It is to be noted that the negative definiteness of $\dot{V}_{i,1}$ and convergence of $Z_{i,1}$ are ensured if $Z_{i,2} = 0$ which will be stabilized in the next step.

Step 2: In this step, the Lyapunov function candidate is chosen as

$$V_{i,2} = V_{i,1} + \frac{1}{2}Z_{i,2}^T Z_{i,2} \tag{6.13}$$

Differentiating V_2 with respect time along the trajectories of the system (6.3) is

$$\begin{aligned}
\dot{V}_{i,2} &= \dot{V}_{i,1} + Z_{i,2}^T\dot{Z}_{i,2} \\
&= -Z_{i,1}^T C_{i,1}Z_{i,1} + (\bar{a}_i + b_i)Z_{i,1}^T S_iZ_{i,2} + Z_{i,2}^T(\varphi_i\Theta_i + G_iu_i^{ET}(t-\tau_i) + \dot{\eta}_{i,2} - \dot{\alpha}_{i,1}) \\
&= -Z_{i,1}^T C_{i,1}Z_{i,1} + (\bar{a}_i + b_i)Z_{i,1}^T S_iZ_{i,2} + Z_{i,2}^T(\varphi_i\Theta_i + G_iu_i^{ET}(t-\tau_i) \\
&+ G_i(u_i^{ET} - u_i^{ET}(t-\tau_i)) - \dot{\alpha}_{i,1}) \\
&= -Z_{i,1}^T C_{i,1}Z_{i,1} + (\bar{a}_i + b_i)Z_{i,1}^T S_iZ_{i,2} + Z_{i,2}^T(\varphi_i\Theta_i + G_iu_i^{ET} - \dot{\alpha}_{i,1})
\end{aligned} \tag{6.14}$$

Let us first assume the case when the robot is actuated by the actual control law i.e. $u_i^{ET} = u_i$. Thus, in order to render $\dot{V}_2$ negative definite, the control law is now designed as follows.

$$u_i(t) = G_i^{-1}\left(-C_{i,2}Z_{i,2} - \varphi_i\Theta_i + \dot{\alpha}_{i,1} - (\bar{a}_i + b_i)Z_{i,1}^T S_iZ_{i,2}\right) \tag{6.15}$$

For simplicity, the internal parameters of the robots are assumed to be known in this chapter. Substituting (6.15) in (6.14), one gets

$$\dot{V}_{i,2} = -Z_{i,1}^T C_{i,1} Z_{i,1} - Z_{i,2}^T C_{i,2} Z_{i,2} \tag{6.16}$$

6.4.1 Triggering conditions

In the previous analysis, it was assumed that the robot is actuated by the actual control law that is updated/transmitted periodically i.e. the event-triggered measurement errors are zero. However, such periodic transmissions result in inefficient utilization of resources. Instead of that, an event-triggering mechanism is placed now to determine when it is necessary to update/transmit the control signal. Due to the incorporation of event-triggered strategy, a new term related to measurement errors will appear in (6.14) as

$$\dot{V}_{i,2} = -Z_{i,1}^T C_{i,1} Z_{i,1} + (\bar{a}_i + b_i) Z_{i,1}^T S_i Z_{i,2} + Z_{i,2}^T (\varphi_i \Theta_i + G_i u_i - G_i e_i^{ET} - \dot{\alpha}_{i,1}) \tag{6.17}$$

With the control law designed as (6.15), one gets

$$\begin{aligned} \dot{V}_{i,2} &= -Z_{i,1}^T C_{i,1} Z_{i,1} - Z_{i,2}^T C_{i,2} Z_{i,2} - Z_{i,2}^T G_i e_i^{ET} \\ &\leq -Z_{i,1}^T C_{i,1} Z_{i,1} - Z_{i,2}^T C_{i,2} Z_{i,2} + \|Z_{i,2}^T G_i\| \|e_i^{ET}\| \\ &\leq -Z_{i,1}^T C_{i,1} Z_{i,1} - Z_{i,2}^T C_{i,2} Z_{i,2} + \frac{\|Z_{i,2}^T G_i\|^2}{2} + \frac{\|e_i^{ET}\|^2}{2} \end{aligned} \tag{6.18}$$

Adding and subtracting the term $\zeta_i (Z_{i,1}^T C_{i,1} Z_{i,1} + Z_{i,2}^T C_{i,2} Z_{i,2})$ from (6.18), yields

$$\begin{aligned} \dot{V}_2 \leq & -(1-\zeta_i)(Z_{i,1}^T C_{i,1} Z_{i,1} + Z_{i,2}^T C_{i,2} Z_{i,2}) \\ & - \zeta_i (Z_{i,1}^T C_{i,1} Z_{i,1} + Z_{i,2}^T C_{i,2} Z_{i,2}) + \frac{\|Z_{i,2}^T G_i\|^2}{2} + \frac{\|e_i^{ET}\|^2}{2}, \end{aligned} \tag{6.19}$$

where ζ_i is an adjustable parameter. Now, if the triggering condition is derived by ensuring that

$$\frac{\|Z_{i,2}^T G_i\|^2}{2} + \frac{\|e_i^{ET}\|^2}{2} \leq \zeta_i (Z_{i,1}^T C_{i,1} Z_{i,1} + Z_{i,2}^T C_{i,2} Z_{i,2}) \tag{6.20}$$

then the derivative of Lyapunov function becomes

$$\dot{V}_2 \leq -(1-\zeta_i)(Z_{i,1}^T C_{i,1} Z_{i,1} + Z_{i,2}^T C_{i,2} Z_{i,2}) \tag{6.21}$$

By choosing $0 < \zeta_i < 1$, the negative semi-definiteness of derivative of Lyapunov function can be ensured. From (6.20), the triggering function can be written as

$$J(e_i^{ET}, Z_{i,1}, Z_{i,2}) = \|e_i^{ET}\|^2 - 2\zeta_i (Z_{i,1}^T C_{i,1} Z_{i,1} + Z_{i,2}^T C_{i,2} Z_{i,2}) + \|Z_{i,2}^T G_i\|^2 \tag{6.22}$$

Proposition 7. *Under the action of control law (6.15) and triggering conditions (6.22), all closed-loop signals are bounded and all followers converge to the leader as $t \to \infty$. Moreover, a minimum inter-event time $(t_{k+1} - t_k)$ is ensured.*

Proof. We choose a Lyapunov function candidate as $V = \sum_{i=1}^{N} V_{i,2}$. From the previous analysis, the derivative of V with respect time along the trajectories of the system (6.3) can be directly written as

$$\dot{V} \leq -\sum_{i=1}^{N}(1-\zeta_i)(Z_{i,1}^T C_{i,1} Z_{i,1} + Z_{i,2}^T C_{i,2} Z_{i,2}) \tag{6.23}$$

Thus, the stability in the sense of Lyapunov is ensured under proposed event-triggered scheme and all closed-loop signals are bounded.

Using Barbalat lemma [97], the convergence of follower to the leader can be proved. From (6.23), we have $\ddot{V} = -2\sum_{i=1}^{N}(1-\zeta)\left(Z_{i,1}^T C_1 \dot{Z}_{i,1} + Z_{i,2}^T C_2 \dot{Z}_{i,2}\right)$. Since $\dot{V}$ is negative semi-definite, all the closed-loop trajectories are bounded. Hence, $Z_{i,1}, Z_{i,2}, \dot{Z}_{i,1}, \dot{Z}_{i,2}$ are bounded for all time. Then, we can easily conclude that $\ddot{V}$ is also bounded. Thus, $\dot{V}$ is uniformly continuous. Now, we can conclude using Barbalat lemma that $\dot{V} \to 0$ as $t \to \infty$ which implies that the error variables converge to zero as $t \to \infty$.

To complete the proof, a lower bound of inter-event time $(t_{k+1} - t_k)$ should be ensured which implies the exclusion of Zeno behavior. From the definition of u_i (6.15), we can conclude that $\dot{u}_i$ is continuous and bounded as u_i is a function of all bounded signals. Thus, we can write $|\dot{u}_i| \leq \epsilon_1^i$ where ϵ_1^i is a positive constant. Meanwhile,

$$\begin{aligned} |u_i(t_{k+1}) - u_i(t_k)| &= \left| \int_{t_k}^{t_{k+1}} \dot{u}_i(\lambda) d\lambda \right| \\ &\leq \int_{t_k}^{t_{k+1}} |\dot{u}_i(\lambda)|\, d\lambda \\ &\leq \int_{t_k}^{t_{k+1}} \epsilon_1^i d\lambda = \epsilon_1^i (t_{k+1} - t_k) \end{aligned} \tag{6.24}$$

Let $e_i^{ET}(t_k) = 0$ and $\lim_{t \to t_{k+1}^-} e_i^{ET}(t) = \epsilon_2^i$ where ϵ_2^i is a positive constant that depends on k, then we can write

$$\epsilon_2^i \leq |u_i(t_{k+1} - u_i(t_k))| \tag{6.25}$$

From (6.24) and (6.25), we get

$$\epsilon_2^i \leq |u_i(t_{k+1} - u_i(t_k))| \leq \epsilon_1^i (t_{k+1} - t_k) \tag{6.26}$$

Accordingly,

$$(t_{k+1} - t_k) \geq \epsilon_2^i / \epsilon_1^i, \tag{6.27}$$

which implies that a lower bound of inter-event time can always be ensured and obtained as $\epsilon_2^i / \epsilon_1^i$ [2]. □

6.5 Simulation Results

To demonstrate the effectiveness of the proposed control scheme, two simulation examples on leader-follower networks, represented by the graphs shown in Fig. 6.1, have been carried out in MATLAB. Agent (0) represents the leader. The agents are assumed to be identical with ideal communications and no loss of connections.

The parameters of the agents are chosen as $m_i = 10\ [kg]$, $r_i = 0.1\ [m]$, $b_i = 0.5\ [m]$, $d_i = 0.5\ [m]$ and $I_i = 2.5\ [kgm^2]$, for $i = 1, \ldots, 6$. The leader moves in a circular trajectory with radius $R_r = 1\ [m]$ and angular speed $W_r = 0.5\ [rad/s]$. Other parameters are chosen as $\kappa_i = 2$, $\zeta_i = 0.6$ and $\tau_i = 0.1[s]$.

Example I: Consensus Control

In this example, the graph shown in Fig. 6.1a, which consists of one leader and four followers, is considered. The consensus error variables are defined as (6.7). The position and orientation of the followers are to be exactly converged to the position and orientation of the leader in this example. The initial position and orientation for each agent are selected as $[x_i(0), y_i(0), \theta_i(0)] = [-1, -1.2, 10]$, $[-0.2, -1.5, 20]$, $[-0.3, -0.8, 20]$ and $[-2, -2, 0]$. The controller parameters are chosen as $C_{i,1} = diag(0.5, 0.5, 1)$ and $C_{i,2} = diag(2, 2)$. The simulation is conducted for a total time $T = 30$ [s] under sampling period equals to $dt = 0.02$ [s].

The trajectories of the followers in $X - Y$ plane are shown in Fig. 6.2. Moreover, the performance and consensus errors in X, Y, and Θ directions are shown in Fig. 6.3. It can be observed that the consensus errors are bounded and converge to a small set around zero. The time-triggered and event-triggered control signals for each agent are shown in Fig. 6.4. It is to be noted that the agents are now actuated by the event-triggered control signals rather than the actual time signals. The triggering instants when the designed conditions are violated are illustrated for each follower in Fig. 6.5. It is worth mentioning that, under the classical time-triggered paradigm, the number of transmissions equals $\frac{T}{dt} = 1500$ as it is continuously updated every dt. The number of triggering events for each agent is shown in Table 6.1. It is clear that the number of transmissions is drastically reduced under the proposed event-triggered mechanism. The bandwidth usage of each agent is reduced more than 90% compared to the traditional time-triggered scenario. The bandwidth usage is calculated as

$$\text{Bandwidth Usage} = 100 \times \text{Number of events} \times \frac{dt}{T} \tag{6.28}$$

The inter-event times between two consecutive triggering instants $(t_k - t_{k-1})$ are also shown in Fig. 6.6. The average and maximum values of inter-event time are also provided

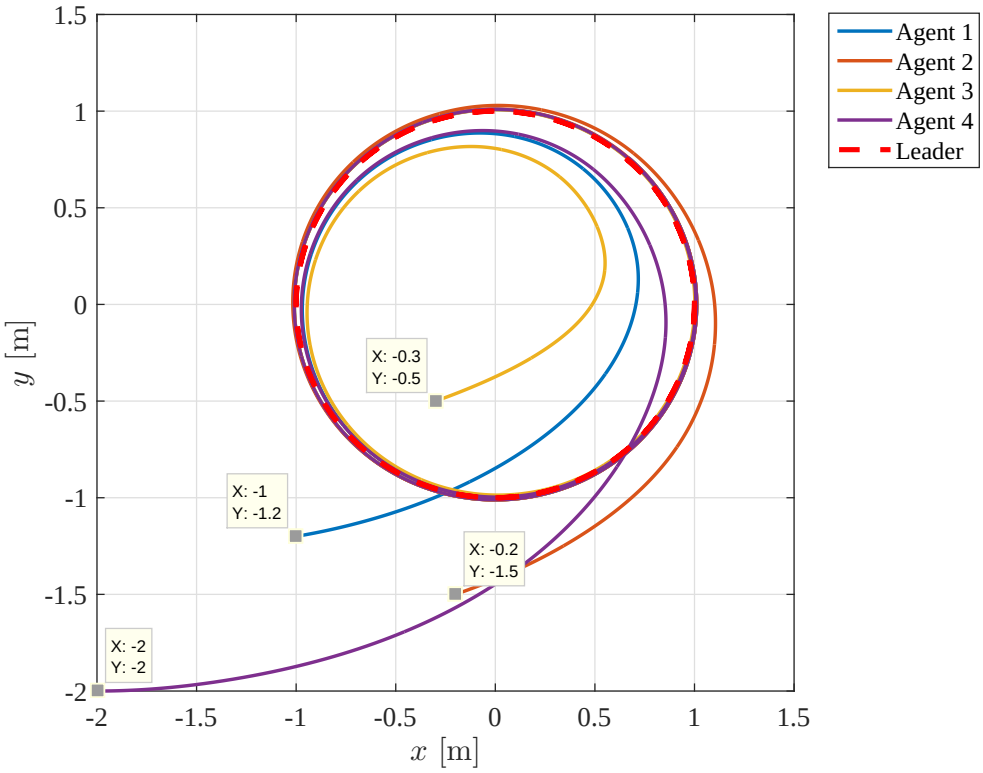

Figure 6.2: Trajectories in the X-Y plane for example I.

in Table 6.1. It is observed that agent 1 who is directly connected with the leader achieves larger inter-event times and less number of triggering events as compared to other agents who are not directly connected with the leader.

Example II: Formation Scenario

In this example, the graph shown in Fig. 6.1b, which consists of one leader and six followers, is considered. In reality, it might be desirable to maintain a fixed distance between the agents rather than converging to the exact quantity. For this purpose, a displacement-vector Δ_i is introduced in this example, and it is defined as follows.

$$\Delta_i = [\frac{\cos(2\Pi(i-1))}{N}R,\ \frac{\sin(2\Pi(i-1))}{N}R,\ 0]^T \tag{6.29}$$

where $i = 1, \ldots, 6$ and R is a positive constant. The consensus error variables in this example are defined as (6.8). Rather than converging to the actual position of the leader, the followers are required to converge to a circle with a radius R around the leader. In our simulation, R is selected equals to R_r. The initial position and orientation for

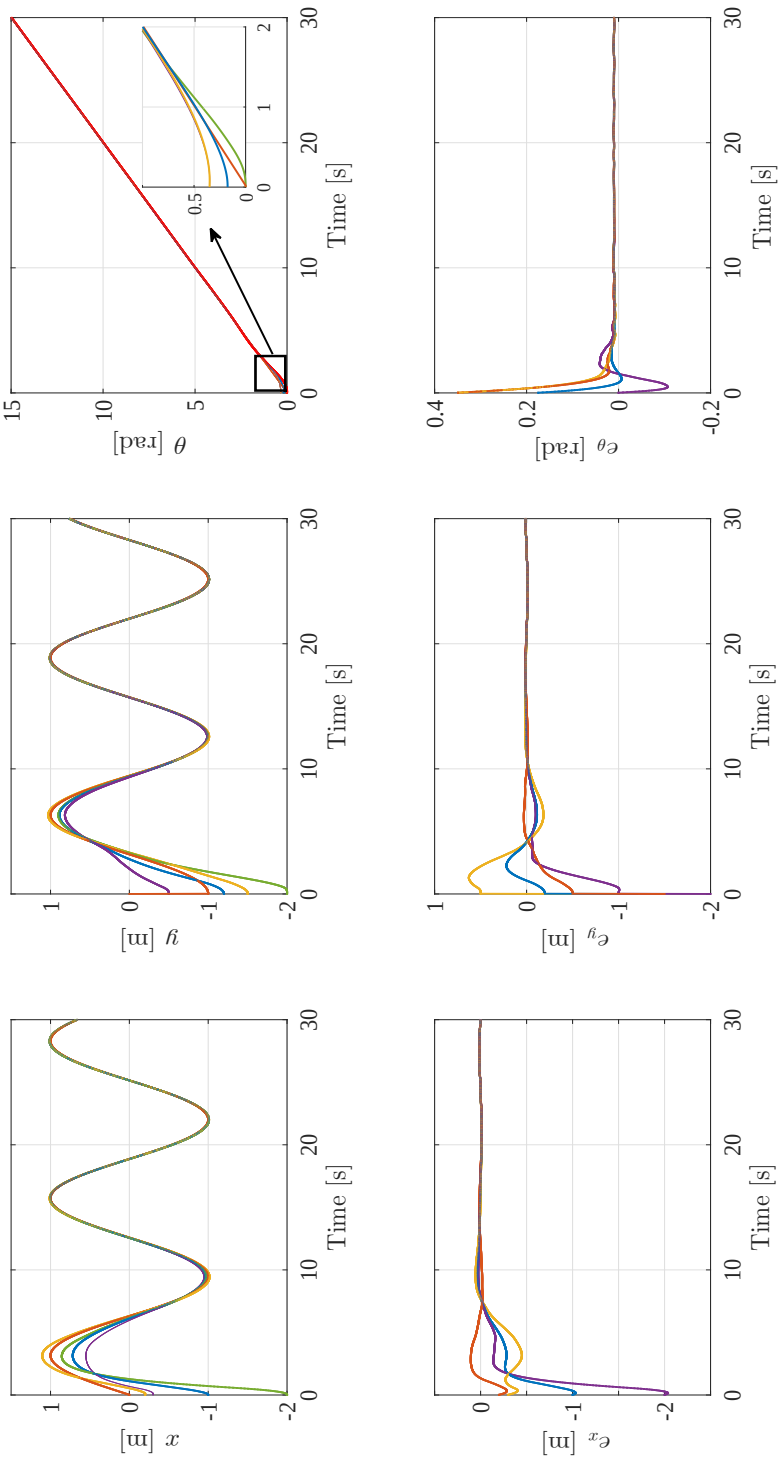

Figure 6.3: Trajectories and consensus errors in X, Y, and Θ directions for example I.

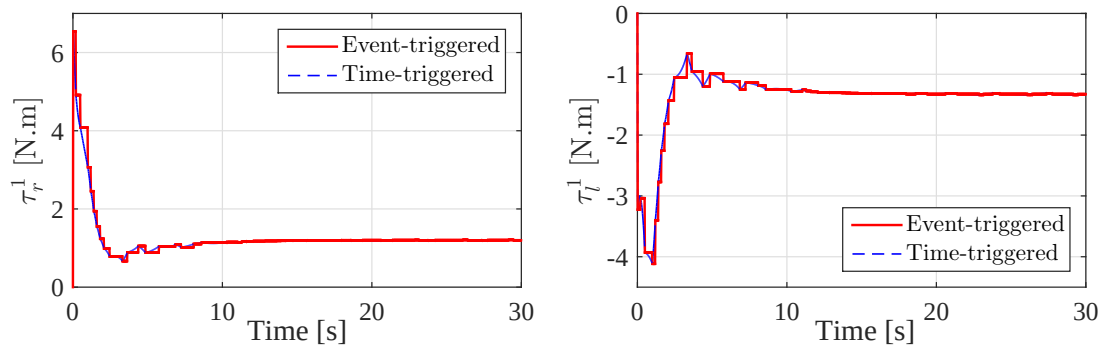

(a) The torques on the right τ_r^1 and left τ_l^1 motors of Agent 1

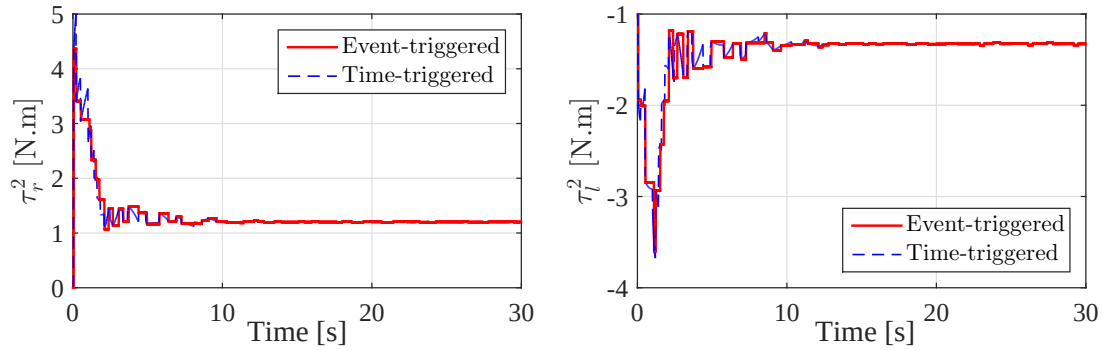

(b) The torques on the right τ_r^2 and left τ_l^2 motors of Agent 2

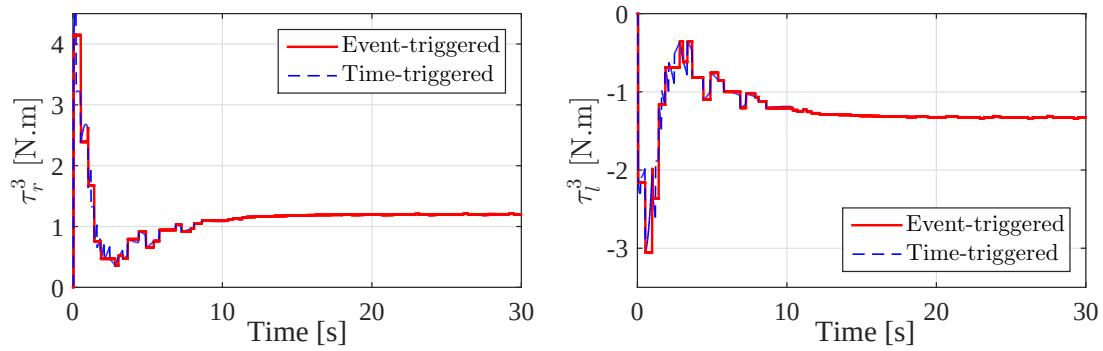

(c) The torques on the right τ_r^3 and left τ_l^3 motors of Agent 3

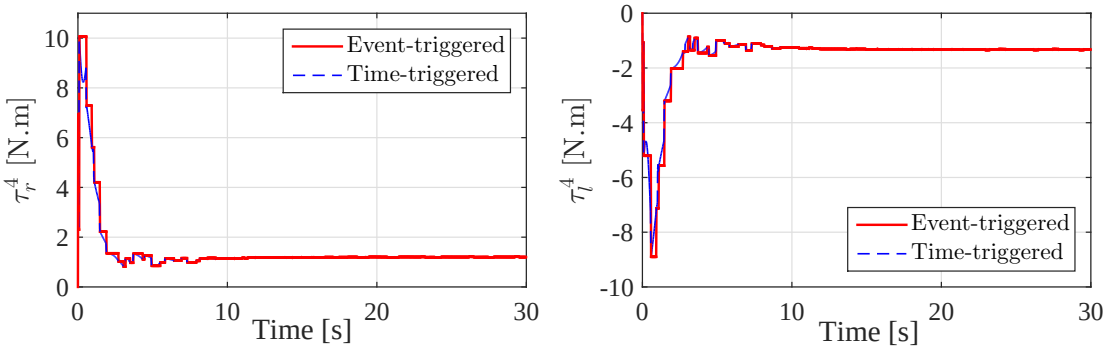

(d) The torques on the right τ_r^4 and left τ_l^4 motors of Agent 4

Figure 6.4: Time-triggered and event-triggered control signals.

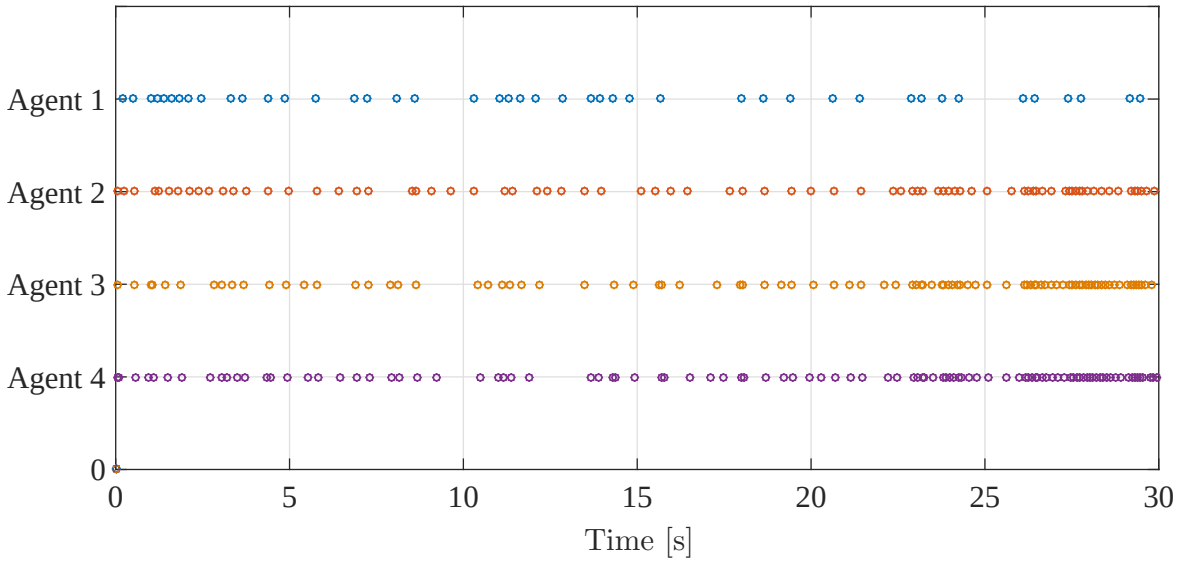

Figure 6.5: Illustration of triggering events for each agent in example I.

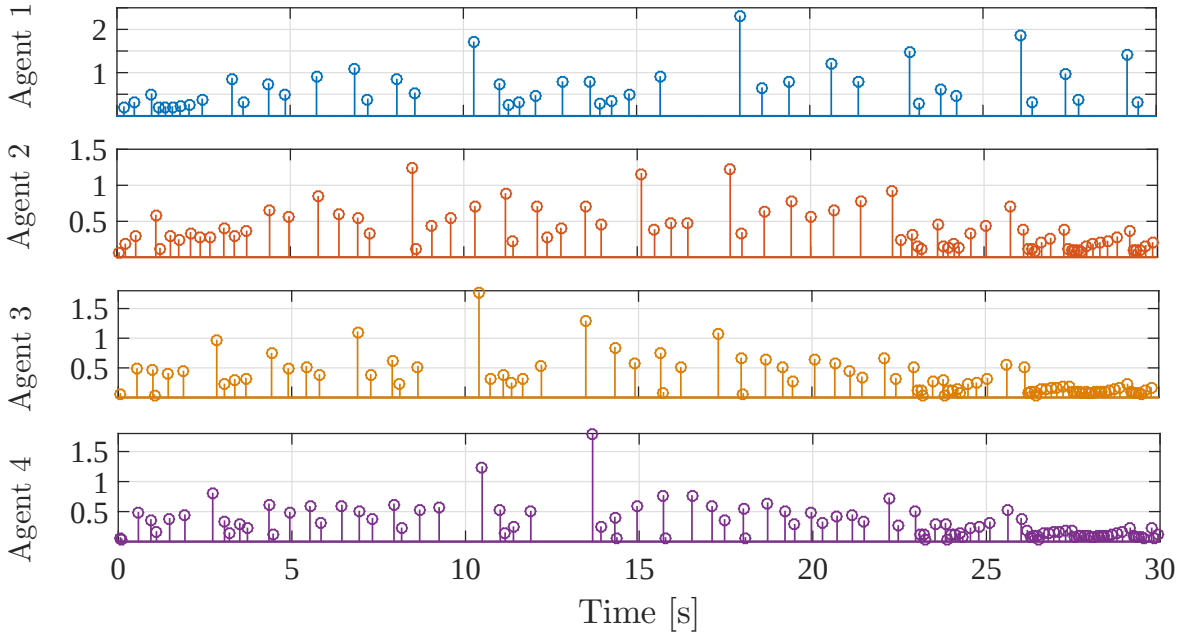

Figure 6.6: Inter-event time $(t_k - t_{k-1})$ for each agent in example I.

Table 6.1: Summarization of simulation results for example I.

	Number of Events	Bandwidth Usage (%)	Inter-event Times (s)	
			Average	Maximum
Agent 1	44	2.9	0.67	2.3
Agent 2	87	5.2	0.38	1.24
Agent 3	91	6.0	0.32	1.76
Agent 4	101	6.7	0.29	1.78

Table 6.2: Summarization of simulation results for example II.

	Number of Events	Bandwidth Usage (%)	Inter-event Times (s)	
			Average	Maximum
Agent 1	45	3.0	0.64	2.26
Agent 2	44	2.9	0.67	4.18
Agent 3	142	9.5	0.21	1.22
Agent 4	221	14.7	0.13	0.58
Agent 5	321	21.4	0.09	0.40
Agent 6	177	11.8	0.17	0.74

each agent are selected as $[x_i(0), y_i(0), \theta_i(0)] = [-1, -1.2, 10]$, $[-0.5, -2, 20]$, $[0.5, -2, 20]$, $[1, -1.2, 20]$, $[0.5, -0.3, 20]$ and $[-0.5, -0.3, 0]$. The controller parameters are chosen as $C_{i,1} = diag(0.5, 0.5, 1)$ and $C_{i,2} = diag(2, 2)$. The simulation is conducted for a total time $T = 30$ [s] under sampling period equals to $dt = 0.02$ [s].

The trajectories of the followers in the $X - Y$ plane are shown in Fig. 6.7. Moreover, the performance and consensus errors in X, Y, and Θ directions are shown in Fig. 6.8. It can be observed that the consensus errors are bounded and converge to a small set around the formation vector Δ. The triggering instants when the designed conditions are violated are illustrated for each follower in Fig. 6.9. The number of triggering events for each agent is shown in Table 6.2. It is clear that the number of transmissions is drastically reduced under the proposed event-triggered mechanism and the bandwidth usage of each agent is reduced more than 90% as compared to the traditional time-triggered scenario. Moreover, it can also be observed that, as compared to agents 1 and 2 who are directly connected to the leader, the agents 3–6 require more triggering events/transmissions to achieve the formation task. This is expected as these agents are not directly connected to the leader. The inter-event times between two consecutive triggering instants $(t_k - t_{k-1})$ are also shown in Fig. 6.10. The average and maximum values of inter-event time are also

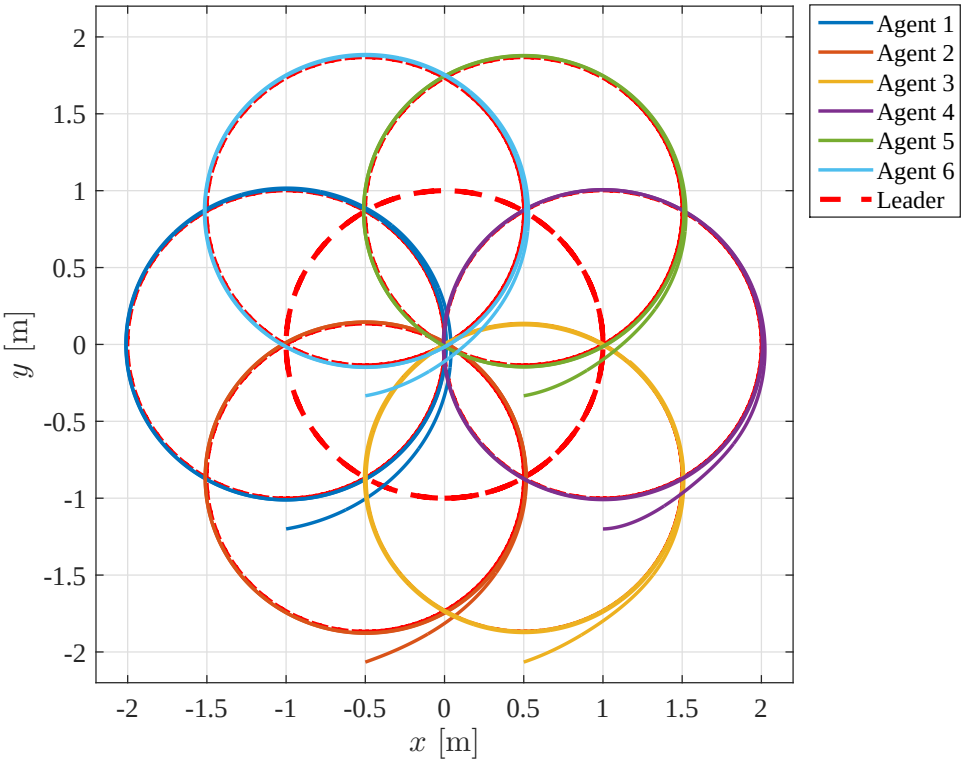

Figure 6.7: Trajectories in the X-Y plane for example II.

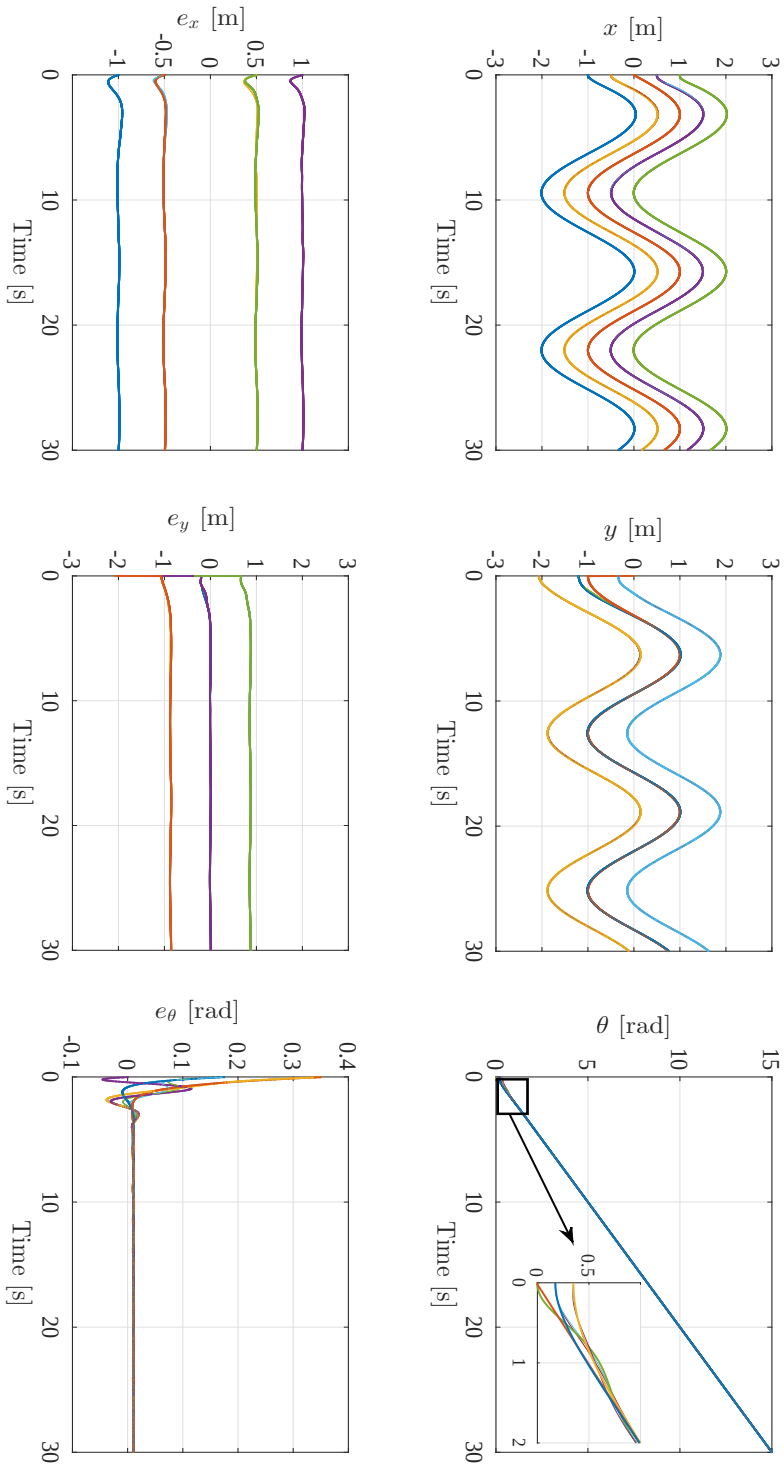

Figure 6.8: Trajectories and consensus errors in X, Y, and Θ directions for example II.

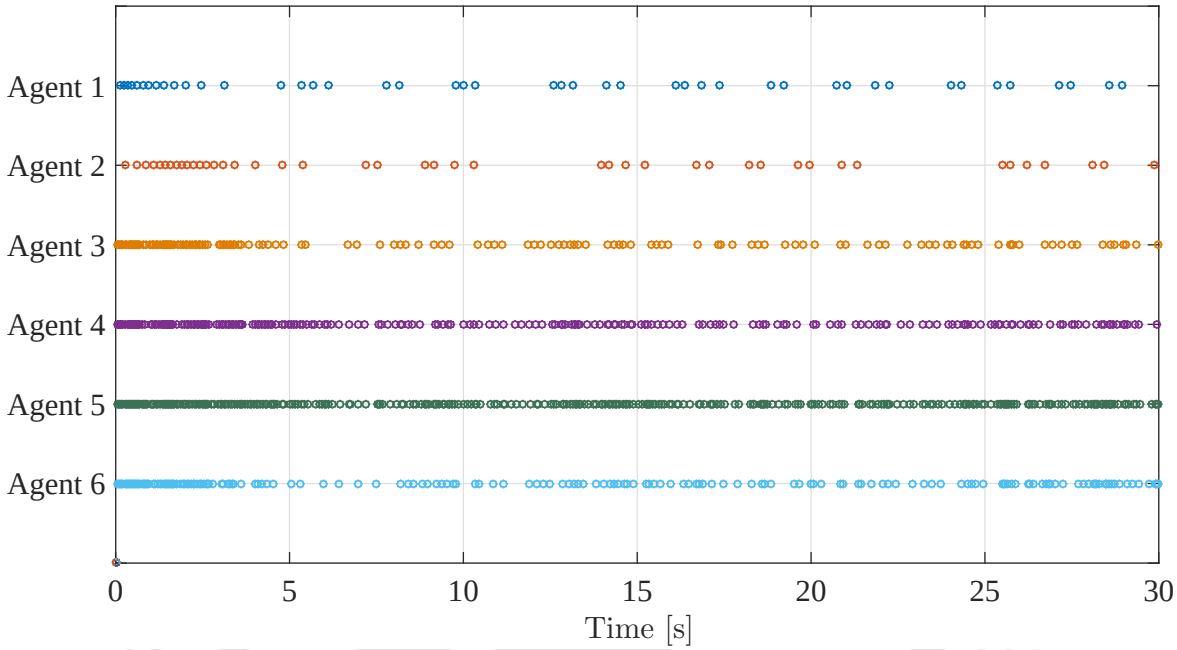

Figure 6.9: Illustration of triggering events for each agent in example II.

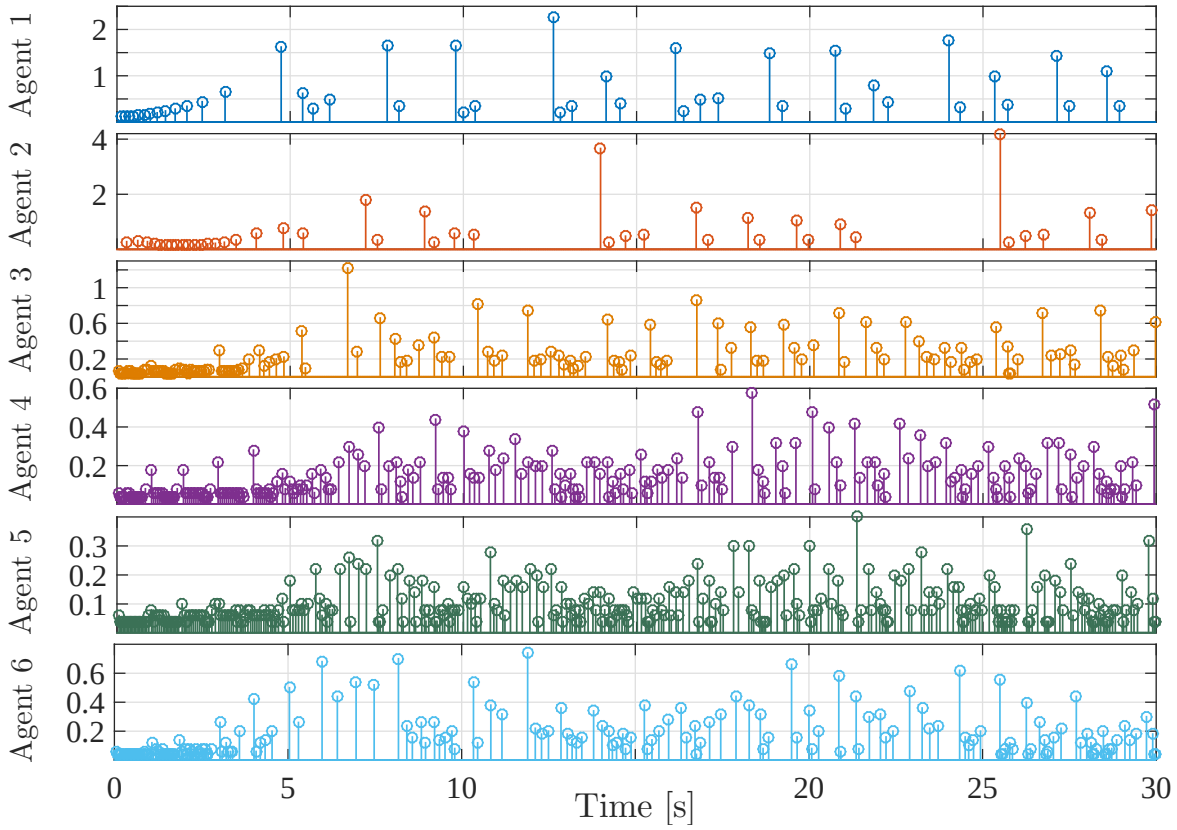

Figure 6.10: Inter-event time $(t_k - t_{k-1})$ for each agent in example II.

provided in Table 6.2. It can be observed that the agents who are not directly connected to the leader achieve smaller inter-event times and a larger number of triggering events, which implies an increase in resource utilization.

6.6 Summary

The consensus tracking control problem has been investigated in this chapter for a leader-followers network of multi-robot systems under limited communication and input delays. For that, an event-triggered consensus controller has been designed based on backstepping while considering both kinematic and dynamic models of mobile robots. A Lyapunov-based event-triggering condition has been incorporated in the controller design resulting in a significant saving of channel bandwidth. Two simulation examples for consensus and formation scenarios have been considered. It is observed from simulations that all agents are practically converged to the leader with significantly less number of transmissions over the network.

7

Conclusion and Scope for Future Work

Contents

7.1 Conclusion

This thesis is an attempt to design an event-triggered adaptive control methodology for a class of nonlinear uncertain systems under network circumstances i.e. induced delays and band-limited channels. It is also an attempt to implement the developed control schemes on a real mobile robot, with possible extension to multi-agent systems. The chapters of the thesis are briefly concluded as follows.

- An event-triggered adaptive control scheme, based on the backstepping technique, was first developed for a class of nonlinear uncertain systems. In *Chapter* 2, the communication restrictions were considered in the controller-to-actuator channel only. Therefore, the triggering mechanism was placed at the controller-end and only input delay was considered. For this purpose, an auxiliary system was introduced to handle such induced delays. Then, the triggering condition was derived in the last step of the backstepping procedure by ensuring the stability of the overall control system. Although this configuration seems simple in design, analysis, and implementation, it is not suitable for applications wherein the communication restrictions occurred in both channels. In *Chapter* 3, the communication restrictions in the sensor-to-controller channel were also considered. Therefore, the triggering mechanism was placed at the sensor-end, which complicated the controller design and triggering conditions. A state-predictor was designed in this chapter to handle the network-induced delays in the state and input signals. The controller was then designed based on the predicted states.

- To show the real-time applicability, the developed event-triggered adaptive control schemes were applied on a nonholonomic mobile robot in *Chapter* 4. The trajectory tracking control problem was formulated with consideration of both kinematic and dynamic models and assuming unknown parameters of the robot. Simulation results showed that the proposed control scheme successfully ensured faithful trajectory tracking with a substantial saving of resources characterized by the number of required control updates and signal transmissions. Furthermore, the developed control schemes were experimentally validated on a real mobile robot (PatrolBot) in *Chapter* 5. To overcome the hardware restriction of commercial mobile robots which are operated by direct velocity commands rather than torques/voltages of the motor, a modified dynamic model was first presented. Thereafter, the proposed control schemes were implemented. The obtained results were consistent with simulations and showed an accurate tracking with a significant saving in channel bandwidth and computational resources in presence of state and input delays.

- Finally, the proposed event-triggered control scheme was extended to multi-agent systems in Chapter 6. The consensus problem of a leader-followers network of multiple mobile robots was considered. It was observed from simulations that all agents were practically converged to the leader with less number of transmissions over the network.

7.2 Recommendations for Future Work

Future possible directions of research based on the event-triggered adaptive control scheme developed in this thesis are outlined as follows.

- All event-triggered control schemes proposed in this thesis assume the availability of all system states. However, this may not be the case in practice. Thus, an observer-based output feedback controller is worth exploring to relax this assumption.

- In the event-triggered control paradigm, the triggering condition is periodically evaluated at each instance to decide whether to update the last-transmitted packet or not. However, this may be inefficient from a computational point of view. This periodic checking can be relaxed in a self-triggered control paradigm wherein the next triggering instance is determined *a priori*. This is an interesting problem worth exploring.

- There are other challenges in NCSs such as packet loss/dropout and attacks that may deteriorate the system performance and even jeopardize the stability of the overall control system. These challenges shall be investigated in the future.

- The thesis is aimed at investigating the deterministic parametric uncertainties in nonlinear networked systems. However, considering these uncertainties as stochastic would be more realistic and is indeed a promising avenue to research upon. Moreover, design and analysis for nonlinear systems simultaneously affected by network perturbation and unknown system uncertainties irrespective of their structure, type of parametrization, and exogenous temporal disturbances can be further investigated in the future.

- This thesis is aimed at investigating the nonlinear systems in the continuous domain. This can be extended to the discrete domain to enhance the flexibility in implementation. Moreover, the extension of the developed control schemes with constraints on system states and outputs is worth exploring due to saturation problems and safety issues.

- The thesis may be extended to investigate time-varying and stochastic network-induced delays, which is a more practical scenario.
- This thesis presents an initial attempt towards the extension of the proposed control scheme to multi-agent systems. It assumes ideal environment with no loss of connections. This attempt shall be proceeded by investigating different graph topologies, agent types, and other challenges related to multi-agent systems.

A

Appendix

Contents

A.1 Event-triggered Sliding Mode Control Scheme (ETSMC) [1]

Here, ETSMC law, event-triggering condition and the relevant parameters used in the simulation section 2.4 of Chapter 2 for the sake of comparison with the proposed ETAC are stated. The control law and triggering rule for system (2.62), are given in the following based on the results reported in [1]. The sliding manifold was designed as

$$S = \left\{ x \in \mathbb{R}^2 : s = c^T x = 0 \right\} \ , \tag{A.1}$$

where $c = [c_1 \quad 1]^T$ with $c_1 \in \mathbb{R}^1$ and $x = [x_1^T \quad x_2]^T$. The sliding mode controller was derived and found to be as

$$u = -0.5x_2 + \frac{MgL}{J} \sin x_1 + \frac{B}{J} x_2 - K \text{sign}(s) \ , \tag{A.2}$$

with the triggering rule was defined in [1],

$$L\|c\|\|e\| \quad < \quad \sigma\alpha \ , \tag{A.3}$$

where $e(t)$ signal was defined as $e(t) = x(t_i) - x(t)$ for $t \in [t_i, t_{i+1})$. The initial states and system parameters were considered the same for all the three controllers for a justified comparison of results. Other relevant parameters were chosen as $q(0) = 20, \dot{q}(0) = 0, c_1 = 0.5, \sigma = 0.8, \alpha = 0.8, L = 6$ and $K = 1$.

A.2 PatrolBot (Mobile Robot)

The autonomous research PatrolBot (shown in Fig. A.1) is a high-quality, differential-drive robot designed for research projects that require reliable, continuous duty cycle or a mid-size payload. The PatrolBot has been designed by Adept Mobilerobots® to carry effectors and sensors over all normal indoor surfaces in wheelchair-accessible facilities. PatrolBot can map buildings and continuously localize within a few centimeters while traveling in mapped areas. With the proper accessories, the robot is able to speak, play and hear audio, transmit a mounted camera view, and drive without supervision.

A.2.1 ARIA- Core Software

ARIA provides a framework for controlling and receiving data from all MobileRobots platforms, as well as most accessories. It includes open source infrastructures and utilities useful for writing robot control software, support for network sockets, and an extensible framework for client-server network programming.

A.2.2 Specifications of the Robot

The physical characteristics of PatrolBot are listed in Table A.1.

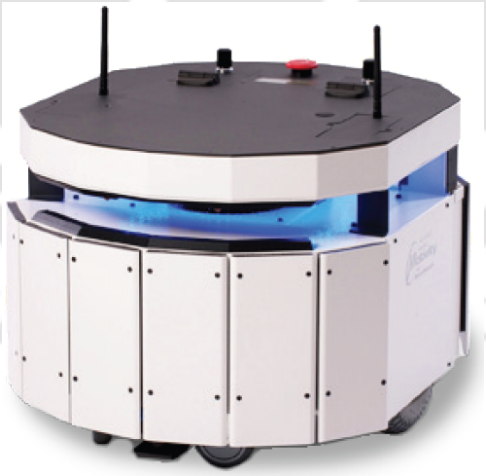

Figure A.1: PatrolBot by Adept MobileRobots.

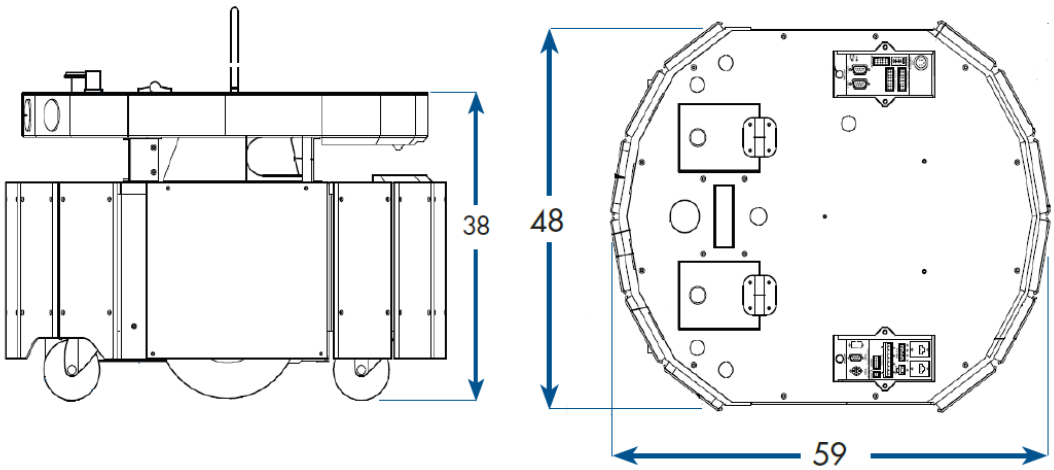

Figure A.2: The dimensions (cm) of PatrolBot by Adept MobileRobots.

Table A.1: The physical characteristics of PatrolBot.

Weight	45 Kg
Payload	12 Kg
Run time	4-6 hrs
Length	59 cm
Width	48 cm
Height	38 cm
Drive Wheel	2 foam-filled rubber; 2 rear-caster balance
Steering	Differential
Wheel Diameter	19 cm
Translate Speed Max	2000 mm/sec
Rotational Speed Max	360 degrees/sec
Position Encoder	30,000 ticks per wheel revolution; 195 ticks per mm

References

[1] A. K. Behera and B. Bandyopadhyay, "Event-triggered sliding mode control for a class of nonlinear systems," *International Journal of Control*, vol. 89, no. 9, pp. 1916–1931, 2016.

[2] L. Xing, C. Wen, Z. Liu, H. Su, and J. Cai, "Event-triggered adaptive control for a class of uncertain nonlinear systems," *IEEE Transactions on Automatic Control*, vol. 62, no. 4, pp. 2071–2076, 2017.

[3] J. Huang and Q.-G. Wang, "Event-triggered adaptive control of a class of nonlinear systems," *ISA Transactions*, vol. 94, pp. 10–16, 2019.

[4] R. Postoyan, M. C. Bragagnolo, E. Galbrun, J. Daafouz, D. Nešić, and E. B. Castelan, "Event-triggered tracking control of unicycle mobile robots," *Automatica*, vol. 52, pp. 302–308, 2015.

[5] X. Ge, F. Yang, and Q.-L. Han, "Distributed networked control systems: A brief overview," *Information Sciences*, vol. 380, pp. 117 – 131, 2017.

[6] R. A. Gupta and M.-Y. Chow, *Overview of Networked Control Systems*, F.-Y. Wang and D. Liu, Eds. London: Springer London, 2008.

[7] D. Zhang, P. Shi, Q.-G. Wang, and L. Yu, "Analysis and synthesis of networked control systems: A survey of recent advances and challenges," *ISA Transactions*, vol. 66, pp. 376 – 392, 2017.

[8] X. Zhang, Q. Han, and X. Yu, "Survey on recent advances in networked control systems," *IEEE Transactions on Industrial Informatics*, vol. 12, no. 5, pp. 1740–1752, Oct 2016.

[9] R. A. Gupta and M.-Y. Chow, "Networked control system: Overview and research trends," *IEEE Transactions on Industrial Electronics*, vol. 57, no. 7, pp. 2527–2535, 2009.

[10] S. M. Amrr, M. U. Nabi, and A. Iqbal, "An event-triggered robust attitude control of flexible spacecraft with modified rodrigues parameters under limited communication," *IEEE Access*, vol. 7, pp. 93 198–93 211, 2019.

[11] F. Shu and J. Zhai, "Event-triggered practical finite-time output feedback stabilisation for switched non-linear time-delay systems," *IET Control Theory & Applications*, vol. 14, no. 6, pp. 824–833, 2020.

[12] Y. Wang, Y. Huang, and E. Yang, "Event-triggered communication for passivity and synchronisation of multi-weighted coupled neural networks with and without parameter uncertainties," *IET Control Theory & Applications*, vol. 14, no. 9, pp. 1228–1239, 2020.

[13] W. Heemels and M. Donkers, "Model-based periodic event-triggered control for linear systems," *Automatica*, vol. 49, no. 3, pp. 698 – 711, 2013.

[14] N. S. Tripathy, I. N. Kar, and K. Paul, "Stabilization of uncertain discrete-time linear system with limited communication," *IEEE Transactions on Automatic Control*, vol. 62, no. 9, pp. 4727–4733, Sept 2017.

[15] M. H. Roohi, I. Izadi, and J. Ghaisari, "Bandwidth allocation, delay bound analysis, and controller synthesis for event-triggered control systems," *IET Control Theory Applications*, vol. 11, no. 16, pp. 2870–2878, 2017.

[16] C.-H. Zhang and G.-H. Yang, "Event-triggered adaptive output feedback control for a class of uncertain nonlinear systems with actuator failures," *IEEE Transactions on Cybernetics*, vol. 50, no. 1, pp. 201–210, 2018.

[17] W. Yang, Y. Pan, and H. Liang, "Event-triggered adaptive fixed-time nn control for constrained nonstrict-feedback nonlinear systems with prescribed performance," *Neurocomputing*, vol. 422, pp. 332–344, 2021.

[18] Y.-X. Li and G.-H. Yang, "Observer-based fuzzy adaptive event-triggered control codesign for a class of uncertain nonlinear systems," *IEEE Transactions on Fuzzy Systems*, vol. 26, no. 3, pp. 1589–1599, 2017.

[19] C.-H. Zhang and G.-H. Yang, "Event-triggered control for a class of strict-feedback nonlinear systems," *International Journal of Robust and Nonlinear Control*, vol. 29, no. 7, pp. 2112–2124, 2019.

[20] A. Yesmin and M. K. Bera, "Design of event-triggered sliding mode controller based on reaching law with time varying event generation approach," *European Journal of Control*, vol. 48, pp. 30–41, 2019.

[21] S. Al Issa and I. Kar, "Event-triggered adaptive control of uncertain non-linear systems under input delay and limited resources," *International Journal of Dynamics and Control*, pp. 1–8, 2021.

[22] C.-H. Zhang and G.-H. Yang, "Event-triggered practical finite-time output feedback stabilization of a class of uncertain nonlinear systems," *International Journal of Robust and Nonlinear Control*, vol. 29, no. 10, pp. 3078–3092, 2019.

[23] L. Liu, X. Li, Y.-J. Liu, and S. Tong, "Neural network based adaptive event trigger control for a class of electromagnetic suspension systems," *Control Engineering Practice*, vol. 106, p. 104675.

[24] C. Wang, L. Guo, C. Wen, Q. Hu, and J. Qiao, "Event-triggered adaptive attitude tracking control for spacecraft with unknown actuator faults," *IEEE Transactions on Industrial Electronics*, vol. 67, no. 3, pp. 2241–2250, 2019.

[25] L. Xing, C. Wen, Z. Liu, H. Su, and J. Cai, "Adaptive compensation for actuator failures with event-triggered input," *Automatica*, vol. 85, pp. 129 – 136, 2017.

[26] W. Chenliang, L. Yun, H. Qinglei, and J. HUANG, "Event-triggered adaptive control for attitude tracking of spacecraft," *Chinese Journal of Aeronautics*, 2019.

[27] H. Pan, W. Sun, J. Zhang, S. Yan, and W. Lin, "Adaptive event-triggered control for vehicle active suspension systems with state constraints," *IFAC-PapersOnLine*, vol. 51, no. 31, pp. 955–960, 2018.

[28] C. Zhu, C. Li, X. Chen, K. Zhang, X. Xin, and H. Wei, "Event-triggered adaptive fault tolerant control for a class of uncertain nonlinear systems," *Entropy*, vol. 22, no. 6, p. 598, 2020.

[29] Y.-X. Li and G.-H. Yang, "Event-triggered adaptive backstepping control for parametric strict-feedback nonlinear systems," *International Journal of Robust and Nonlinear Control*, vol. 28, no. 3, pp. 976–1000, 2018.

[30] T. Li, J. Fu, and Z. Ma, "Improved event-triggered control for a class of continuous-time switched linear systems," *IET Control Theory Applications*, vol. 12, no. 7, pp. 1000–1005, 2018.

[31] W. Xiang and T. T. Johnson, "Event-triggered control for continuous-time switched linear systems," *IET Control Theory Applications*, vol. 11, no. 11, pp. 1694–1703, 2017.

[32] X. Meng and T. Chen, "Event-driven communication for sampled-data control systems," in *2013 American Control Conference*, June 2013, pp. 3002–3007.

[33] S. Tarbouriech, A. Seuret, J. M. G. da Silva, and D. Sbarbaro, "Observer-based event-triggered control co-design for linear systems," *IET Control Theory Applications*, vol. 10, no. 18, pp. 2466–2473, 2016.

[34] S. Al Issa, A. Chakravarty, and I. Kar, "Improved event-triggered adaptive control of non-linear uncertain networked systems," *IET Control Theory & Applications*, vol. 13, no. 13, pp. 2146–2152, 2019.

[35] M. Abbas, S. Al Issa, and S. K. Dwivedy, "Event-triggered adaptive hybrid position-force control for robot-assisted ultrasonic examination system," *Journal of Intelligent & Robotic Systems*, vol. 102, no. 4, pp. 1–19, 2021.

[36] A. K. Behera and B. Bandyopadhyay, "Robust sliding mode control: An event-triggering approach," *IEEE Transactions on Circuits and Systems II: Express Briefs*, vol. 64, no. 2, pp. 146–150, Feb 2017.

[37] M. Cucuzzella and A. Ferrara, "Practical second order sliding modes in single-loop networked control of nonlinear systems," *Automatica*, vol. 89, pp. 235 – 240, 2018.

[38] L. Wu, Y. Gao, J. Liu, and H. Li, "Event-triggered sliding mode control of stochastic systems via output feedback," *Automatica*, vol. 82, pp. 79 – 92, 2017.

[39] M. M. Azimi, A. A. Afzalian, and R. Ghaderi, "Decentralized stabilization of a class of large scale networked control systems based on modified event-triggered scheme," *International Journal of Dynamics and Control*, pp. 1–11, 2020.

[40] A. Rahnama, M. Xia, and P. J. Antsaklis, "Passivity-based design for event-triggered networked control systems," *IEEE Transactions on Automatic Control*, pp. 1–1, 2017.

[41] M. Krstic, P. V. Kokotovic, and I. Kanellakopoulos, *Nonlinear and adaptive control design*. John Wiley & Sons, Inc., 1995.

[42] D. Zhang, P. Shi, Q.-G. Wang, and L. Yu, "Analysis and synthesis of networked control systems: A survey of recent advances and challenges," *ISA Transactions*, vol. 66, pp. 376–392, 2017.

[43] C. Santos, M. Mazo Jr, and F. Espinosa, "Adaptive self-triggered control of a remotely operated p3-dx robot: Simulation and experimentation," *Robotics and Autonomous Systems*, vol. 62, no. 6, pp. 847–854, 2014.

[44] J. Ma, S. Xu, G. Zhuang, Y. Wei, and Z. Zhang, "Adaptive neural network tracking control for uncertain nonlinear systems with input delay and saturation," *International Journal of Robust and Nonlinear Control*, vol. 30, no. 7, pp. 2593–2610, 2020.

[45] K. Liu, A. Selivanov, and E. Fridman, "Survey on time-delay approach to networked control," *Annual Reviews in Control*, vol. 48, pp. 57–79, 2019. [Online]. Available: https://www.sciencedirect.com/science/article/pii/S1367578819300021

[46] J. Ghommam and F. Mnif, "Predictor-based control for an inverted pendulum subject to networked time delay," *ISA Transactions*, vol. 67, pp. 306–316, 2017. [Online]. Available: https://www.sciencedirect.com/science/article/pii/S0019057817301180

[47] M. Sharma and I. Kar, "Control of a quadrotor with network induced time delay," *ISA Transactions*, vol. 111, pp. 132–143, 2021. [Online]. Available: https://www.sciencedirect.com/science/article/pii/S0019057820304791

[48] H. Li, L. Wang, H. Du, and A. Boulkroune, "Adaptive fuzzy backstepping tracking control for strict-feedback systems with input delay," *IEEE Transactions on Fuzzy Systems*, vol. 25, no. 3, pp. 642–652, 2016.

[49] J. Ma, S. Xu, G. Cui, W. Chen, and Z. Zhang, "Adaptive backstepping control for strict-feedback non-linear systems with input delay and disturbances," *IET Control Theory & Applications*, vol. 13, no. 4, pp. 506–516, 2018.

[50] J. K. Hale and S. M. V. Lunel, *Introduction to functional differential equations*. Springer Science & Business Media, 2013, vol. 99.

[51] R. Postoyan, M. C. Bragagnolo, E. Galbrun, J. Daafouz, D. Nešić, and E. B. Castelan, "Nonlinear event-triggered tracking control of a mobile robot: design, analysis and experimental results," *IFAC Proceedings Volumes*, vol. 46, no. 23, pp. 318–323, 2013.

[52] C. Santos, M. Martínez-Rey, F. Espinosa, A. Gardel, and E. Santiso, "Event-based sensing and control for remote robot guidance: An experimental case," *Sensors*, vol. 17, no. 9, p. 2034, 2017.

[53] C. Santos, F. Espinosa, M. Martinez-Rey, D. Gualda, and C. Losada, "Self-triggered formation control of nonholonomic robots," *Sensors*, vol. 19, no. 12, p. 2689, 2019.

[54] E. A. Martínez, H. Ríos, and M. Mera, "Robust tracking control design for unicycle mobile robots with input saturation," *Control Engineering Practice*, vol. 107, p. 104676.

[55] T.-Y. Zhang and G.-P. Liu, "Tracking control of wheeled mobile robots with communication delay and data loss," *Journal of Systems Science and Complexity*, vol. 31, no. 4, pp. 927–945, 2018.

[56] M. Takahashi, T. Suzuki, H. Shitamoto, T. Moriguchi, and K. Yoshida, "Developing a mobile robot for transport applications in the hospital domain," *Robotics and Autonomous Systems*, vol. 58, no. 7, pp. 889–899, 2010.

[57] N. I. Katevas, N. M. Sgouros, S. G. Tzafestas, G. Papakonstantinou, P. Beattie, J. Bishop, P. Tsanakas, and D. Koutsouris, "The autonomous mobile robot senario: a sensor aided intelligent navigation system for powered wheelchairs," *IEEE Robotics & Automation Magazine*, vol. 4, no. 4, pp. 60–70, 1997.

[58] D. Sanders, "Comparing ability to complete simple tele-operated rescue or maintenance mobile-robot tasks with and without a sensor system," *Sensor Review*, 2010.

[59] C. Trevai, J. Ota, and T. Arai, "Multiple mobile robot surveillance in unknown environments," *Advanced Robotics*, vol. 21, no. 7, pp. 729–749, 2007.

[60] R. Solea, A. Filipescu, and G. Stamatescu, "Sliding-mode real-time mobile platform control in the presence of uncertainties," in *Proceedings of the 48h IEEE Conference on Decision and Control (CDC) held jointly with 2009 28th Chinese Control Conference*. IEEE, 2009, pp. 7747–7752.

[61] S. Alshamali, "A backstepping design approach to a class of mobile robots," in *2017 11th Asian Control Conference (ASCC)*. IEEE, 2017, pp. 1341–1344.

[62] T. Fukao, H. Nakagawa, and N. Adachi, "Adaptive tracking control of a nonholonomic mobile robot," *IEEE Transactions on Robotics and Automation*, vol. 16, no. 5, pp. 609–615, 2000.

[63] B. S. Park, S. J. Yoo, J. B. Park, and Y. H. Choi, "A simple adaptive control approach for trajectory tracking of electrically driven nonholonomic mobile robots," *IEEE Transactions on Control Systems Technology*, vol. 18, no. 5, pp. 1199–1206, 2010.

[64] D. Nganga-Kouya and F. A. Okou, "Adaptive backstepping control of a wheeled mobile robot," in *2009 17th Mediterranean Conference on Control and Automation*. IEEE, 2009, pp. 85–91.

[65] Z.-G. Hou, A.-M. Zou, L. Cheng, and M. Tan, "Adaptive control of an electrically driven nonholonomic mobile robot via backstepping and fuzzy approach," *IEEE Transactions on Control Systems Technology*, vol. 17, no. 4, pp. 803–815, 2009.

[66] M. G. Villarreal-Cervantes, J. F. Guerrero-Castellanos, S. Ramírez-Martínez, and J. P. Sánchez-Santana, "Stabilization of a (3, 0) mobile robot by means of an event-triggered control," *ISA Transactions*, vol. 58, pp. 605–613, 2015.

[67] Q. Cao, Z. Sun, Y. Xia, and L. Dai, "Self-triggered mpc for trajectory tracking of unicycle-type robots with external disturbance," *Journal of the Franklin Institute*, vol. 356, no. 11, pp. 5593–5610, 2019. [Online]. Available: https://www.sciencedirect.com/science/article/pii/S0016003219302753

[68] C. Santos, F. Espinosa, E. Santiso, and D. Gualda, "Lyapunov self-triggered controller for nonlinear trajectory tracking of unicycle-type robot," *International Journal of Control, Automation and Systems*, vol. 18, no. 7, pp. 1829–1838, 2020.

[69] D. Chwa, "Tracking control of differential-drive wheeled mobile robots using a backstepping-like feedback linearization," *IEEE Transactions on Systems, Man, and Cybernetics - Part A: Systems and Humans*, vol. 40, no. 6, pp. 1285–1295, Nov 2010.

[70] C. De La Cruz and R. Carelli, "Dynamic modeling and centralized formation control of mobile robots," in *IECON 2006-32nd Annual Conference on IEEE Industrial Electronics*. IEEE, 2006, pp. 3880–3885.

[71] F. N. Martins, W. C. Celeste, R. Carelli, M. Sarcinelli-Filho, and T. F. Bastos-Filho, "An adaptive dynamic controller for autonomous mobile robot trajectory tracking," *Control Engineering Practice*, vol. 16, no. 11, pp. 1354–1363, 2008.

[72] C. De La Cruz and R. Carelli, "Dynamic model based formation control and obstacle avoidance of multi-robot systems," *Robotica*, vol. 26, no. 3, pp. 345–356, 2008.

[73] H. C.-H. Hsu and A. Liu, "Multiagent-based multi-team formation control for mobile robots," *Journal of Intelligent and Robotic Systems*, vol. 42, no. 4, pp. 337–360, 2005.

[74] X. Dong, Y. Zhou, Z. Ren, and Y. Zhong, "Time-varying formation tracking for second-order multi-agent systems subjected to switching topologies with application to quadrotor formation flying," *IEEE Transactions on Industrial Electronics*, vol. 64, no. 6, pp. 5014–5024, 2016.

[75] V. Lesser, C. L. Ortiz Jr, and M. Tambe, *Distributed sensor networks: A multiagent perspective*. Springer Science & Business Media, 2012, vol. 9.

[76] D. Liu and G.-H. Yang, "A dynamic event-triggered control approach to leader-following consensus for linear multiagent systems," *IEEE Transactions on Systems, Man, and Cybernetics: Systems*, 2020.

[77] D. Zhang and G. Feng, "A new switched system approach to leader-follower consensus of heterogeneous linear multiagent systems with dos attack," *IEEE Transactions on Systems, Man, and Cybernetics: Systems*, 2019.

[78] Y. Cai, H. Zhang, J. Zhang, and Q. He, "Distributed bipartite leader-following consensus of linear multi-agent systems with input time delay based on event-triggered transmission mechanism," *ISA Transactions*, vol. 100, pp. 221–234, 2020.

[79] D. Zhao, T. Zou, S. Li, and Q. Zhu, "Adaptive backstepping sliding mode control for leader–follower multi-agent systems," *IET Control Theory & Applications*, vol. 6, no. 8, pp. 1109–1117, 2012.

[80] W. Wang, H. Liang, Y. Zhang, and T. Li, "Adaptive cooperative control for a class of nonlinear multi-agent systems with dead zone and input delay," *Nonlinear Dynamics*, vol. 96, no. 4, pp. 2707–2719, 2019.

[81] J. Huang, W. Wang, C. Wen, J. Zhou, and G. Li, "Distributed adaptive leader–follower and leaderless consensus control of a class of strict-feedback nonlinear systems: a unified approach," *Automatica*, vol. 118, p. 109021, 2020.

[82] Q. Yang, H. Fang, M. Cao, and J. Chen, "Distributed trajectory tracking control for multiple nonholonomic mobile robots," *IFAC-PapersOnLine*, vol. 49, no. 4, pp. 31–36, 2016.

[83] M. Guinaldo, E. Fábregas, G. Farias, S. Dormido-Canto, D. Chaos, J. Sánchez, and S. Dormido, "A mobile robots experimental environment with event-based wireless communication," *Sensors*, vol. 13, no. 7, pp. 9396–9413, 2013.

[84] D. Ayedi, M. Boujelben, and C. Rekik, "A multiagent architecture for mobile robot navigation using hierarchical fuzzy and sliding mode controllers," *Mathematical Problems in Engineering*, vol. 2018, 2018.

[85] L. Ding, Q.-L. Han, X. Ge, and X.-M. Zhang, "An overview of recent advances in event-triggered consensus of multiagent systems," *IEEE Transactions on Cybernetics*, vol. 48, no. 4, pp. 1110–1123, 2017.

[86] L. Zhang, H. Gao, and O. Kaynak, "Network-induced constraints in networked control systems a survey," *IEEE Transactions on Industrial Informatics*, vol. 9, no. 1, pp. 403–416, 2013.

[87] D. Fyler, B. Sullivan, and I. A. Raptis, "Distributed object manipulation using a mobile multi-agent system," in *2015 IEEE International Conference on Technologies for Practical Robot Applications (TePRA)*. IEEE, 2015, pp. 1–6.

[88] H. Kitano, S. Tadokoro, I. Noda, H. Matsubara, T. Takahashi, A. Shinjou, and S. Shimada, "Robocup rescue: Search and rescue in large-scale disasters as a domain for autonomous agents research," in *IEEE SMC'99 Conference Proceedings. 1999 IEEE International Conference on Systems, Man, and Cybernetics (Cat. No. 99CH37028)*, vol. 6. IEEE, 1999, pp. 739–743.

[89] D. I. Tapia, J. F. De Paz, S. Rodriguez, J. Bajo, and J. M. Corchado, "Multi-agent system for security control on industrial environments," *International Transactions on System Science and Applications Journal*, vol. 4, no. 3, pp. 222–226, 2008.

[90] R. Fierro and F. L. Lewis, "Control of a nonholomic mobile robot: Backstepping kinematics into dynamics," *Journal of robotic systems*, vol. 14, no. 3, pp. 149–163, 1997.

[91] K. D. Do, Z.-P. Jiang, and J. Pan, "Simultaneous tracking and stabilization of mobile robots: an adaptive approach," *IEEE Transactions on Automatic Control*, vol. 49, no. 7, pp. 1147–1151, 2004.

[92] B. S. Park, S. J. Yoo, J. B. Park, and Y. H. Choi, "A simple adaptive control approach for trajectory tracking of electrically driven nonholonomic mobile robots," *IEEE Transactions on Control Systems Technology*, vol. 18, no. 5, pp. 1199–1206, 2009.

[93] S. Al Issa, M. Sharma, and I. Kar, "Event-triggered backstepping control scheme for networked mobile robots," in *Proceedings of the Advances in Robotics 2019*, 2019, pp. 1–5.

[94] S. Al Issa, A. Chakravarty, and I. Kar, "Adaptive control of a networked mobile robot subject to parameter uncertainties and limited communications," in *2019 Sixth Indian Control Conference (ICC)*. IEEE, 2019, pp. 308–313.

[95] F. N. Martins, M. Sarcinelli-Filho, and R. Carelli, "A velocity-based dynamic model and its properties for differential drive mobile robots," *Journal of Intelligent & Robotic Systems*, vol. 85, no. 2, pp. 277–292, 2017.

[96] L. Xing, Y. Mishra, Y.-C. Tian, G. Ledwich, C. Zhou, W. Du, and F. Qian, "Distributed state-of-charge balance control with event-triggered signal transmissions for multiple energy storage systems in smart grid," *IEEE Transactions on Systems, Man, and Cybernetics: Systems*, vol. 49, no. 8, pp. 1601–1611, 2019.

[97] J.-J. E. Slotine, W. Li *et al.*, *Applied nonlinear control*. Prentice hall Englewood Cliffs, NJ, 1991, vol. 199, no. 1.

[98] L. Behera and I. Kar, *Intelligent systems and control principles and applications*. Oxford University Press, Inc., 2010.

[99] S. Al Issa and I. Kar, "Design and implementation of event-triggered adaptive controller for commercial mobile robots subject to input delays and limited communications," *Control Engineering Practice*, vol. 114, p. 104865, 2021.

[100] ——, "Adaptive backstepping control of multiple mobile robots under limited communication; an event-triggered approach," in *Communication and Control for Robotic Systems*. Springer, 2022, pp. 107–122.